

論文 / 著書情報  
Article / Book Information

題目(和文)	
Title(English)	Immunomodulatory effect of Surface Layer Protein B coated lactobacilli
著者(和文)	YINTingyu
Author(English)	Tingyu Yin
出典(和文)	学位:博士(工学), 学位授与機関:東京工業大学, 報告番号:甲第12578号, 授与年月日:2023年9月22日, 学位の種別:課程博士, 審査員:山本 直之,一瀬 宏,越川 直彦,折原 芳波,吉田 啓亮
Citation(English)	Degree:Doctor (Engineering), Conferring organization: Tokyo Institute of Technology, Report number:甲第12578号, Conferred date:2023/9/22, Degree Type:Course doctor, Examiner:,,,,,
学位種別(和文)	博士論文
Type(English)	Doctoral Thesis

# **Immunomodulatory effect of Surface Layer Protein B coated lactobacilli**

YIN Tingyu

Supervisor: Prof. Naoyuki Yamamoto

Human Centered Science and Biomedical Engineering Course

Department of Life Science and Technology

Tokyo Institute of Technology



## Abstract

Lactic acid bacteria (LAB) are known to exert immunomodulatory effects in the gastrointestinal tract of the host. Surface layer protein (Slp) is one of the critical components of LAB that closely linked with the uptake of lactobacilli into the host cell and cytokines production via the interaction with host immune dendritic cells (DCs). However, only a few functional Slps have been reported and the key receptors for Slps remain unknown.

In this research, SlpB isolated from *Levilactobacillus brevis* JCM 1059 has been identified and investigated as the essential component involved in the uptake of lactobacilli into DCs. Various lactobacilli enhanced the immunomodulation by SlpB coating and the receptor for SlpB was purified from DCs and identified as adenylyl cyclase-associated protein 1 (CAP-1). Also, the core binding peptides derived from SlpB showed interactions with lactobacilli and DCs were detected.

These results strongly suggest that the SlpB coating on lactobacilli plays a crucial role in the uptakes of lactobacilli into THP-1 DCs and activates the immune responses with cytokine productions.

# Abbreviation

Adenylyl cyclase-associated protein 1 (CAP-1)

Adherens junctions (AJs)

Antigen-presenting cells (APCs)

Antimicrobial peptides (AMPs)

Coomassie Brilliant Blue (CBB)

Dendritic cells (DCs)

Differentially expressed genes (DEG)

Dimethyl sulfoxide (DMSO)

Ethylenediaminetetraacetic acid (EDTA)

Fetal bovine serum (FBS)

Fluorescein isothiocyanate (FITC)

Follicle-associated epithelium (FAE)

Gut-associated lymphoid tissues (GALT)

Interferon- $\beta$  (IFN- $\beta$ )

Interleukin-1 (IL-1)

Interleukin-4 (IL-4)

Interleukin-6 (IL-6)

Interleukin-8 (IL-8)

Interleukin-10 (IL-10)

Interleukin-12 (IL-12)

Interleukin-25 (IL-25)

Interleukin-1 receptor associated kinase (IRAK)

Intestinal epithelial cells (IECs)

Isoelectric point (PI)

Isolated lymphoid follicles (ILF)

Lactic acid bacteria (LAB)

Lithium chloride (LiCl)

Macrophage-inducible C-type lectin (Mincle)

Major histocompatibility complex (MHC)

Microfold cells (M cells)

Mucoprotein 3 (MUC3)

Multiplicity of infection (MOI)

Myeloid differentiation primary response 88 gene (Myd88)

Nuclear factor kappa B (NF- $\kappa$ B)

Paraformaldehyde (PFA)

Phorbol 2-myristate 13-acetate (PMA)

Phosphate-buffered saline (PBS)

Polyvinylidene difluoride (PVDF)

Secretory IgA molecule (SIgA)

Sodium dodecyl sulphate-polyacrylamide gel electrophoresis (SDS-PAGE)

Sulfo-Cyanine3 (Cy3)

Surface layer protein (Slp)

T-cell receptor (TCR)

Tight junctions (TJs)

TNF receptor associated factor (TRAF)

Toll like receptors (TLRs)

Transforming growth factor- $\beta$  (TGF- $\beta$ )

Tumor necrosis factor- $\alpha$  (TNF- $\alpha$ )

# Content

<b>ABSTRACT</b> .....	- 1 -
<b>ABBREVIATION</b> .....	- 2 -
<b>CHAPTER 1 INTRODUCTION</b> .....	- 9 -
1.1 GENERAL INTRODUCTION OF LACTIC ACID BACTERIA.....	- 9 -
1.1.1 <i>Health effects of lactic acid bacteria on hosts</i> .....	- 9 -
1.1.2 <i>The role of lactobacilli in intestinal immunity</i> .....	- 11 -
1.2 LACTOBACILLI INVOLVED IN INTESTINAL IMMUNITY .....	- 13 -
1.2.1 <i>The importance of the intestinal barrier in immune regulation</i> .....	- 13 -
1.2.2 <i>The key role of surface proteins in lactobacilli for the intestinal immunity</i> .....	- 15 -
1.3 CLASSIFICATION AND CHARACTERISTICS OF SLPS IN LACTOBACILLI .....	- 18 -
1.4 INTESTINAL IMMUNE RELATED SIGNALING PATHWAYS. ....	- 20 -
1.4.1 <i>Toll like receptors pathway</i> .....	- 20 -
1.4.2 <i>NF-<math>\kappa</math>B Pathway</i> .....	- 22 -
1.5 INTESTINAL IMMUNE TISSUE AND IMMUNE CELLS.....	- 25 -
1.6 OBJECTIVE OF THIS RESEARCH .....	- 28 -
<b>CHAPTER 2 ROLE OF SURFACE LAYER PROTEINS IN IMMUNOMODULATORY EFFECTS OF LACTOBACILLI</b> .....	- 29 -
2.1 INTRODUCTION.....	- 29 -
2.2 MATERIALS AND METHODS.....	- 30 -
2.2.1 <i>Bacteria and the cultivation</i> .....	- 30 -
2.2.2 <i>Differentiation of monocytic THP-1 to dendritic cells (THP-1 DCs)</i> .....	- 30 -

2.2.3 Strain Sulfo-Cyanine3 Labelling .....	- 31 -
2.2.4 Isolation and identification of surface layer proteins from LAB .....	- 32 -
2.2.5 Fluorescent observation <i>L. brevis</i> JCM 1059 SlpB on <i>L. plantarum</i> JCM 1149 .....	- 32 -
2.2.6 SlpB coating capacity on LAB strains .....	- 33 -
2.2.7 Uptake of <sup>Cy3</sup> SlpB coated LAB by THP-1 DCs .....	- 33 -
2.2.8 Cytokines Measurement .....	- 34 -
2.2.9 RNA sequencing and data analysis .....	- 34 -
2.2.10 in vivo uptake assay of SlpB coated <i>L. plantarum</i> JCM 1149 .....	- 34 -
2.2.11. Statistical Analysis .....	- 35 -
2.3 RESULTS .....	- 36 -
2.3.1. Induction of DC-SIGN on THP-1 cells .....	- 36 -
2.3.2. Uptake of LAB by THP-1 DC and IL-12 induction .....	- 38 -
2.3.3 Key Slps on <i>L. brevis</i> JCM 1059 and role in the uptake .....	- 41 -
2.3.4 SlpB coating ability on different LAB strains .....	- 46 -
2.3.5 SlpB coating LAB strains increased the uptake ratio into THP-1 DCs .....	- 49 -
2.3.6 Gene expressions in THP-1 DCs after the treatment with SlpB coated <i>L. brevis</i> JCM 1059 .....	- 53 -
2.3.7 SlpB-coated <sup>Cy3</sup> <i>L. plantarum</i> JCM 1149 in mouse Peyer's patches .....	- 55 -
2.4 SUMMARY .....	- 58 -
<b>CHAPTER 3 IDENTIFICATION OF SLPB RECEPTOR ON THP-1 DCS .....</b>	<b>- 60 -</b>
3.1 INTRODUCTION .....	- 60 -
3.2 MATERIALS AND METHODS .....	- 62 -
3.2.1 Cell differentiation and protein collection .....	- 62 -
3.2.2 Isolation the SlpB binding receptors on THP-1 DCs .....	- 62 -

3.2.3 Identification of affinity purified protein.....	- 62 -
3.2.4 CAP-1 Expression on THP-1 DCs.....	- 63 -
3.2.5 Western blotting analysis.....	- 64 -
3.2.6 Inhibition of SlpB binding to THP-1 DCs by specific antibody.....	- 64 -
3.2.7 Fluorescent observation of CAP-1 and Actin on THP-1 DCs.....	- 65 -
3.2.8. Statistical Analysis.....	- 65 -
3.3 RESULTS.....	- 66 -
3.3.1 Identification of surface proteins from THP-1 DCs.....	- 66 -
3.3.2 CAP-1 expression and immunostaining on THP-1 DCs.....	- 70 -
3.3.3 Western Blotting Analysis for surface receptors.....	- 72 -
3.3.4 SlpB Binding to THP-1 DCs by Antibodies.....	- 74 -
3.3.5 Immunostaining of CAP-1 and Actin on THP-1 DCs.....	- 76 -
3.4 SUMMARY.....	- 78 -

#### CHAPTER 4 PREDICTION OF MAJOR SLPB REGIONS INVOLVED IN BINDINGS WITH

<b>BACTERIA AND THP-1 DCS.....</b>	<b>- 80 -</b>
4.1 INTRODUCTION.....	- 80 -
4.2 MATERIALS AND METHODS.....	- 82 -
4.2.1 SlpB digestion and HPLC analysis.....	- 82 -
4.2.2 Identification of bacteria binding fragments.....	- 82 -
4.2.3 Identification of CAP-1 binding fragments.....	- 83 -
4.2.4 Glycan competition test with SlpB on THP-1 DCs.....	- 84 -
4.2.5 SlpB deglycosylation and THP-1 DCs binding test.....	- 84 -
4.2.6 Peptide analysis and prediction.....	- 84 -
4.2.7 Statistical Analysis.....	- 85 -

4.3 RESULTS .....	- 86 -
4.3.1 Peptide fragments at different enzymatic hydrolysis times.....	- 86 -
4.3.2 Identification of binding fragments to bacteria.....	- 88 -
4.3.3 Involvement of polysaccharide of SlpB for CAP-1 binding.....	- 93 -
4.3.4 Identification of binding fragments to CAP-1 .....	- 95 -
4.3.5 Prediction of bacteria binding peptides .....	- 97 -
4.4 SUMMARY .....	- 100 -
<b>CHAPTER 5 DISCUSSION AND CONCLUSION .....</b>	<b>- 102 -</b>
5.1 DISCUSSION .....	- 102 -
5.1.1 SlpB on <i>L. brevis</i> JCM 1059 plays important role for bacterial uptake by THP-1 DCs .....	- 102 -
5.1.2 SlpB can coat other LAB strains and enhance the bacterial immune ability. -	103 -
5.1.3 NF- $\kappa$ B involved in TLRs signal pathway triggered by SlpB in THP-1 DCs.....	- 106 -
5.1.4 CAP-1 as a novel receptor for SlpB on THP-1 DCs.....	- 108 -
5.1.5 The exploration of SlpB functional binding peptides.....	- 112 -
5.2 CONCLUSION.....	- 116 -
<b>REFERENCE.....</b>	<b>- 117 -</b>
<b>ACKNOWLEDGEMENT .....</b>	<b>- 135 -</b>



# Chapter 1 Introduction

## 1.1 General introduction of lactic acid bacteria

### 1.1.1 Health effects of lactic acid bacteria on hosts

Lactic acid bacteria (LAB) are a type of gram-positive, non-spore-producing bacteria, including *Lactobacillus*, *Bifidobacterium*, *Lactococcus*, etc. LAB are widely present in soil, water, and plants in nature, as well as applied in the food industry [1]. In recent years, it has been shown that LAB have important effects on host health, these microbes play beneficial roles in supporting the host by controlling the composition of the gut microbiota, strengthening immunological function, and improving digestive tract health through a variety of mechanisms [2, 3].

#### (1) Regulation of gut microbiota composition

The gut microbiota is one of the most complex and numerous microbial communities in our body, and as one important exist, LAB play an important role in many aspects. LAB can affect the growth of other harmful microorganisms through competitive inhibition and the production of antibacterial substances, such as lactic acid and hydrogen peroxide, which inhibit the growth and reproduction of bacteria, fungi, viruses, and other pathogens, thus maintaining the balance of intestinal microorganisms [4, 5].

#### (2) Regulation of immune function

The immune system is an important defense line for protecting the human body, and LAB have been shown to influence immunological function through various pathways. LAB can enhance the host's immune response, promote the activation of immune cells, and secrete immune factors [6]. LAB can also inhibit

the occurrence of inflammatory reactions and alleviate the symptoms of inflammatory related diseases [7]. In addition, the allergic response of the host can be mitigated by LAB through the regulation of immune tolerance [8]. Lactobacilli is the main strain for the fermentation of various vegetables, and has a variety of probiotic effects such as immune enhancement activity, improvement of chronic intestinal inflammation and irritable bowel syndrome [9, 10].

### (3) Improvement of gastrointestinal health

By assisting to establish an optimal environment in the gastrointestinal tract, LAB could enhance digestion and nutrient absorption. The gastrointestinal tract's pH can be reduced by LAB, preventing infections and diarrhea by suppressing the development of pathogenic bacteria. Cellulases, proteases, and other enzymes produced by LAB can decompose the complex components in food, contribute to the digestion and absorption of nutrients, improve food utilization, and reduce the production of excreta [11, 12].

### (4) The impact of LAB on mental health

Recent studies have also found that LAB have a certain impact on mental health. LAB can regulate the communication mechanism of the gut-brain axis [13], regulate neurotransmitters related to emotions and behavior in the brain, and improve psychological problems such as stress, anxiety, and depression [14].

Clearly, LAB play a key role in maintaining gut health, boosting immunity, and warding off gastrointestinal disorders. By focusing on the study of LAB will help us better improve human health and prevent related diseases.

### 1.1.2 The role of lactobacilli in intestinal immunity

Lactobacilli is a type of LAB that plays an important role in the maintenance of intestinal health compared to other LAB [15-18]. By modulating the activity of the intestinal immune system, lactobacilli assist in fending off infections, reducing inflammation, and promoting host immunity, while simultaneously maintaining the microbiota balance in the gut [19]. With the increased attention to intestinal health, the mechanism investigation and application of lactobacilli have become a research focus.

The gut mucosal barrier is a crucial part of the immune system. Lactobacilli plays an important role in maintaining the integrity and normal function of the intestinal mucosal barrier [20-22]. Although the existing report cannot fully reveal the immune regulatory mechanisms involved in lactobacilli, based on current research, we can understand that lactobacilli can synthesize and secrete the antibacterial components such as lactic acid or lactate peroxide, inhibiting the growth and invasion of pathogens [23]. Also, lactobacilli can stimulate the intestinal epithelial cells to produce mucoprotein, preventing bacterial adhesion. *Lactobacillus casei* GG induces the high expression of mucoprotein 3 (MUC3) mRNA on Caco-2 cells, promotes the secretion of MUC3, and thus reduces the adhesion of *E. coli* [24].

More importantly, lactobacilli exhibited an anti-inflammatory ability, inflammatory reactions are inevitable products of the body's immune response process. if the inflammatory response is excessive or persistent, it can lead to pathological damage. However, lactobacilli can inhibit the production of inflammatory mediators and the activation of inflammatory signaling pathways,

promote the regulatory function of T cells, and regulate the balance of inflammatory responses by reducing infiltration of inflammatory cells and alleviating tissue damage, exerting anti-inflammatory effects, and reducing the occurrence of inflammatory related diseases. In the intestine, lactobacilli regulate the secretion and activity of immune cells to regulate the immune response, including enhancing the phagocytic ability of macrophages, activating dendritic cells, and enhancing NK cell activity, to enhance the body's immune system [25-28].

Despite research has found that lactobacilli can enhance intestinal barrier function, more detailed mechanisms, including the functional components of lactobacilli involved in immune regulation and the regulated immune cells, still need further research.

## **1.2 Lactobacilli involved in intestinal immunity**

### **1.2.1 The importance of the intestinal barrier in immune regulation**

The intestinal barrier is a complex system composed of epithelial cells and mucosal epithelial cells present in the intestine [29, 30]. It is one of the most important parts of the human digestive system and plays a crucial role in the human immune system. Not only affects defending against external pathogens and antigenic substances but also maintains immune balance by regulating the activity and function of immune cells.

The intestinal barrier is mainly composed of intestinal epithelial cells, which are tightly bound together by tight junction proteins and adhesion proteins to form a sealed barrier. In addition to the intercellular junction, the intestinal barrier also includes the mucus layer and antibacterial peptides on the surface of mucosal epithelial cells. The mucus layer can prevent the invasion of pathogens, while antibacterial peptides can kill pathogens (Figure 1.1) [31]. Also, the intestinal barrier has immune regulatory functions, that can maintain immune balance by regulating the activity of immune cells and the release of cytokines. Research has found that intestinal epithelial cells can release soluble factors such as interleukin-25 (IL-25), which inhibits the activity of immune cells [32, 33]. At the same time, mucosal immune cells can also secrete immune regulatory factors, such as transforming growth factor- $\beta$  (TGF- $\beta$ ) and IL-10 to maintain immune balance [34]. Eventually prevent the occurrence of autoimmune diseases and reduce the risk of chronic inflammation.

Overall, the intestinal barrier is the first line of defense against external pathogens and antigenic substances entering the human body. It can selectively

allow beneficial microorganisms and nutrients to pass through while preventing harmful bacterial communities and toxins from entering the body. The rupture of the intestinal barrier can lead to the invasion of pathogens and the activation of the immune system, causing inflammation and immune response. Therefore, maintaining the integrity of the intestinal barrier is crucial for preventing infection and disease.

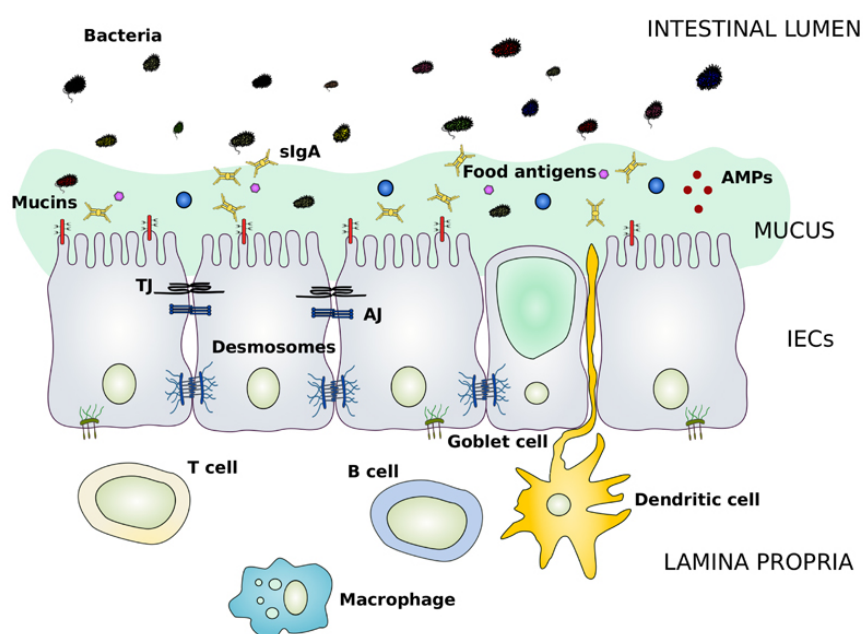


**Figure 1.1. Schematic representation of the main components of the intestinal barrier and immune system [31]** The mucus layer present as a sieve-like structure on the surface of intestinal epithelium, secreting antimicrobial peptides (AMPs) and secretory IgA molecule (sIgA). Monolayer intestinal epithelial cells (IECs) tightly attached to each other by tight junction (TJs) and adherens junctions (AJs). The main immune cells involved are T cells, B cells, macrophages, and dendritic cells.

### **1.2.2 The key role of surface proteins in lactobacilli for the intestinal immunity**

The functional components of lactobacilli mainly include polysaccharides, proteins, vitamins, enzymes etc. (Figure 1.2) [35] Polysaccharides could enhance immune cell activity, regulate immune responses, and have anticancer effects. Proteins, as important antigens of lactobacilli, can induce immune responses and enhance protective immunity in the body. In addition, lactobacilli can also produce a variety of vitamins, such as vitamin K, vitamin B group and antioxidant enzymes, which help to maintain the normal function of the immune system [36-40]. Among these components, the surface proteins of lactobacilli exhibit effects in maintaining bacterial stability, adhesion to the hosts and especially immune regulation [41].

In the process of interaction between bacteria and host cells, adhesion and colonization in the intestine are the prerequisite and foundation for lactobacilli to exert its functions. Surface protein is one of the main components that can assist lactobacilli adhere to the host cell, being recognized by the host cell, and further triggering the subsequent reaction. The cell wall surface proteins and extracellular secretory proteins of lactobacilli have been reported to secrete adhesins, which can be recognized by specific adhesin receptors on the host cell surface and bind to them [42, 43]. Meanwhile, there is a special type of surface layer protein (Slp) with a single-molecule crystalline arrangement on some lactobacillus strains that is also found to be involved in the adhesion of lactobacilli [44, 45].

Slp is a protein composed of repeatedly arranged protein units with high structural stability and self-assembly ability, which can enhance the stability and tolerance of bacteria, enabling bacteria to survive in extreme environmental

conditions, such as low pH, high salinity, and high temperature [46, 47]. It can act as an adhesion molecule between bacteria and host cells, participating in host immune response and regulating the balance of gut microbiota. In addition, Slp also be found can inhibit the growth and attachment of some pathogenic microorganisms, thus playing an important role in maintaining the intestinal microbalance. Also, Slp has potential applications such as biological repair and biological separation [48-50].

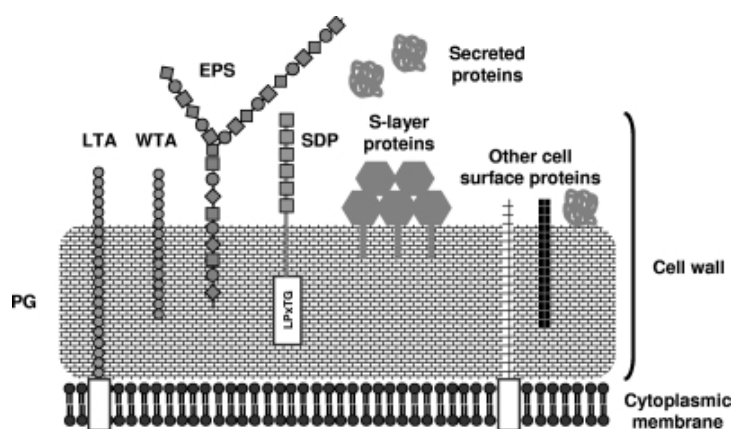


**Figure 1. 2. Cell surface architecture of lactobacilli [35].** multilayered peptidoglycan (PG) decorated with wall teichoic acid (WTA) and or lipoteichoic acid (LTA), exopolysaccharides (EPSs) and proteins exist in most gram-positive bacteria. On the surface of lactobacilli also exist sortase-dependent proteins (SDPs) and S-layer proteins (Slps) structures.

Although current research indicates the Slp of lactobacilli has an immune regulating effect, only a few Slps revealed the adhesin effect. The mechanism of adhesion and the recognition receptor on immune cells, especially the involved immune regulation effect remain unclear. Thus, we need deep research on Slp to



understand its functional effect and its role in intestinal immune regulation for lactobacilli.

### 1.3 Classification and characteristics of Slps in lactobacilli

Slps in LAB is mainly produced by lactobacilli, and there have been no reports of Slps in lactococci. The Slps were found in *Lactobacillus acidophilus*, *Lactobacillus brucei*, *Lactobacillus helveticus*, *Lactobacillus delbrueckii* subsp. *bulgaricus* and *Lactobacillus brevis* [51-53]. The Slps in these species have the similar characteristics, with molecular weight between 25 to 71 kD [54] and isoelectric point (pI) between 9.35 to 10.04. Although glycosylated structures of Slps have been found in many gram-positive bacteria [55], in most LAB, Slps are non-glycosylated, and currently glycosylated structures have only been found in *Lactobacillus brevis* [56]. The Slp crystals have oblique, square, and hexagonal shapes. According to different lattice types, Slps can be composed of 1, 2, 4, 5 or 6 proteins subunits [57]. In most bacteria, Slps exhibit adhesion to extracellular matrix such as fibrin, laminin, or other collagen proteins [58].

Slps have self-assembly property, and the Slp monomers isolated from the surface of lactobacilli can be reassembled in many matrices, such as solid surfaces, gas-liquid interfaces, liposomes, and suspensions (Figure 1.3) [59]. Meanwhile, the Slp also exhibits high expression and stability, the tightly arranged protein molecules present a network like, uniform hexagonal or square structure on the cell surface. It can cover the entire cell to form a dense protective layer, prevent the invasion of harmful substances from the outside, stabilize the cell morphology, and have a protective effect on the cell [60, 61].

In general, Slps differ in amino acid sequence, molecular weight, pI and glycosylation modification. Resulting the different structural characteristics and

functions. Thus, leading the Slp of *Lactobacillus* strains can not only resist the adhesion and invasion of pathogenic bacteria, but also induce cellular immune response by triggering immune cell responses (such as Th1 and Th17), thereby regulating intestinal inflammation [62, 63]

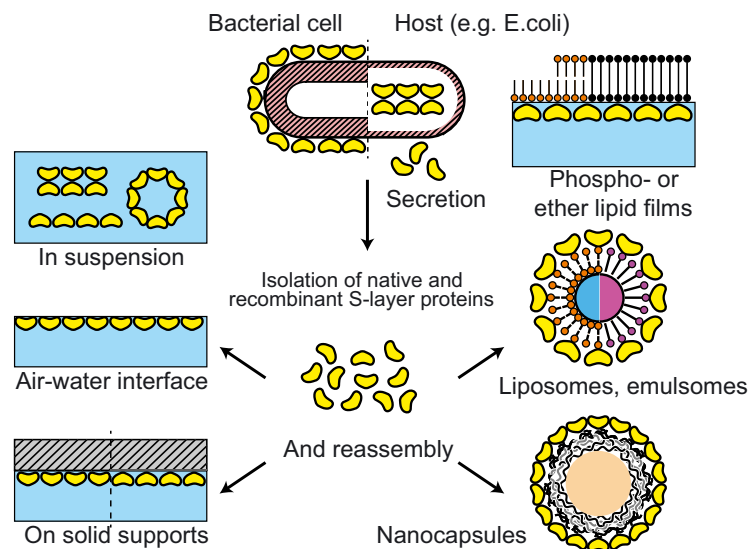


**Figure 1.3. reassembly of isolated S-layer in different mediums [59].** The example host is *Escherichia coli*.

## **1.4 Intestinal immune related signaling pathways.**

Intestinal regulation related signaling pathways refer to a series of signaling pathways that play a crucial role in the intestinal immune system. To understand the basic signal pathways are important to investigate the interaction of lactobacilli on intestinal immunomodulatory effect.

### **1.4.1 Toll like receptors pathway**

Toll like receptors (TLRs) are a class of transmembrane proteins that mainly exist on the surface of immune cells, such as macrophages, dendritic cells, and epithelial cells [64]. The TLRs pathway can initiate immune responses by identifying surface molecules of pathogenic microorganisms, such as bacterial endotoxins or viral nucleic acids. When pathogenic microorganisms enter the intestinal tract, TLRs will bind to its specific ligand, triggering a series of signal transduction pathways, including activation of various cytokines and cytokine receptor (Figure 1.4) [64]. Thus plays an important role in intestinal immunity.

Toll like receptors (TLRs) are the core of this pathway, and a total of 10 different types of TLRs (TLR1 to TLR10) have been discovered in humans [65]. These receptors can recognize and bind to different pathogens, viruses, and microbial components, initiating immune responses [66, 67]. Myeloid differentiation primary response 88 gene (MyD88) is the main pathway for TLRs signal transduction. When TLRs bind to their ligands, they interact with the MyD88 protein [68], activating downstream inflammation and immune responses. TNF receptor associated factor (TRAF) family genes encode TRAF proteins, including TRAF3, TRAF6, etc. Interleukin-1 receptor associated kinase (IRAK) family genes

encode IRAK proteins, including IRAK1, IRAK2, and IRAK4 [69, 70]. They also play an important role in the TLRs pathway, participating in signal transduction and regulating inflammatory responses. They interact with other proteins in the TLRs signaling pathway to regulate inflammation and immune response [71]. Nuclear factor kappa B (NF- $\kappa$ B) is a transcription factor that is considered an important regulator of the TLRs pathway [72, 73]. Promotes the expression of inflammation and immune genes. After activation of TLRs, the TLRs signaling pathway can also initiate interferon type immune responses. Interferon- $\beta$  (IFN- $\beta$ ) is an important interferon that can inhibit virus replication and spread and promote the development of antiviral immunity [74, 75].

The TLRs pathway can also regulate the function of intestinal epithelial cells [76]. Through TLRs activation, intestinal epithelial cells can produce mucus, strengthen the function of the intestinal mucosal barrier, and prevent the invasion of pathogenic microorganisms. And promote the secretion of immune regulation cytokines by intestinal epithelial cells, such as TGF- $\beta$  and IL-10 [77, 78].

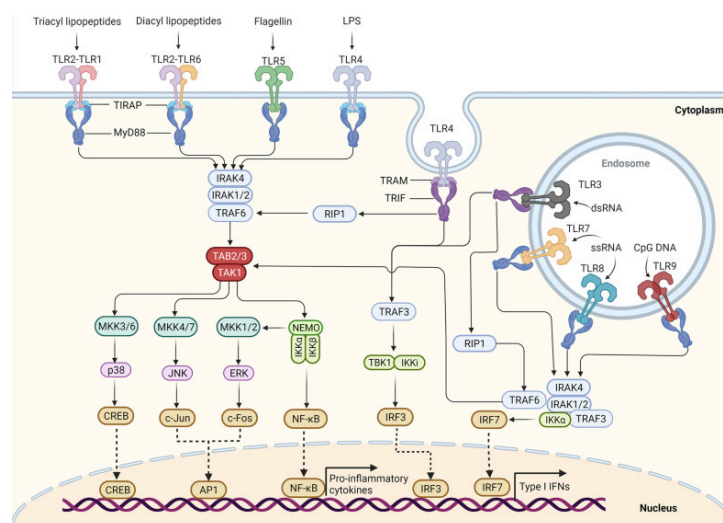


**Figure 1.4. TLRs signaling pathway in innate immune cells.[64]**

### 1.4.2 NF- $\kappa$ B Pathway

NF- $\kappa$ B is the main transcription factor that regulates inflammatory and immune responses. In intestinal immunity, the TLRs and NF- $\kappa$ B signaling pathways have a mutual influence relationship. After activation of the TLRs signaling pathway, ligands bound to TLRs trigger a series of signaling reactions, ultimately leading to the activation and translocation of NF- $\kappa$ B (Figure 1.5) [79]. With the stimulation, I $\kappa$ B protein will be degraded and release NF- $\kappa$ B. Subsequently, NF- $\kappa$ B enters the nucleus and binds to specific sequences on DNA, initiating or inhibiting the transcription of related genes (Figure 1.5) [72, 80-82].

IL-1 $\beta$  and tumor necrosis factor- $\alpha$  (TNF- $\alpha$ ) are the main regulatory molecules of inflammatory response, and their expression is regulated by NF- $\kappa$ B. They can trigger the activation and inflammatory response of immune cells and promote the chemotaxis and proliferation of immune cells [83, 84]. IL-8 is a chemokine that can attract the migration of inflammatory cells such as neutrophils, eosinophil, and monocyte. NF- $\kappa$ B plays an important role in the migration and inflammatory response of inflammatory cells by regulating the expression of IL-8 [85]. NF- $\kappa$ B can also binds to the promoter region of the Bcl-2 family (which includes a series of genes that promote and inhibit cell apoptosis), reducing the expression of intracellular inhibitory genes and increasing the likelihood of cell apoptosis [86]. In addition, the activation of NF- $\kappa$ B pathway can promote the expression of apoptosis-inducing factor (such as FasL and TRAIL) [87, 88]. These factors can bind to apoptosis related receptors on the cell membrane, further activating the apoptotic signaling pathway within the cell, leading to cell apoptosis.

In general, the NF- $\kappa$ B pathway plays a crucial role in the development, normal

function, and defense response of the intestinal immune system. Any abnormal regulation of this pathway may lead to the occurrence or development of immune diseases.

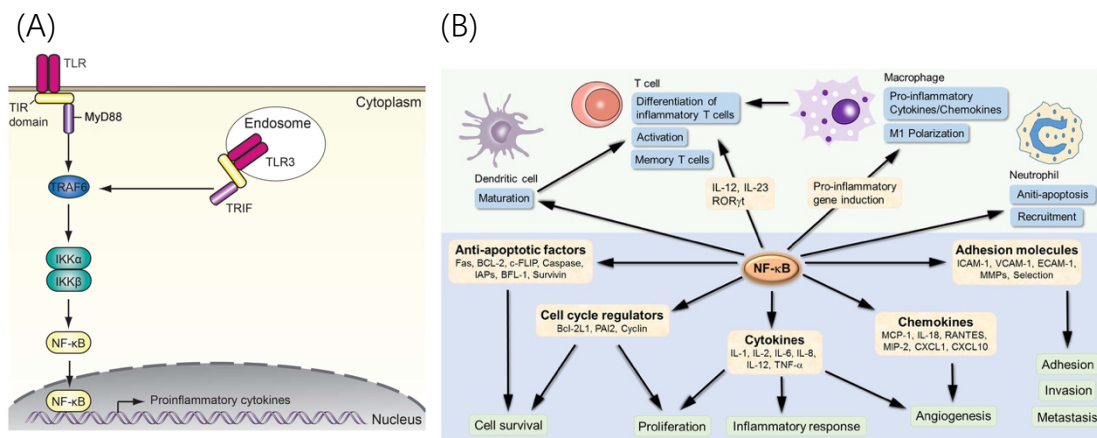


**Figure 1.5.** (A) Activation of NF-κB through TLRs signaling [79]. (B). NF-κB target genes involved in inflammation development and progression [72]

The signal pathway also includes: T-cell receptor (TCR) pathway: TCR is a receptor on T cells and can recognize antigens in the intestine [89]. After TCR activation, it triggers the activation and proliferation of T cells, participating in the intestinal immune response. IL-23 pathway: IL-23 is a cytokine that can promote the differentiation and functional enhancement of intestinal immune cells by activating specific receptors [90, 91]. The IL-23 pathway plays an important role in the pathogenesis of intestinal inflammatory diseases. Cell apoptosis pathway: In intestinal immunity, cell apoptosis is an important immune response mode. It includes apoptosis, necrosis, autophagy, etc., which can clear the source of infection and regulate inflammatory reactions [92]. These signaling pathways work

together to regulate the intensity and timing of the intestinal immune response, maintain intestinal immune balance, and protect the body from pathogen invasion and inflammatory damage.

Moreover, reports showed the Slp of lactobacilli has the ability to regulate immune related signaling pathways and immune cells, thereby achieving immune regulation. Via recognition of the TLR2 pathway, SlpA from *Lactobacillus helveticus* MIMLh5 triggers human macrophage pro-inflammatory factors TNF- $\alpha$  and COX-2 to stimulate the innate immune system [93]. Immune cells such as macrophages and lymphocytes play a crucial role in the immune response. The Slp can interact with immune cells, regulate the activity of cellular signaling pathways, alter cellular function, and thus affect the process of immune response [94].

The involvement of regulating immune related signaling pathways makes the Slp have potential application value in immune diseases and immune function regulation. However, further research and validation are needed to investigate the mechanism of Slp-mediated immune modulation.



## 1.5 Intestinal immune tissue and immune cells

The immune tissues involved in intestinal immunity include the intestinal epithelial barrier, Peyer's patches, gut-associated lymphoid tissue and isolated lymphoid follicles. Immune cells include intestinal epithelial cells, dendritic cells, macrophages, B cells, and T cells [95]. Have a fully understand of these tissues and cells can help us better resolve the operational mechanisms of the intestinal immune system:

**Intestinal epithelial barrier:** Intestinal epithelial cells are the outermost defense barrier in the intestine. They maintain interlock condition through tight junction protein and adhesion protein [96], which limits the passage of bacteria and other pathogenic microorganisms under normal conditions.

**Peyer's patches:** Peyer's patches are lymphoid tissues residing in the intestinal segment, mainly composed of T and B cells [95, 97]. T cells include CD4+ helper T cells, CD8+ cytotoxic T cell and regulatory T cells, which play a key role in immune response and immune regulation [98, 99]. B cells are responsible for producing and secreting antibodies to cope with pathogenic microorganisms in the intestine [100].

**Gut-associated lymphoid tissues (GALT):** GALT is the lymphoid tissue distributed throughout the entire intestinal wall. It includes the intestinal bulb gland, solitary lymph nodules, and lymphatic sinus of intestinal wall [101, 102]. GALT is the main distribution area of immune cells, including T cells, B cells, dendritic cells, etc. [103] They carry on immune responses through antigen presentation, antibody generation, and cytotoxic accumulation [104].

Isolated lymphoid follicles (ILF): ILF is a specific lymph node distributed under the intestinal mucosa, mainly consisting of T cells, B cells, and dendritic cells [105]. They play a role in monitoring bacteria and other pathogenic microorganisms in the intestine.

Intestinal immune cells have different immune defending mechanisms: B cells secrete immunoglobulin antibodies, especially IgA antibodies, which can neutralize bacteria and toxins in the intestine, thereby protecting the intestinal mucosa [106]; Intestinal epithelial cells present as regulators for partial immune responses, regulate immune responses by secreting immunosuppressive factors and pro-inflammatory cytokines [107]; T cells in the intestine can regulate immune responses, including CD4+helper T cells and regulatory T cells, to maintain immune balance [108]; Dendritic cells (DCs) are important antigen-presenting cells (APCs), which capture antigens in the intestine and present them to T cells to activate T cell immune response [109]; At the same time, inflammatory cells, such as neutrophils, eosinophil and macrophages, play a role in clearing pathogens and releasing inflammatory mediators in the intestinal inflammatory reaction [110].

Among them, APCs including dendritic cells, play an important role in intestinal immunity [111, 112]. DCs are a kind of specialized immune cells with highly differentiated dendritic morphology. They are the main APCs in intestinal mucosa. When the intestine is invaded by foreign antigens (such as bacteria, viruses, etc.), DCs first recognize and capture these antigens through specific surface receptors. After that, they internalize and decompose the antigen into small fragments through endocytosis. These small fragments will bind to major histocompatibility complex (MHC) molecules and transport to the cell surface

[113]. In this way, the antigen fragments are presented to the surrounding immune cells.

DCs mainly participate in intestinal immunity through two ways. Firstly, they can directly stimulate sensitized T cells [114, 115]. The antigen MHC complex on the surface of dendritic cells interacts with the T-cell receptor on the surface to activate T cells and trigger an immune response. This stimulation can cause the proliferation and differentiation of T cells, and then trigger cellular and humoral immunity immune responses. Secondly, DCs can indirectly participate in the immune response by present antigen fragments to immune B cells [116-118]. Through the interaction with B cells, DCs can promote the activation and differentiation of B cells and transform them into antibody secreting plasma cell. In addition, DCs are also involved in regulating the balance of intestinal immunity. They can recognize and decompose the food ingredients in the intestine and the metabolites produced by probiotics, to maintain the immune tolerance state of the intestine. At the same time, DCs can also recognize and eliminate abnormal cells and pathogenic microorganisms, protecting the intestine from infection.

Overall, including DCs, the intestinal immune cells and immune tissues forms the intestinal immune system, protecting the intestine from the invasion of pathogenic microorganisms and maintaining the immune balance of the intestine.

## 1.6 Objective of this research

Based on the existing reports, it can be confirmed that Slp is involved in the important bacteria-immune cell recognition process [119-122]. According to research, the surface protein SlpA of *Lactobacillus* can react with CD11c and SIGNR3, the two intestinal immune dendritic cell surface receptors [123, 124]. By binding to these receptors, intestinal immune dendritic cells will engulf lactobacilli into the cell through endocytosis to form endosomes [125]. In the endosomes, lactobacilli are digested and processed into small fragments, which are combined with antigen presenting molecules such as MHC-II molecules. In this way, the antigen fragments of lactobacilli can be presented through the surface of dendritic cells to other immune cells, such as helper T cells [27]. Then, by activating the helper T cells, releasing cytokines and signaling molecules, these components can further promote the activation and proliferation of other immune cells, such as B cells and cytotoxic T cells, thereby enhancing the immune response.

However, Slps from various *Lactobacillus* strains have different recognition receptors on distinct immune cells. These functional Slps and specific immune cells receptors remain unclear. Thus, the object of this study is to identify the Slps involved in the interaction between lactobacilli and immune cells and clarify the roles of Slps in the immunomodulation effects. Investigate the specific receptor of Slps on immune cells and understand the interaction signal pathway triggered by this Slp. Explore the structure of the target Slp, have a complete understanding of this component, and further help us to have a deeper cognition of the Slp generated lactobacilli and its immunomodulatory effect on the host.

# Chapter 2 Role of surface layer proteins in immunomodulatory effects of lactobacilli

## 2.1 Introduction

Although there are various components on the surface of LAB, including lipoteichoic acids, polysaccharides and surface layer proteins, that can react with host cells [126], Slps are considered as the key components to enhance the host-bacteria interactions and accelerate the host intestinal immune responses [127]. Since Masuda [128] first isolated Slps from *L. brevis* with high concentration of urea in 1979, most Slps can be released from the cells by washing with chaotropic reagents [129]. Guanidinium chloride and lithium chloride (LiCl) are often used as the common reagents to release Slps [130, 131]. SlpA released with LiCl from *L. acidophilus* has been reported that can enhance the cell interaction with DC-SIGN receptors on the surface of differentiated DC cells and help immunoregulation effect [123, 124].

In previous laboratory studies, different types of surface proteins released with 5M LiCl have been detected in various LAB strains. However, other types of Slps from the tested strains and the role in the immunomodulatory effect remain unknown. So, in this chapter, I tried to compare the Slps and understand the importance of the major Slps in the immunomodulation effect. The major Slp observed in the specific *Lactobacillus* strains was identified. Then, host cell responses after stimulation via the isolated Slp were predicted by RNA-seq analysis.

## 2.2 Materials and Methods

### 2.2.1 Bacteria and the cultivation

All lactic acid bacterial strains were obtained from the Japan Collection of Microorganisms (JCM). LAB strains were cultured in Man Rogosa Sharpe (MRS, Becton, Dickinson and Company, Sparks, MD, USA) medium at 30 °C or 37 °C for 20 h, as described in Table 2.1.

**Table 2.1.** LAB strains obtained from the Japan Collection of Microorganisms (JCM), origin and culture conditions in MRS medium. showed.

Strain	Temperature (°C)	Origin
<i>Levilactobacillus brevis</i> JCM 1059	30	Human feces
<i>Lactiplantibacillus plantarum</i> subsp. <i>plantarum</i> JCM 1149	30	Pickled cabbage
<i>Lactococcus lactis</i> subsp. <i>lactis</i> IL1403	30	Cheese
<i>Lactobacillus amylovorus</i> JCM 1126	37	Cattle waste
<i>Lactobacillus helveticus</i> JCM 1120	37	Cheese
<i>Lactobacillus acidophilus</i> JCM 1132	37	Human feces

### 2.2.2 Differentiation of monocytic THP-1 to dendritic cells (THP-1 DCs)

Roswell Park Memorial Institute 1640 (RPMI 1640) supplemented with 10% fetal bovine serum (FBS), 100 U/mL penicillin, and 100 g/mL streptomycin was used to culture human-origin THP-1 monocyte cells obtained from RIKEN Cell Bank (JRFB0112) at 37 °C in a 5% CO<sub>2</sub> humidified incubator. To stimulate the growth of THP-1 DCs, THP-1 cells were seeded in 24-well culture plates ( $5 \times 10^5$  cells/mL) and treated for 2 days with 50 nM phorbol 2-myristate 13-acetate (PMA, Adipogen Life Science, Liestal, Switzerland) and 2 days with 20 ng/mL IL-4 (Peprotech, Cranbury, NJ, USA).

The cell surface expression of DC-SIGN was evaluated by flow cytometry (EC800, SONY) with the addition of anti-DC-SIGN (Novus Biologicals USA, CO, USA) to verify the differentiation of THP-1 cells into DCs. The cells were treated with 4% paraformaldehyde (PFA) for 10 minutes before being harvested. Following the addition of 1 mM ethylenediaminetetraacetic acid (EDTA)-phosphate-buffered saline (PBS), the cells in each well were detached and transferred to a 1.5 mL plastic microtube. DC-SIGN expression was then examined by flow cytometry at 490/525 nm after the cells had been washed three times with PBS. The cells were treated with anti-DC-SIGN at a concentration of 5 ng/mL before being incubated at room temperature for 1 h. Anti-IgG-Alexa 488 (50 ng/mL, Thermo Fisher Scientific Company) was added to the cells after PBS wash and then incubated at 25 °C for 1 h.

### **2.2.3 Strain Sulfo-Cyanine3 Labelling**

According to the manufacturer's instructions, a sulfo-cyanine3 (Cy3) Mono-reactive dye labelling kit (GE Healthcare Bio-Sciences KK, Tokyo, Japan) was used to label all tested LAB strains. In brief, LAB strains were cultured in 50 mL MRS medium at 30 °C or 37 °C for 20 h, harvested by centrifugation at 6,000 ×*g* for 10 min, and then washed twice with PBS. The amount of 1×10<sup>10</sup> washed bacteria cells were suspended in 500 μL of 1 M NaHCO<sub>3</sub> (pH 9.3) and combined with the 1 mg Cy3-containing reagent at 25 °C for 2 h in dark. The cells were then centrifugation at 6,000 ×*g* for 10 min after being washed twice with PBS to remove the supernatant that contained unlabeled Cy3. The Cy3 labelled LAB strains were used for the further THP-1 DCs uptake study.

#### **2.2.4 Isolation and identification of surface layer proteins from LAB**

*L. brevis* JCM 1059 was cultured in MRS medium at 30 °C for 20 h as described above, after PBS wash, the bacterial cells were suspended in 1M LiCl solution for 40 min to remove the surface layer proteins. Then target surface layer proteins from JCM 1059 were collected in 40 min treated with 5M LiCl and dialyzed against 300 times volume of 20 mM phosphate buffer (pH 6.8) in 4 °C for 24 h. The isolated 5M LiCl Slps were analysed using sodium dodecyl sulphate-12.5% polyacrylamide gel electrophoresis (SDS-12.5%PAGE). To predict the major proteins observed in SDS-PAGE. Before the proteome analysis, de-staining the gel by incubated with 30% acetonitrile and 50 mM NH<sub>4</sub>HCO<sub>3</sub> for 30min. Then, de-hydration the gel by 60% acetonitrile and 20 mM NH<sub>4</sub>HCO<sub>3</sub>. 1%(w/w) trypsin (Promega Japan, Tokyo, Japan) was added into the dried gel to digest the protein into peptides at 37 °C for 24h. The gel-released peptides were subsequently exposed to mass spectrometric analysis using an UltrafleXtreme TOF/TOF MS (Bruker Daltonics GmbH, Bremen, Germany) operating in positive reflection ion mode between m/z 0 and 5000 Da. The Zip Tip with 0.6 µL C<sub>18</sub> resin (Merck Millipore, Cork, Ireland) pipette tips were used for concentrating and desalting the peptides following by the manufacturer's protocol before the TOF MS analysis.

#### **2.2.5 Fluorescent observation *L. brevis* JCM 1059 SlpB on *L. plantarum* JCM 1149**

*L. plantarum* JCM 1149 cells collected after cultivation in MRS medium were treated with 5M LiCl to remove the Slps from bacterial cell surface and washed with PBS twice. Then, 1 mg fluorescein isothiocyanate (FITC) from ICN Biomedicals (Costa Mesa, CA, USA) was incubated with  $1 \times 10^{10}$  JCM 1149 cells at 30°C for 1 h.



Then incubated with <sup>Cy3</sup>SlpB at 30°C for 2 h. The coating condition was observed under ZOE Fluorescent Cell Imager (Bio-Rad, CA, USA).

### **2.2.6 SlpB coating capacity on LAB strains**

Prepare the Cy3 labelled SlpB from 0 to 15 µg and co-culture with 10 µl *L. plantarum* JCM 1149 ( $5.4 \times 10^9$ /mL) at 30 °C for 1h. After remove the supernatant by centrifugation at 6,000 xg, 10min, suspended with 100 µl PBS and triplicate seeded into 96-wells microplate. Read the florescence with a plate reader (Thermo Fisher Scientific, Varioskan LUX SkanIt Software 4.0) to create a coating curve. Repeat the coating test to other LAB strains include *L. brevis* JCM 1059, *L. acidophilus* JCM 1132, *L. helveticus* JCM 1120, *L. amylovorus* JCM 1126, *L. plantarum* JCM 1149 and *L. lactis* IL 1403 with the same bacteria number of  $1 \times 10^8$  to 10 µg <sup>Cy3</sup>SlpB.

### **2.2.7 Uptake of <sup>Cy3</sup>SlpB coated LAB by THP-1 DCs**

THP-1 DCs at a concentration of  $5 \times 10^5$  cells/mL were differentiated from THP-1 cells as described above. Co-cultured with Cy3 labelled LAB strains (MOI = 50) or 5M LiCl treated strains (MOI = 50, with or without <sup>Cy3</sup>SlpB coating) for 2 h in 24-well culture plates with 1mL/well RPMI 1640 medium. After cultivation, THP-1 DCs were washed thrice with PBS and harvested by adding 10 mM EDTA containing cold PBS. Uptake of LAB strains with different treatment were measured using a SONY EC800 flow cytometry analyzer (Sony Biotechnology, IL, USA). Flow cytometric analyses were performed at 550/570 nm.

### 2.2.8 Cytokines Measurement

THP-1 DCs were cultured as described above. *Lactobacillus* strains with or without SlpB coating were incubated with THP-1 DCs ( $5 \times 10^5$  cells/mL, MOI = 50) at 37 °C for 24 h. After incubation, the culture supernatant was collected and centrifugated at  $6,000 \times g$  for 5 min to precipitate the suspended lactobacilli cells. A plate reader (Thermo Fisher Scientific, Varioskan LUX SkanIt Software 4.0) and ELISA kits from BioLegend Inc. (San Diego, CA, USA), and R&D Systems (Minneapolis, MN, USA), respectively, were utilized to quantify IL-6, IL-10, and IL-12p40 (IL-12) in the supernatant. The measurements were performed in triplicates.

### 2.2.9 RNA sequencing and data analysis

THP-1 DCs were stimulated as described above. 5M LiCl treated *L. brevis* JCM 1059 with or without SlpB coating were incubated with THP-1 DCs (MOI = 50) at 37 °C for 24 h. after co-culture, remove the supernatant and harvest the THP-1 DCs with cold PBS. Total RNA from THP-1 DCs was extracted by using RNeasy Mini Kit (QIAGEN, Hilden, Germany). RNA sequence was analysed at the Bioengineering Lab (Kanagawa, Japan).

### 2.2.10 *in vivo* uptake assay of SlpB coated *L. plantarum* JCM 1149

BALB/c mice (male, 12 weeks of age, n=3) were obtained from Charles River Laboratory, Japan. 5M LiCl treated <sup>Cy3</sup>*L. plantarum* JCM 1149 with or without SlpB coating ( $2.5 \times 10^8$ /mouse) were oral administrated to mice for 1 h. Euthanize the mice and excise the Peyer's patches contain intestinal parts. The collected intestines were fixed by 4% formaldehyde after PBS wash. Before the histological

operation, dehydrate the tissue by 2h 15% sucrose-PBS soaking and 30% sucrose-PBS soaking overnight at 4°C, then cladding the tissue with Optimal Cutting Temperature Compound (OCT compound, Sakura Fine Tech Japan, Tokyo, Japan) and snap freeze under -80°C. After the preparation, perform the serial sagittal plane sections by using a cryostat to collect a 5 µm thickness tissue section. The section was observed and the number of bacteria on the area of Peyer's patches was counted under ZOE Fluorescent Cell Imager (Bio-Rad, CA, USA). Antigen-presenting cells on Peyer's patches are stained with mouse CD23 antibody (Novus Biologicals, Centennial, CO, USA) against FITC-rabbit IgG (Sigma-Aldrich Japan, Tokyo, Japan). Animal experiments were approved by the Animal Experiment Committees at Tokyo Institute of Technology and carried out in accordance with the guidelines.

#### **2.2.11. Statistical Analysis**

Statistical significance was analysed using GraphPad Prism software version 9.1. Each data point represents the mean of triplicated test samples and SD. Statistically significant differences were set at  $p < 0.05$  by using one-way analysis of variance (ANOVA) followed by Duncan's test.

## 2.3 Results

### 2.3.1. Induction of DC-SIGN on THP-1 cells

According to a previous investigation, SlpA binding is required for the basal level expression of DC-SIGN on THP-1 DCs [132, 133]. In this study, THP-1 cells were treated with PMA and IL-4 in accordance with a previous report. [132]. While PMA (for 2 d) followed by IL-4 (for 2 d), the structure of THP-1 cells resembled that of dendritic-like cells (Figure 2.1 A). applying the anti-DC-SIGN antibody, the expression of DC-SIGN on THP-1 DCs was quantified as one of the differentiation markers by flow cytometry (Figure 2.1 B). Results revealed that providing PMA or PMA coupled with IL-4 for 1 day was ineffective in promoting DC-SIGN expression (induced less than 2%) (Figure 2.1 C). However, treatment with PMA for 2 d, PMA for 1 d and IL-4 for 1 d, or PMA along with IL-4 for 2 d resulted in enhanced DC-SIGN expression on THP-1 cell surface (8.5, 9.2, and 10.3%, respectively), despite the effect of extra IL-4 on DC-SIGN induction remained uncertain (Figure 2.1 C). The most significant levels of DC-SIGN have been detected on the cell surfaces of THP-1 DCs treated for 2 d with PMA, then for 2 d with IL-4 (23.3%) (Figure 2.1 C).

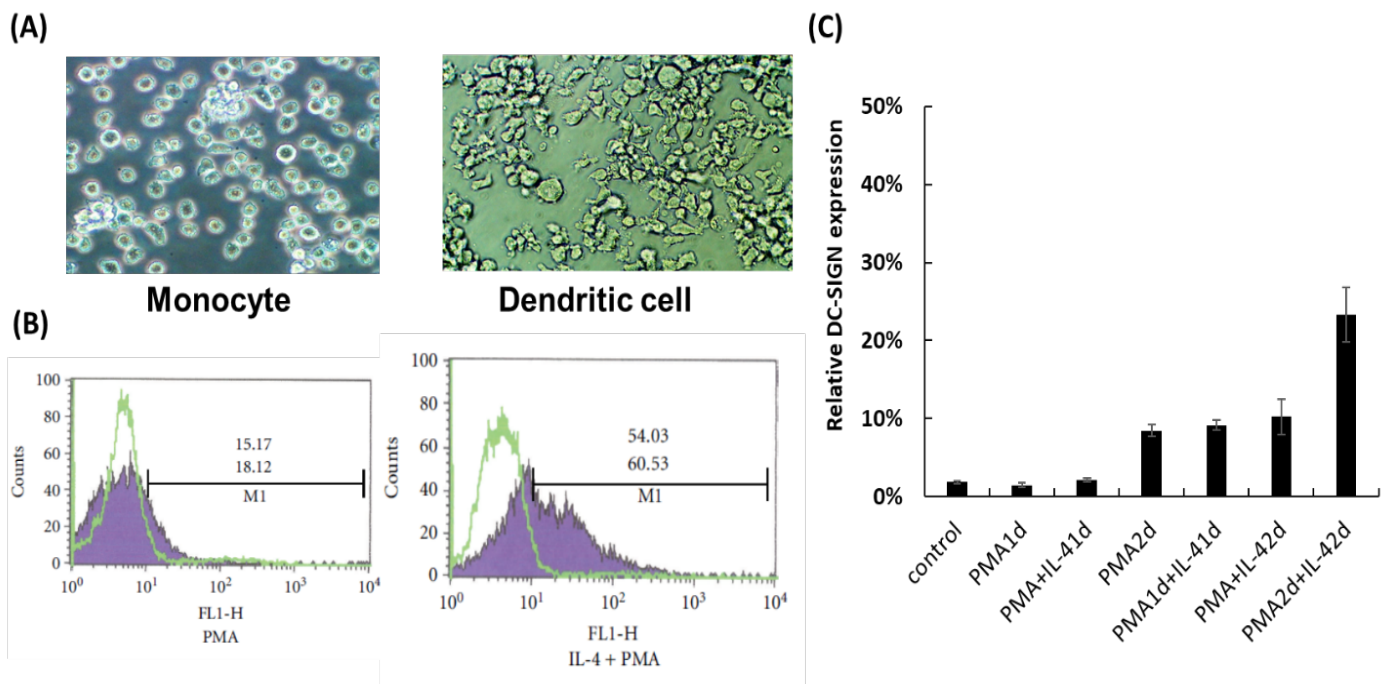


**Figure 2. 1.** (A) Phorbol 2-myristate 13-acetate (PMA) and interleukin-4 (IL-4) treatment induces differentiation of monocytic THP-1 cells into dendritic-like THP-1 cells (THP-1 DCs). (B) Expression of DC-specific ICAM-3-grabbing nonintegrin (DC-SIGN) on the surface of THP-1 DC against anti-DC-SIGN antibody was evaluated by flow cytometer. (C) Measurement of DC-SIGN expressed on THP-1 cells treated with PMA and IL-4.

### 2.3.2. Uptake of LAB by THP-1 DC and IL-12 induction

Slps from 12 different LAB strains have been examined and released by 5M LiCl (Figure 2.2). SlpA from lanes 8 and 9 have been confirmed in the SDS-10%PAGE results. On particular LAB strains, SlpA is the protein that interacts with the DC-SIGN on THP-1 DCs and plays an important role in the subsequent immune response. Nevertheless, little has been discovered of other LAB cell surface proteins have the potential to interact THP-1 DCs.

Flow cytometry was applied to examine the uptake of <sup>Cy3</sup>SlpA-labelled LAB strains into THP-1 DCs. The results revealed notable differences in the uptake ratio of the 12 examined LAB strains (Figure 2.3). *L. helveticus* JCM 1120, *L. delbrueckii* subsp. *bulgaricus* JCM 1002, *L. kefir* JCM 5818, *L. acidophilus* JCM 1132, *L. plantarum* JCM 1100, and *L. brevis* JCM 1059 all had significantly higher uptake ratio than *L. paracasei* subsp. *paracasei* JCM 8130. Following it, Slps produced from the LAB strains with the chaotropic reagent 5 M LiCl treatment were coupled with FITC-OVA conjugated microbeads and the impact of Slps in microbead uptake by THP-1 DC was assessed. The uptake ratio of microbeads combined with Slps from varied LAB strains differed among those analyzed strains. Microbeads-coupled with the Slps from *L. helveticus* JCM 1120, *L. acidophilus* JCM 1132, *L. brevis* JCM 1059, *L. plantarum* JCM 1100, and *L. kefir* JCM 5818 showed higher uptake ratio than other Slps coupled microbeads (Figure 2.3). Result shows these Slps have the ability to function as binding components for THP-1 DCs.

Furthermore, after treating THP-1 DCs with 6 different LAB strains, we detected IL-12 production in order to clarify how LAB intake influences cytokine production. Of the examined lactobacilli, three strains, *L. helveticus* JCM 1120, *L.*

*acidophilus* JCM 1132, and *L. brevis* JCM 1059 had higher intake ratios than others and produced more IL-12, and two *L. lactis* subspecies with lower uptake ability showed lower IL-12 production. As a result, the enhanced uptake of LAB strains into THP-1 DCs by Slps may be crucial for the activation of IL-12 production in THP-1 DCs. Bacterial cells collected at various growth stages did not produce significantly different levels of cytokines (Data not shown).

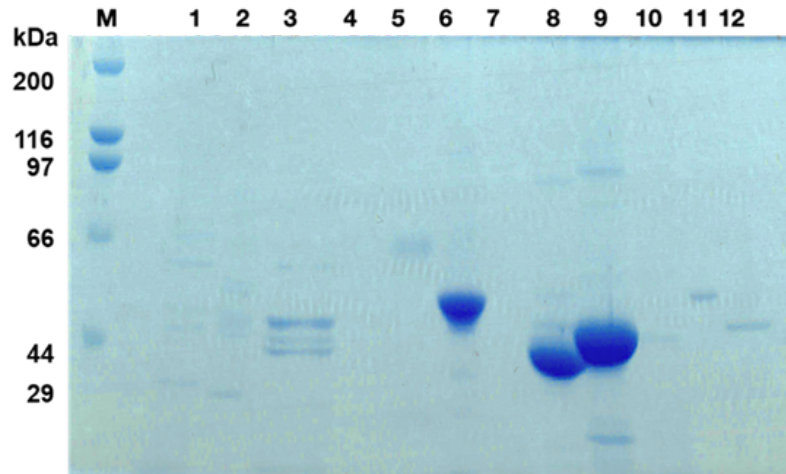


**Figure 2.2** SDS-10%PAGE analysis of 5 M LiCl released proteins. Lane 1: *L. plantarum* subsp. *plantarum* JCM 1149, lane 2: *L. lactis* subsp. *cremoris* NZ 9000, lane 3: *L. amylovorus* JCM 1126, lane 4: *L. paracasei* subsp. *paracasei* JCM 8130, lane 5: *L. kefir* JCM 5818, lane 6: *L. brevis* JCM 1059, lane 7: *L. plantarum* JCM 1100, lane 8: *L. helveticus* JCM 1120, lane 9: *L. acidophilus* JCM 1132, lane 10: *L. plantarum* TIN- KL 001, lane 11: *L. lactis* subsp. *lactis* IL1403, lane 12: *L. rhamnosus* JCM 1136 and lane M: Marker proteins.

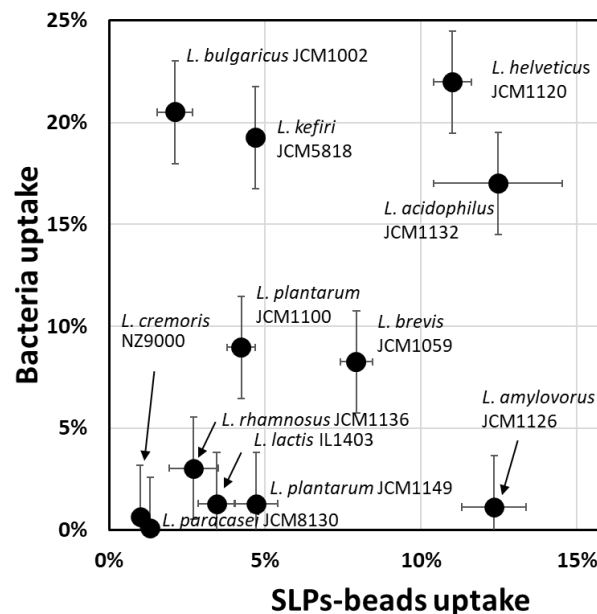


**Figure 2.3** Uptakes of Cy3 labelled surface layer protein A ( $^{Cy3}$ SlpA) lactic acid bacteria (LAB) and Sips-coupled microbeads by THP-1 DCs.



### 2.3.3 Key Slps on *L. brevis* JCM 1059 and role in the uptake

Under the same culture condition and the number of bacteria strains, *L. plantarum* JCM 1149, *L. acidophilus* JCM 1132 and *L. brevis* JCM 1059 showed different uptake ratios into THP-1 DCs (Figure 2.4 A). Among the 3 strains, JCM 1059 showed the most significant uptake ratio into THP-1 DCs compared with SlpA containing JCM 1132 and non-Slps containing JCM 1149. However, after removing the Slps from *L. brevis* JCM 1059 by 5M LiCl treatment, the uptake ratio significantly reduced compared with the complete strain (Figure 2.4 B). The results suggest that the Slps on *L. brevis* JCM 1059 is the main component that affects the uptake process into the immune THP-1 DCs of *L. brevis* JCM 1059.

To identify the target proteins on *L. brevis* JCM 1059, the SDS-12%PAGE showed with 1M LiCl pre-treatment removes the surface layer-associated proteins, 5M LiCl could release only one major protein (Figure 2.5 A). Directly cut and digested the protein from the gel, and performed the proteome analysis, depended on the analysis from the MASCOT database, this 5M LiCl released surface layer protein from *L. brevis* JCM 1059 has been confirmed as *L. brevis* SlpB (Figure 2.5 C). With the sequence comparison, SlpB only shows a 19.5% overlap protein sequence with SlpA (Figure 2.5 D).

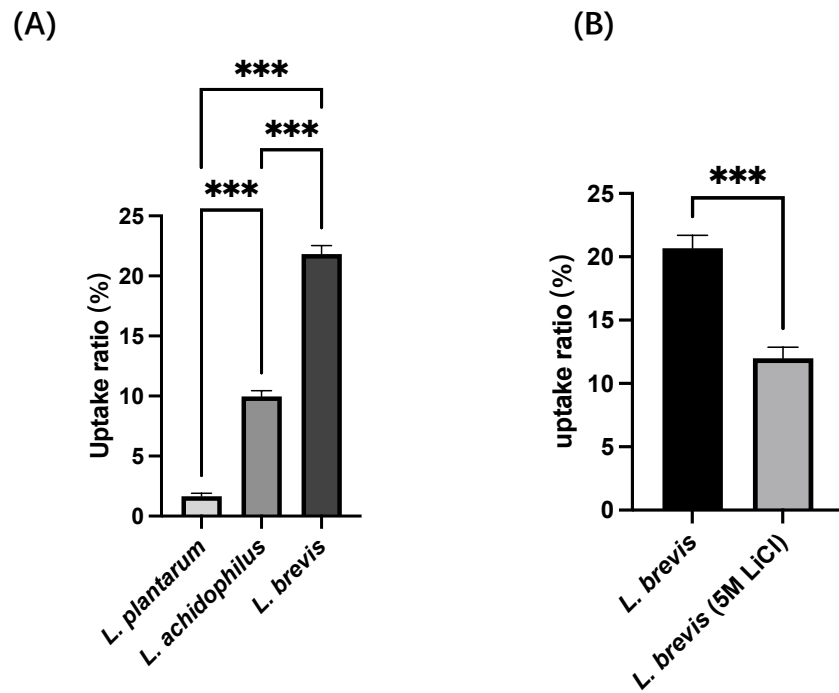
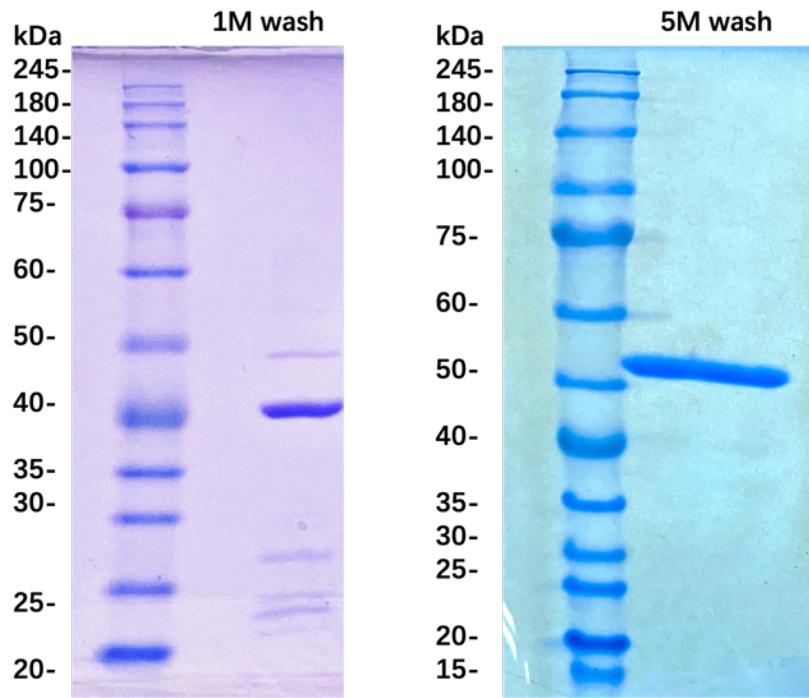
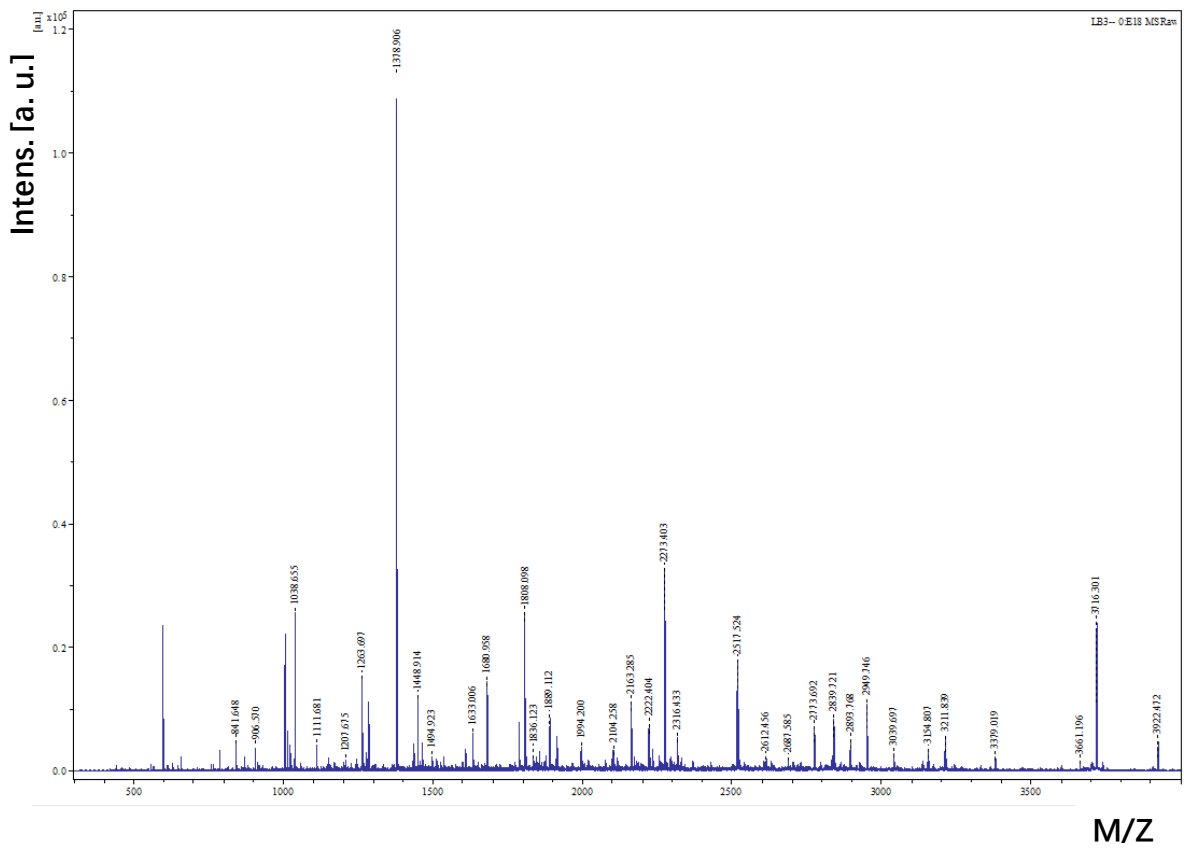


**Figure 2.4.** (A) Uptake ratio of <sup>Cy3</sup>*L. plantarum* JCM 1149, <sup>Cy3</sup>*L. acidophilus* JCM 1132 and <sup>Cy3</sup>*L. brevis* JCM 1059 into THP-1 DCs. (B) Uptake ratio of <sup>Cy3</sup>*L. brevis* JCM 1059 and 5M LiCl treated <sup>Cy3</sup>*L. brevis* JCM 1059 into THP-1 DCs. (Means ± SD, \*\*\*  $p < 0.001$ ).

(A)



(B)



(C)

 **MASCOT Search Results**

**Protein View: Q8GFE5**

**Surface layer protein SlpB OS=Lactobacillus brevis OX=1580 GN=slpB PE=4 SV=1**

**Database:** uniprot-lactobacillus-brevis  
**Score:** 129  
**Expect:** 1.9e-009  
**Monoisotopic mass (M<sub>r</sub>):** 50894  
**Calculated pI:** 9.54

Sequence similarity is available as [an NCBI BLAST search of Q8GFE5 against nr.](#)

**Search parameters**

**Enzyme:** Trypsin: cuts C-term side of KR unless next residue is P.  
**Mass values searched:** 88  
**Mass values matched:** 16

**Protein sequence coverage: 51%**

Matched peptides shown in **bold red**.

```
1  MQSSLKKSLY  LGLAALSFAS  VAVVSTTASA  KSAAKVTSDK  VLTTDATKRN
51 VNLTCGTNAIY  SKPCITVKGAK  VVATTTTAKN  LNKSTTSREN  FRAYRVAKTN
101 RGSIIYKVVVS  YNKAYRGWVY  G GKSDTAFAG  GLTSYDTFKE  GTLTADQKSG
151 NYKLANPGKT  EAGLTYKQPA  WTQYKIGKTI  ADTTAYKDAT  FSVDKVGTRT
201 REGDTWVHVV  NQNTADTKAD  GWILLSNLTQ  TNAFNEASQV  KVNINNLKGE
251 TLKSFNYNVG  TTATNTNAAD  NTVYDSTATP  TKFADGFAAT  VKNALAGTGY
301 TVDGTNALNR  VANLKSGSTL  TIYATEGTQK  PSTVSVFAQY  PDTPSINQVK
351 VATADQTKDG  VADAATAQNL  INQPAATTLF  TGVEGKSFTA  TEALAYLNGN
401 ASMKKLTSPS  WTETSGSTSV  TYQWVLTSPQ  AFAGQYGSPF  SAIYTAKKTV
451 VPATGSNDNN  TDNPIANGVV  SSTPTANPTD  TTK
```

(D)

19.5% identity in 456 residues overlap; Score: 171.0; Gap frequency: 6.6%

```
SlpA      10 AAAAALLAVAPVAASAVSTVSAATTINASSSAIN-TNTNAKYDVDVTPSVSAVAANTA--
SlpB      19 ASVAAVSTTASAKSAAKVTSDKVLTTDATKRVNVLGTNAIYSKPGTVKGAKVVATTTTA
          *  **   *   *   *   *   *   *   *   *   *   *   *   *   *
SlpA      67 ---NNTPAIAGNLTGTISASYN-GKTYTANLKADTENATITAAGSTTAVKPAELAAGVAY
SlpB      79 KNLNKSTTSRENFRAIRVAKTNRGSIYYKVVSYNKAYRGWVYGGKSDTAFAGGLTSYDTF
          *   *   *   *   *   *   *   *   *   *
SlpA     123 ---TVTVNDVSNFNGSENAGKT---VTLGSANSNVKFTGTNSDNQTETNVSTLKVKLDQN
SlpB     139 KEGTLTADQKSGNYKLANPGKTEAGLTYKQPAWTQYKIGKTIADTTAYKDATFSV---DKV
          *  *   *  *   *  **   *   *   *   *   *   *   *
SlpA     177 GVASLTNVSIAINVYAINTTDSNVNFYDVTSGATVTNGAVSVNADNQGQVNVANVVA-AI
SlpB     197 GTRTREGDTWVHVVNQNTAD-TKADGWILLSNLTQTN---AFNEASQVKVINNLKGETL
          *   *   **  *   *   *   *   *   *   *   *   *
SlpA     236 NSKYFAAQYADKKNLNRTRTANTEDAIIKAALKDQKIDVNSVGYFKAPHTFTVNVKATSN--T
SlpB     253 KSFNYNVGTTATNTNAADNTVYDSTATPTKFADGFAATVKNALAGTGYTVDGTNALNRVA
          *   *   *   *   *   *   *   *   **   *
SlpA     294 NGKSATLPVVVTPVNAEPTVASVSKRI-----MHNAYYYDKDAKRVGT-DSVKRYNSVS
SlpB     313 NLKSGSTLTIYATEGTQKPSTVSVFAQYPDTPSINQKVATADQTKDGVADAATAQNLI
          *  **   *   **   *   *   *   *   *
SlpA     348 VLPNTTTINGKTYQVVENKAVDKYINAANIDGTRTLKHNAYVYASSKKRA-NKVVLK
SlpB     373 QPAATTLFTGVEGKSFTATEALAYLNGNASMKKLTSPSWTETSGSTSVTYQWVLTSPQAF
          **  *   *   **   *
SlpA     407 KGEVVTTYGASYTFKNGQKYYKIGDNTDKTYVKVAN
SlpB     433 AGQYGSPFSAIYTAKK-TVVPATGSNDNNTDNPIAN
          *   *  **  *   *   *   *   **
```

**Figure 2.5.** (A) SDS-12%PAGE analysis of 1M and 5M LiCl released proteins from *L. brevis* JCM 1059. (B) TOF/MS analysis of the 5M LiCl released proteins from *L. brevis* JCM 1059 with the trypsin treatment. (C) MASCOT database analysis of trypsin digested peptide fragment from the 50 kDa protein in SlpB sequence of *L. brevis* (52kDa). (D) 19.5% of the amino acid sequence overlapped between SlpA and SlpB. (SlpA original from *Lactobacillus acidophilus*, SlpB original from *Levilactobacillus brevis*. Data from <https://www.uniprot.org> )

### 2.3.4 SlpB coating ability on different LAB strains

Under the fluorescence image telescope observation, it is very clear to observe that the SlpB coating on the surface of FITC labelled JCM 1059. Especially, the merge picture suggests the wrapping of <sup>Cy3</sup>SlpB (red) around the green fluorescence (<sup>FITC</sup>*L. plantarum*), which preliminarily indicates the surface coating effect of SlpB (Figure 2.6 A). Then, the binding curve of SlpB to *L. plantarum* JCM 1059 showed a saturated binding of SlpB. With the different amounts of <sup>Cy3</sup>SlpB from 0 µg to 12 µg, the fluorescence intensity tended to saturate after 4.78 µg of <sup>Cy3</sup>SlpB coating on  $5.4 \times 10^7$  *L. plantarum* JCM 1059 (Figure 2.6 B). In another way to say, 1 µg of <sup>Cy3</sup>SlpB has the coating ability on the number of  $1.13 \times 10^7$  *L. plantarum* JCM 1059 and further increasing the amount of <sup>Cy3</sup>SlpB will not significantly increase the coating intensity.

To confirm the coating ability of SlpB on other LAB strains, add 10 µg of <sup>Cy3</sup>SlpB with  $1 \times 10^8$  of LAB strains including *L. brevis* JCM 1059, *L. helveticus* JCM 1120, *L. acidophilus* JCM 1132, *L. lactis* IL 1403, *L. amylovorus* JCM 1126 and *L. plantarum* JCM 1149 pre-treated with 5M LiCl. The results showed all tested LAB strains increased the fluorescence intensity after coating of <sup>Cy3</sup>SlpB significantly (Figure 2.7). The results confirmed at this coating recipe, SlpB can successfully cover all test LAB strains. Indicates SlpB could adhere to different bacterial surfaces, providing a stable and feasible attachment relationship for subsequent functional testing experiments.

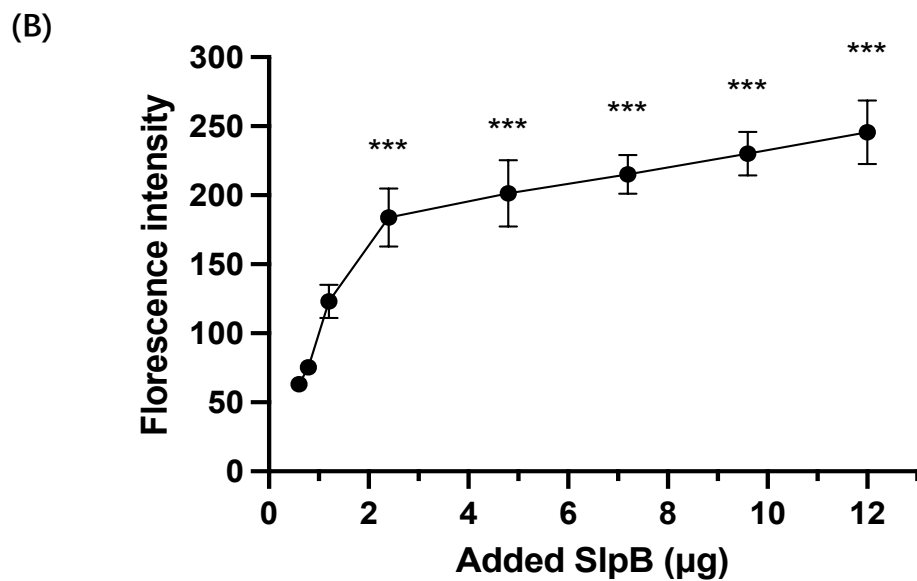
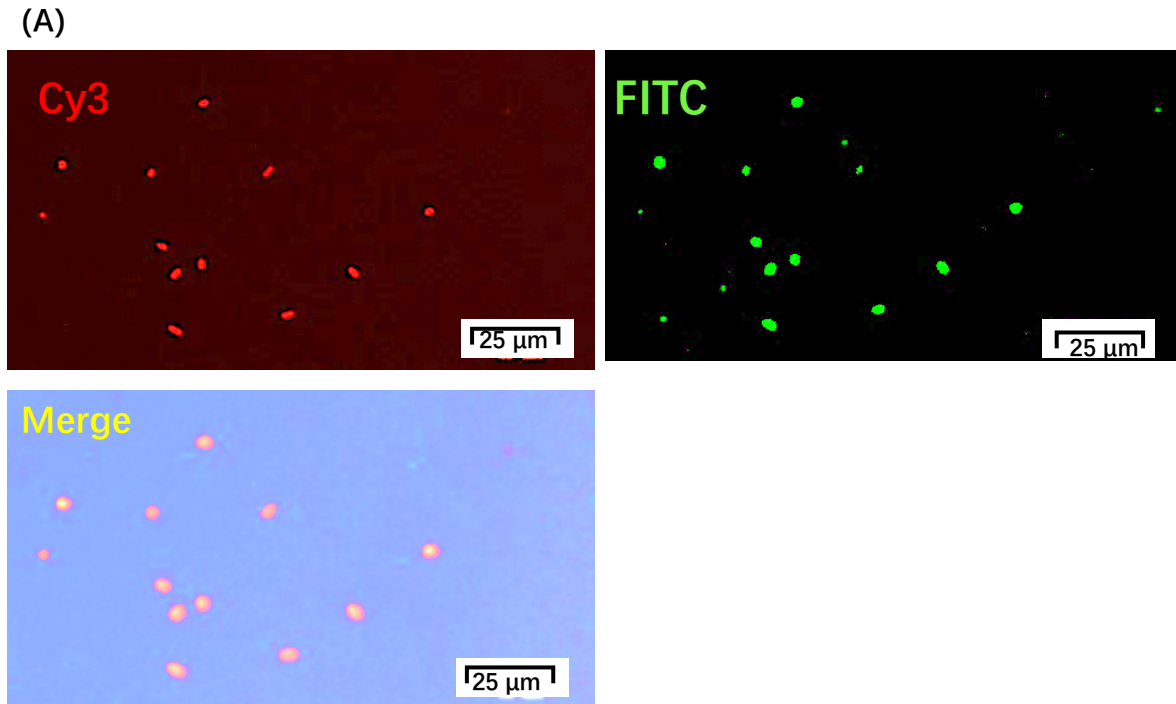


**Figure 2.6.** (A) <sup>Cy3</sup>SlpB coating *L. plantarum* JCM 1059 (red), <sup>FITC</sup>*L. plantarum* JCM 1059 (Green) and the merge image of <sup>Cy3</sup>SlpB coating with <sup>FITC</sup>*L. plantarum* JCM 1059 observed under fluorescence microscope. The scale bars are 25 μm. (B) the coating curve of different amount <sup>Cy3</sup>SlpB with *L. plantarum* JCM 1059. (Means ± SD, \*\*\*  $p < 0.001$ ; each point represents triplicated)

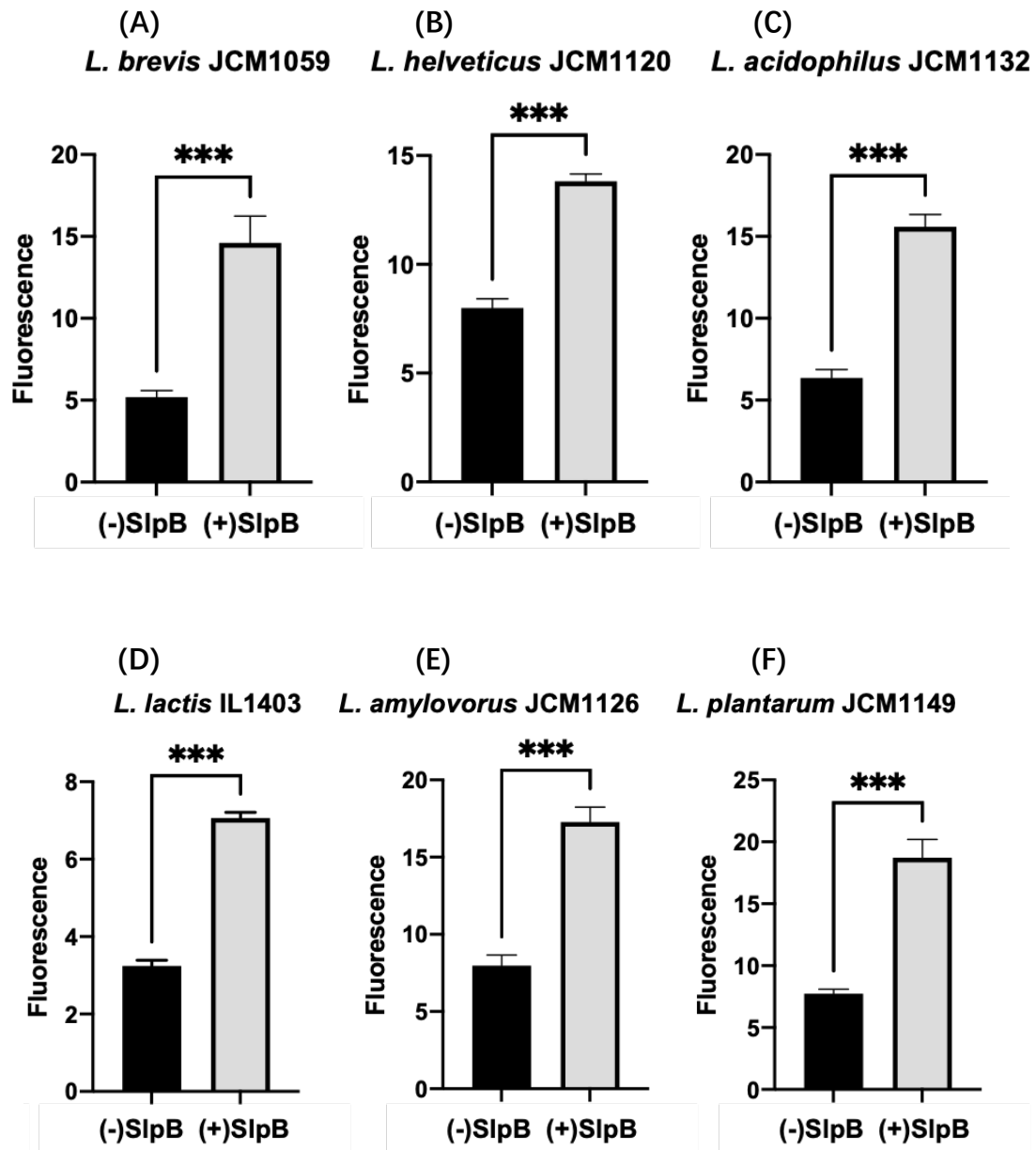


**Figure 2.7.** (A) fluorescence intensity of *L. brevis* JCM 1059 (B) *L. helveticus* JCM 1120 (C) *L. acidophilus* JCM 1132 (D) *L. lactis* IL1403 (E) *L. amylovorus* JCM 1126 (F) *L. plantarum* JCM 1149 with or without <sup>Cy3</sup>SlpB coating. (Means  $\pm$  SD, \*\*\*  $p < 0.001$ )



### 2.3.5 SlpB coating LAB strains increased the uptake ratio into THP-1 DCs.

After confirming the SlpB coating on other LAB strains, 4 *Lactobacillus* strains including *L. brevis* JCM 1059, *L. plantarum* JCM 1149, *L. amylovorus* JCM 1126 and *L. lactis* IL1403 were selected to evaluate the bacterial uptake by THP-1 DCs with or without SlpB coating. Except for *L. brevis* JCM 1059, other strains showed low THP-1 DCs uptake rates in the previous experiment without any additional treatment. However, after the coating with SlpB, all tested strains increased uptakes into THP-1 DCs (Figure 2.8). Especially *L. plantarum* JCM 1149 showed a significant increase in the uptake (Figure 2.8 B) compared with *L. amylovorus* JCM 1126 and *L. lactis* IL1403.

With the increased THP-1 DCs uptake, immune responses expected in THP-1 DCs after co-cultivations with *L. brevis* JCM 1059 and *L. plantarum* JCM 1149 were evaluated. IL-12, IL-10 and IL-6 productions in THP-1 DCs culture supernatant were evaluated by ELISA kit. Although IL-10 and IL-6 were increased on both tested strains (Figure 2.9, Figure 2.10), IL-12 showed a most significant increase on *L. plantarum* JCM 1149 after coating of SlpB (Figure 2.10 A). These results suggest that SlpB not only can help the uptake of bacterial cells into THP-1 DC, but also enhance the cytokine productions in THP-1 DCs especially IL-12 production of JCM 1149.

Cytokine production results of *L. brevis* JCM 1059 and *L. plantarum* JCM 1149 showed the most significant increase in IL-12 production by *L. plantarum* JCM 1149 and IL-10 by *L. brevis* JCM 1059. So, to compare the production of IL-12 in THP-1 DC after co-incubation of bacterial cells with or without SlpB, *L. amylovorus* JCM 1126 and *L. lactis* IL1403 were added in this analysis. *L. amylovorus* JCM 1126

and *L. lactis* IL1403 also showed an increase of bacterial cell uptakes into THP-1 DCs (Figure 2.11).

In summary, the tested 4 kinds of LAB strains showed increased uptakes into THP-1 DCs by coating with SlpB. Of interest, increased cytokine productions in THP-1 DCs after treatment of these SlpB-coated LAB were slightly different. Among the tested strains, *L. plantarum* JCM 1149 showed a significant increase in IL-12 production after coating with SlpB (Figure 2.12).

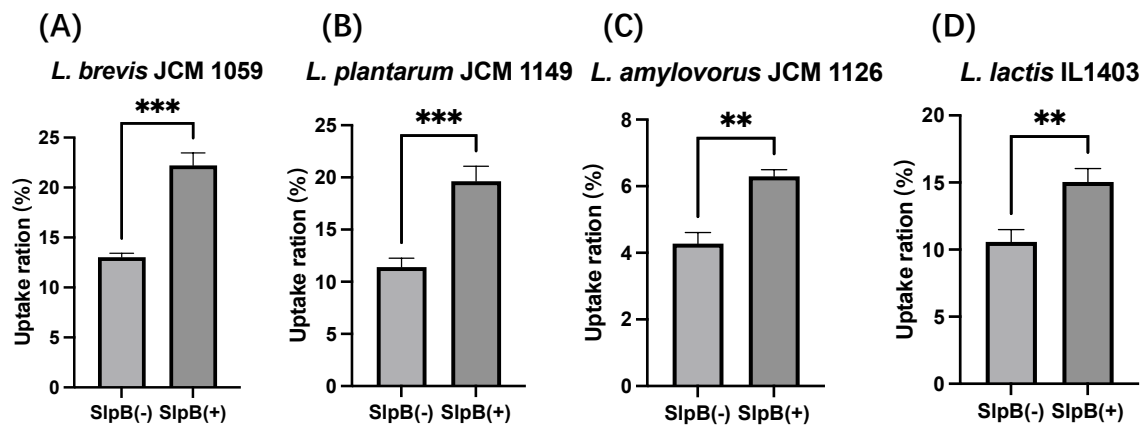


**Figure 2.8.** Uptake of Cy3 labelled (A) *L. brevis* JCM 1059 (B) *L. plantarum* JCM 1149 (C) *L. amylovorus* JCM 1126 (D) *L. lactis* IL1403 with 5M LiCl treated (slpB-) and SlpB coating (slpB +) strain group into THP-1 DC. (Means  $\pm$  SD. \*\*  $p < 0.01$ , \*\*\*  $p < 0.001$ ; n=3).

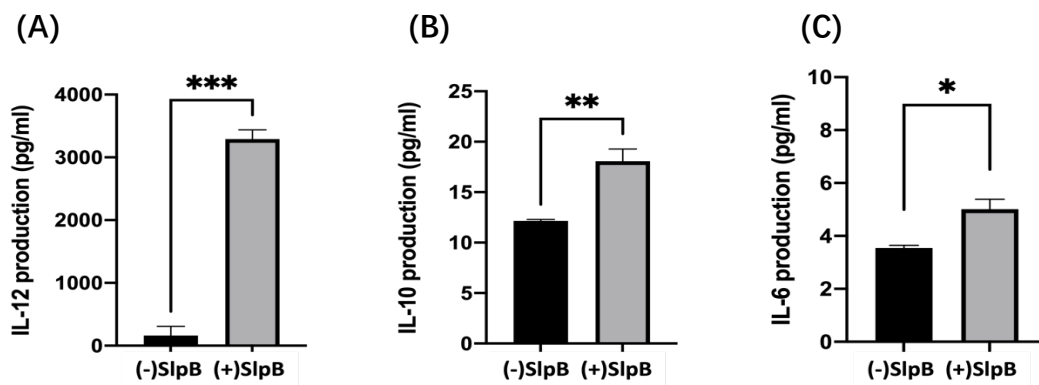


**Figure 2.9.** (A) IL-12, (B) IL-10 and (C) IL-6 production by THP-1 DCs after treatment with *L. brevis* JCM 1059 with (+) or without (-) SlpB. (Means  $\pm$  SD. \*  $p < 0.05$ , \*\*  $p < 0.01$ ; n=3).

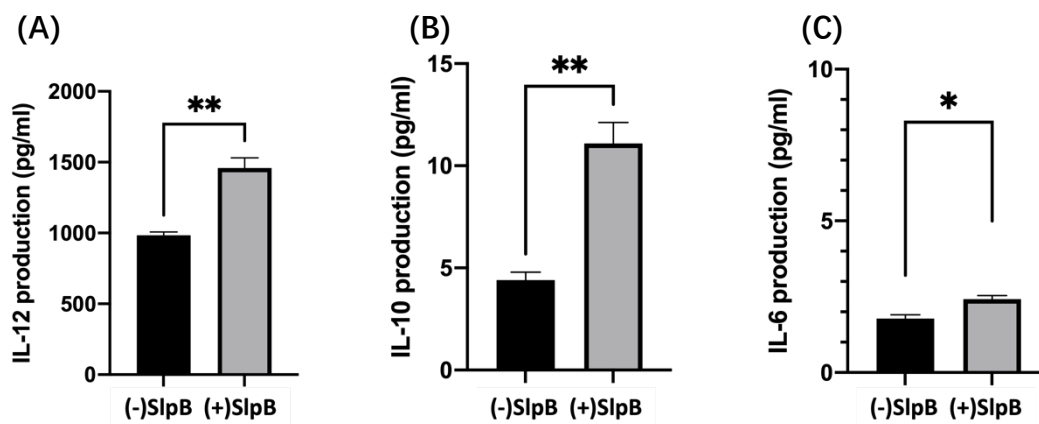


**Figure 2.10.** (A) IL-12, (B) IL-10 and (C) IL-6 production by THP-1 DCs after treatment with *L. plantarum* JCM 1149 with (+) or without (-) SlpB. (Means  $\pm$  SD. \*  $p < 0.05$ , \*\*  $p < 0.01$ , \*\*\*  $p < 0.001$ ; n=3).

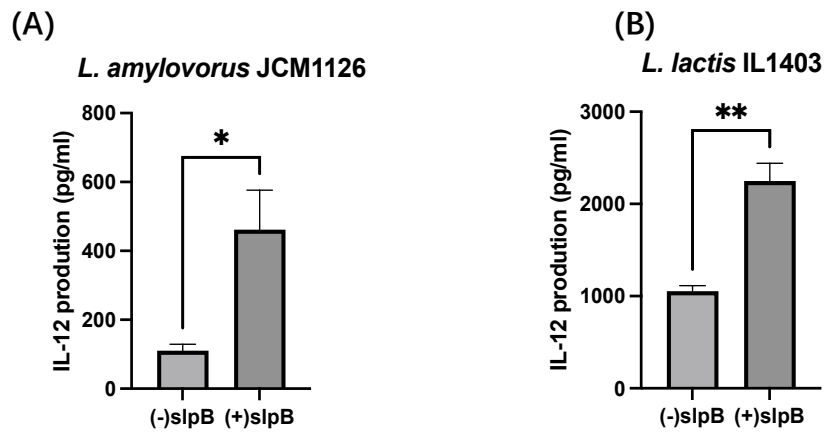


**Figure 2.11.** (A) IL-12 productions in THP-1 DC after treatments with *L. amylovorus* JCM 1126 and *L. lactis* IL1403 with or without SlpB coating. (Means  $\pm$  SD. \*  $p < 0.05$ , \*\*  $p < 0.01$ )

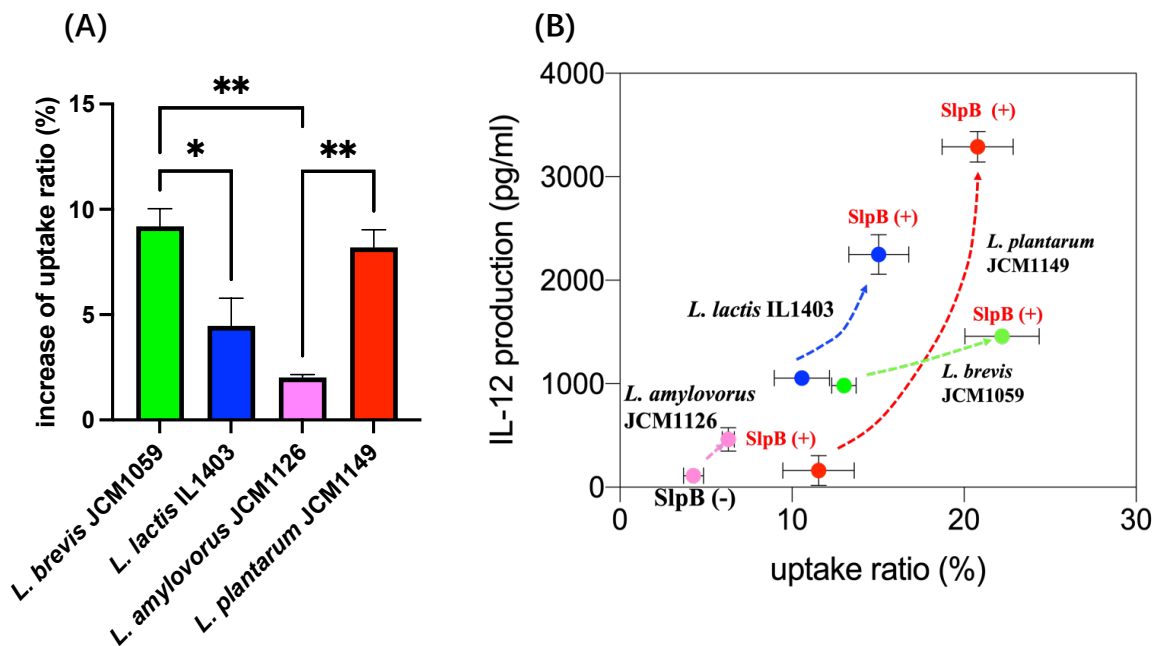


**Figure 2.12.** (A) Summary of increased uptakes of Cy3-labelled *L. brevis* JCM 1059, *L. lactis* IL1403, *L. amylovorus* JCM 1126 and *L. plantarum* JCM 1149 after SlpB coating. (B) IL-12 productions in THP-1 DCs after treatment with *L. brevis* JCM 1059, *L. lactis* IL1403, *L. amylovorus* JCM 1126 and *L. plantarum* JCM 1149 with (+) or without (-) SlpB. (Means  $\pm$  SD. \*  $p < 0.05$ , \*\*  $p < 0.01$ ).

### **2.3.6 Gene expressions in THP-1 DCs after the treatment with SlpB coated *L. brevis* JCM 1059**

The gene expressions in THP-1 DCs co-culture with *L. brevis* JCM 1059 with or without SlpB were compared. The differentially expressed genes (DEGs) from expression profiles were screened based on the fold change (+SlpB/-SlpB), up regulated genes were represented as fold change  $> 1.3$  and down regulated genes were represented as fold change  $< 0.769$ ,  $p < 0.05$ . among all detected genes, a total of 697 genes were upregulated, and 44 genes down regulated on SlpB coated group. The most related genes were organized by using STRING analysis (<https://string-db.org/>) (Figure 2.11). And the genes were separated into 3 different clusters based on the gene function (Table 2.2). 32 genes linked and participated in immune response, cytokine chemokine production, and cell inflammation. 15 genes associated with transcriptional regulation and 15 genes active by SlpB coated *L. brevis* JCM 1059 group effect on adhesion function.

The gene expression results suggest SlpB coated bacteria first activate a complex gene network in THP-1 DCs. Multiple genes are involved in and eventually stimulate the immune THP-1 DCs to produce cytokine.



### 2.3.7 SlpB-coated <sup>Cy3</sup>*L. plantarum* JCM 1149 in mouse Peyer's patches

The fluorescence staining section results can clearly observe the attachment of the <sup>Cy3</sup>*L. plantarum* JCM 1149 to the immune structure in the mouse intestine. After labelling two sets of sections with the same CD23 marker protein against FITC-rabbit IgG to represent the Antigen-presenting cells, (-SlpB)<sup>Cy3</sup>*L. plantarum* JCM 1149 group and (+SlpB)<sup>Cy3</sup>*L. plantarum* JCM 1149 group both observed the FITC green fluorescence (Figure 2.12), however, only on the section of (+SlpB)<sup>Cy3</sup>*L. plantarum* JCM 1149 group can be easily observed in the Cy3 labelled strains (red, Figure 2.12 B).

To further count the bacteria number in each section, each section is divided into 16 counting regions, and 5 counting regions from each section are randomly selected to count the red fluorescent labelled <sup>Cy3</sup>*L. plantarum* JCM 1149 (Figure 2.14 A; B). Triplicated repeat the counting on each section to have an average counting number of <sup>Cy3</sup>*L. plantarum* JCM 1149 in the 5 regions and represent as N. Total <sup>Cy3</sup>*L. plantarum* JCM 1149 number on one section =  $\frac{N}{5} \times 16$ , each group contains three sections. According to the above counting method to count the <sup>Cy3</sup>*L. plantarum* JCM 1149 numbers on the section and compare the results. And the results further indicate that <sup>Cy3</sup>*L. plantarum* JCM 1149 encapsulated in SlpB are more attached to the intestine (Figure 2.14 C). Combined with previous cell experiments, a more comprehensive understanding of the binding relationship between SlpB and immune cells has been revealed. Not only can the SlpB coating bacteria be more absorbed by immune THP-1 cells. In the complex gastrointestinal tract of animals, SlpB can also stably envelop the bacterial body, allowing it to adhere more to the intestinal immune tissue, thereby unleashing the

potential efficacy of the LAB strain.

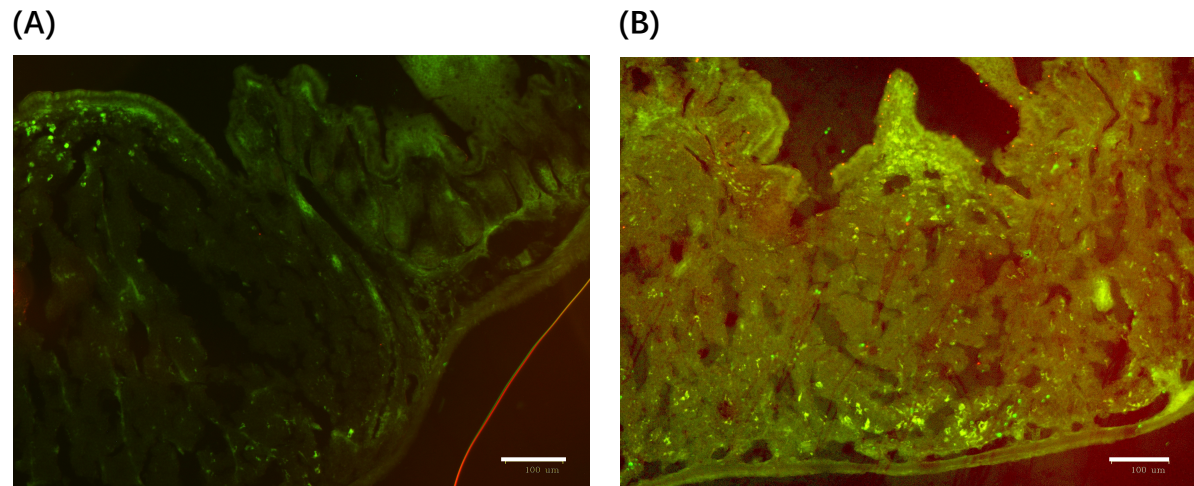


**Figure 2.14.** (A) *Cy3* *L. plantarum* JCM 1149 (red) in mice Peyer's patches. (B) SlpB coated *Cy3* *L. plantarum* JCM 1149 (red) in mice Peyer's patches. Antigen-presenting cells on Peyer's patches are stained with mouse CD23 antibody against FITC-rabbit IgG (Green). The scale bars are 100 μm.



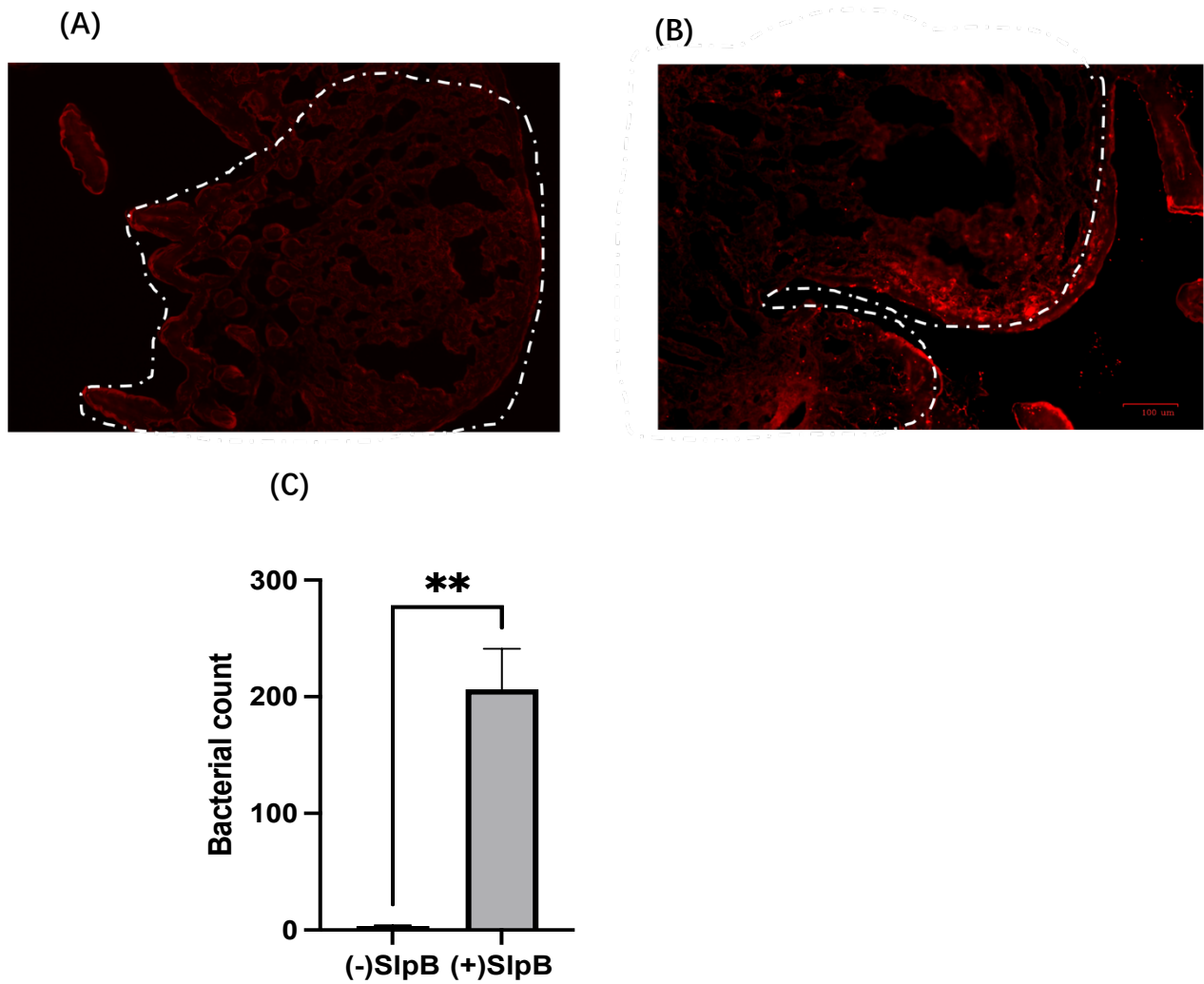


**Figure 2.15.** Mice Peyer's patches section of (A) *Cy3-L. plantarum* JCM 1149 group and (B) SlpB coated *Cy3-L. plantarum* JCM 1149 group for bacteria counting. The scale bars are 100  $\mu$ m. (C) Bacteria numbers on mice Peyer's patches section compared between *Cy3-L. plantarum* JCM 1149 with (+SlpB) or without SlpB (-SlpB) coating group. (Means  $\pm$  SD. \*\*  $p < 0.01$ ).

## 2.4 Summary

In this chapter, SlpB has been identified as the major surface layer protein on *L. brevis* JCM 1059. SlpB showed the stable coating on all tested different lactobacilli including *L. brevis* JCM 1059, *L. helveticus* JCM 1120, *L. acidophilus* JCM 1132, *L. lactis* IL 1403, *L. amylovorus* JCM 1126 and *L. plantarum* JCM 1149. With the SlpB coating, the bacteria thus improved the uptake ratio into THP-1 DCs. By improve the interaction effect between bacteria and immune cell, further stimulate THP-1 DCs to produce cytokines. As the results, with SlpB coating, *L. brevis* JCM 1059, *L. lactis* IL1403, *L. amylovorus* JCM 1126 and *L. plantarum* JCM 1149 not only increased the uptake ratio into THP-1 DCs, but also significantly stimulate the THP-1 DCs to produce cytokine IL-12, especially in *L. plantarum* JCM 1149.

The further gene expression analysis revealed after SlpB enhanced *L. brevis* JCM 1059 interaction with THP-1 DCs, the endosome recognizes the bacteria released effect component through TLR3, and continues active various regulate genes response for inflammation, cytokine, and chemokine production. SlpB is the key to initiating cellular immune recognition. Without the recognition response of SlpB to immune THP-1 DC cells, the LAB strains will not be captured by immune cells, and subsequent complex immune activities unable to be activated.

The role of SlpB was further validated in the *in vivo* experiments. *L. plantarum* JCM 1149 can stably pass through the gastrointestinal tract of mice with the coating of SlpB and attach to the immune Peyer's patch in the small intestine. Without the encapsulation of SlpB, it is difficult for the bacteria to remain in the

intestinal tract of mice, and thus the immune efficacy of the strain cannot be exerted.

Therefore, in this chapter, SlpB, as a key component in combination with immune cells, fully demonstrates that SlpB can not only act as a carrier protein to stably coat different types of lactobacilli, but also can improve the uptake effect of lactobacilli into THP-1 DCs, promote immune cells to produce immune pro-inflammatory cytokine IL-12, and activate the entire immune response.

# Chapter 3 Identification of SlpB receptor on THP-1 DCs

## 3.1 Introduction

In Chapter 2, the role of SlpB in enhancing the immune efficacy of lactobacilli has been demonstrated. Meanwhile, the upregulated immune responses of THP-1 DCs via slpB have also been discovered. However, the mechanism in the binding process between SlpB and THP-1 DCs remains unclear.

The dendritic cell is an important antigen-presenting cell for the cellular immunity process [134]. Probiotics protect the host intestinal barrier by promoting immune response and upregulating anti-inflammatory factors on gut GALT [135]. microfold cells (M cells) are specialized antigen transport cells in the follicle-associated epithelium (FAE). M cells intake LAB and transport it to macrophages or DCs. Macrophages or DCs recognize the antigen and enter the Peyer's patch to activate T and B cells. Thus, understanding the lactobacilli interaction with DCs is essential for immune activation within GALT lymphoid follicles [136, 137].

In the experiment, DCs are induced by THP-1 monocyte lines [132], utilized as the SlpB interacts with immune cells. Therefore, the identification of the SlpB receptor protein on the immune cell is the screening of the DC surface protein. Although the specific presenting protein DC-SIGN of DCs has been reported as the receptor for *Lactobacillus acidophilus* originated SlpA [123]. The interaction of DC-SIGN and SlpB has not been reported. Moreover, by the protein sequence comparison, SlpB didn't share the same protein sequence with SlpA, the different

structure implies the possible different receptor for SlpB on THP-1 DCs. So, it has a high possibility of a novel receptor exists on DCs to SlpB, and exploring the recognition receptors for SlpB on the cell surface will be the major object in this chapter.

## **3.2 Materials and Methods**

### **3.2.1 Cell differentiation and protein collection**

THP-1 cells ( $3 \times 10^5$  cells/mL) were suspended in 15 mL RPMI 1640 media supplemented with 10% FBS, 100 U/mL penicillin, and 100 g/mL streptomycin. Add 50nM PMA for 2 d and 20ng/mL IL-4 for 2 d at 37 °C in a 5% CO<sub>2</sub> humidified incubator to differentiate monocyte THP-1 cells into THP-1 DCs. THP-1 DCs were collected using iced-PBS and cell surface components were lysed using 0.1% Triton X-100-PBS. The cell surface protein extract was separated from the cell supernatant by centrifugation at 1000  $\times g$  for 5 min at 4°C. The concentration of protein was determined using the Bradford assay.

### **3.2.2 Isolation the SlpB binding receptors on THP-1 DCs**

In this experiment, Profinity epoxide resin (Bio-Rad) was used to create a SlpB coupled resin tube. 1 g dry Profinity epoxide resin powder pre-swelled with 8 mL distilled water overnight, then mixed with 2 mg SlpB, and rotated overnight at room temperature. PBS was administered to remove unreacted SlpB, and the SlpB-resin was blocked for 4 hours with 0.05 M glycine-NaOH (pH 8.8). The resin was then washed twice with 5 M LiCl to remove the aggregated SlpB before performing an SDS-PAGE analysis with a 1 M NaCl elution to confirm that all unbound SlpB was removed. SlpB-resin was washed with 0.15 M NaCl PB containing 0.1% Triton-X 100 before being mixed with THP-1 cell extract.

### **3.2.3 Identification of affinity purified protein**

The SlpB coupled resin tube was combined with the lysate THP-1 proteins (1

mg/mL) and stood for 1 hour. 0.5 M, 1 M, 1.5 M, and 2 M of 0.1% Triton-X 100 containing NaCl solutions were used to elute the THP-1 proteins attached to the SIpB-resin. Following the application of SDS-PAGE to confirm the elute proteins result.

The potential target proteins were extracted from the gel. Two protein bands around 46 kDa and 57 kDa were cut from SDS-PAGE gel. To remove the dye from the gel, the gel bands were crushed and dissolved in a de-staining solution (30% acetonitrile, 50 mM  $\text{NH}_4\text{HCO}_3$ ) for 30 minutes. The gel was then de-hydrated with a de-hydrating solution (60% acetonitrile, 20 mM  $\text{NH}_4\text{HCO}_3$ ). The dried gel was then treated with 5% (w/w) trypsin (Promega Japan, Tokyo, Japan) and incubated at 37 °C for 12 h. Peptides were detected by mass spectrometry using an UltrafleXtreme TOF/TOF MS (Bruker Daltonics GmbH, Bremen, Germany) in positive reflection ion mode between m/z 0 and 5000 Da.

### **3.2.4 CAP-1 Expression on THP-1 DCs**

THP-1 cells ( $3 \times 10^5$  cells/mL) were cultured with 50 nM PMA for two days, or 50 nM PMA for two days, followed by 20 ng/mL IL-4 for two days at 37 °C. To prepare the cells for harvesting, cells were first incubated in 4% PFA for 10 min. Iced PBS was added to detach the cells, and then placed in a 1.5 mL microtube. Anti-CAP-1 antibody at a concentration of 5 ng/mL was added to the cells and then left to incubate at room temperature for 1 h. After that, the cells were washed with PBS and mixed with anti-IgG-Alexa 488 (50 ng/mL, Thermo Fisher Scientific Company, Waltham, MA, USA), then placed in an incubator at 25°C for 1 h. Flow cytometry was applied to examine the levels of CAP-1 expression present in each

THP-1 differentiation group at 490/525 nm.

### **3.2.5 Western blotting analysis**

THP-1 cell extract and purified proteins were analysed by sodium dodecyl sulphate-10% polyacrylamide gel electrophoresis (SDS-10%PAGE). Staining gels with Coomassie Brilliant Blue (CBB) displayed protein bands. Protein Ladder One Plus (Nacalai Tesque, Kyoto, Japan) was the marker. Proteins in the gel were transferred to polyvinylidene difluoride (PVDF) membranes for 1 h at 150 mA in Tris-HCl buffer, pH 8.3 (190 mM glycine, 5 mM Tris-HCl, 20% methanol). Specific proteins were identified using antibodies against 1000-fold diluted Mincle (NK MAX, Santa Ana, CA, USA), DC-SIGN (SAB, Greenbelt, MD, USA), Actin, and CAP-1 (Novus Biological, Centennial, CO, USA) after biotinylated anti-rabbit IgG dilution and avidin-peroxidase reaction. Eventually, the band emerged by using 4-Chloro-1-naphthol as a substrate (Wako, Japan).

### **3.2.6 Inhibition of SIpB binding to THP-1 DCs by specific antibody**

THP-1 DCs ( $3 \times 10^5$  cells/mL, differentiated with 50 nM PMA for 2 days and 20 ng/mL IL-4 for 2 days) were washed with iced PBS and harvested before being fixed with 4% PFA for 10 min. 1000-fold diluted antibodies Mincle (NK MAX, Santa Ana, CA, USA), DC-SIGN (SAB, Greenbelt, MD, US), Actin and CAP-1 (Novus Biological, Centennial, CO, USA) were cultured with THP-1 DCs for 1 h at 37 °C. After washing the cells with PBS, 2 ug/cell culture well Cy3 labelled SIpB was added and cultured with THP-1 DCs for 1 h at 37 °C. the expression of Cy3-SIpB on THP-1 DCs was evaluated using a SONY EC800 flow cytometer. Flow cytometric



analyses was performed at 550/570 nm.

### **3.2.7 Fluorescent observation of CAP-1 and Actin on THP-1 DCs**

THP-1 DCs ( $3 \times 10^5$  cells/mL, differentiated with 50 nM PMA for 2 days and 20 ng/mL IL-4 for 2 days) were washed with PBS and fixed by 4% PFA for 10 min at 4°C directly on the cell culture plate. To confirm the expression of each receptor, 1000-fold diluted anti-CAP-1 and anti-Actin were added into THP-1 DCs for 2 h at 37 °C separately. Following the 1 h culture with 1000-fold diluted FITC-anti-IgG after PBS washing.

To view the division of two receptors on the cell surface, fluorescent labelling the anti-CAP-1 with FITC and anti-Actin with Cy3. Briefly, 1 mg dimethyl sulfoxide (DMSO) dissolved Cy3 or FITC was 1% (w/w) diluted and supplemented with 1000-fold anti-CAP-1 and anti-Actin in 0.1 M NaHCO<sub>3</sub> buffer (pH=9.3). The mixture was stood in the dark for 4 h and dialysis by deionized water (100 volume against) at 4°C for 24 h in the dark. FITC-anti-CAP-1 and Cy3-anti-Actin were added into THP-1 DCs for 2 h at 37 °C together. After PBS washing, the immunostaining condition was observed under ZOE Fluorescent Cell Imager (Bio-Rad, CA, USA).

### **3.2.8. Statistical Analysis**

Statistical significance was analysed using GraphPad Prism software version 9.1. Each data point represents the mean of triplicated test samples and SD. Statistically significant differences were set at  $p < 0.05$  by using one-way analysis of variance (ANOVA) followed by Duncan's test.

## 3.3 Results

### 3.3.1 Identification of surface proteins from THP-1 DCs

To identify the SlpB receptor expected on the surface of differentiated THP-1 cells, SlpB coupled Profinity Epoxide resins (SlpB-resin) were prepared. THP-1 cells were differentiated into THP-1 DCs and lysed the surface extract (THP-1 DCs extract) with expect receptor proteins by 0.1% Triton-PBS and mixed the THP-1 DCs extract to SlpB-resin. The potential SlpB bound components were eluted by NaCl-PB with different concentrations. Release of various sizes of components was observed in 0.5 M NaCl elution by SDS-10%PAGE analysis, however, only two major bands, 46kDa and 57 kDa, were observed in 1M NaCl fraction (Figure 3.1). The 46 kDa band was increased in 1M fraction whereas the 57 kDa band was mainly observed in 0.5M fraction. This suggests that SlpB has a higher affinity with the 57 kDa protein than the 46 kDa protein.

To predict these two proteins, each band was cut, and peptides released from the protein by trypsin treatment were analyzed by TOF-Mass (Figure 3.2). By the proteome analysis, the peptides from the 57 kDa protein showed the best matching to adenylyl cyclase-associated protein 1 (CAP-1) and the 46 kDa showed matching to Actin, cytoplasmic 1 (Figure 3.2) in the MASCOT Database analysis. Compared with actin participates in basic functions such as cell movement and control of cell shape widely present in eukaryotic cells [138], CAP-1 was reported as a receptor protein for resistin on monocytes in humans [139]. So, CAP-1 has been preliminarily considered as a possible receptor for SlpB on the surface of THP-1 DCs.

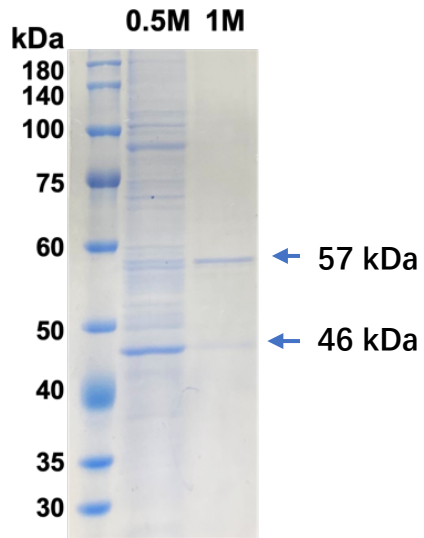



**Figure 3.1.** SDS-10%PAGE analysis of proteins in 0.5M and 1M NaCl fractions purified from THP-1 DCs cell extract by SlpB affinity resin.

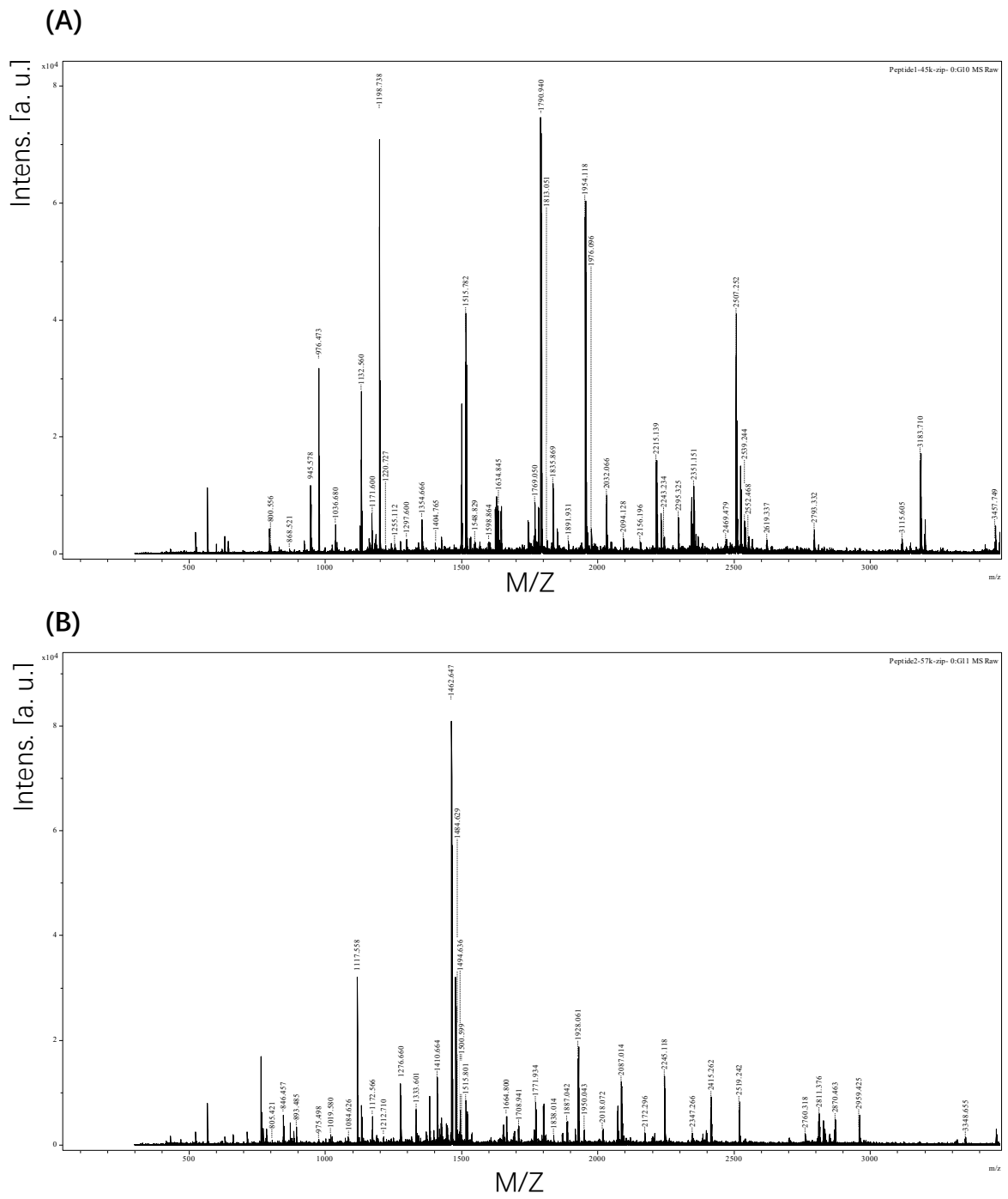


**Figure 3.2.** TOF-Mass analyses of the trypsin treated (A) 46 kDa and (B) 57 kDa proteins.

(A)

 **MASCOT Search Results**

**Protein View: ACTB\_HUMAN**

Actin, cytoplasmic 1 OS=Homo sapiens OX=9606 GN=ACTB PE=1 SV=1

Database: SwissProt  
Score: 257  
Expect: 4.1e-022  
Monoisotopic mass (M<sub>r</sub>): 41710  
Calculated pI: 5.29  
Taxonomy: [Homo sapiens](#)

Sequence similarity is available as [an NCBI BLAST search of ACTB\\_HUMAN against nr.](#)

**Search parameters**

Enzyme: Trypsin: cuts C-term side of KR unless next residue is P.  
Mass values searched: 91  
Mass values matched: 25

**Protein sequence coverage: 59%**

Matched peptides shown in **bold red**.

```
1 MDDDIALLVV DNGSGMCKAG FAGDDAPRAV FPSIVGRPRH QGMVMGMGQK
51 DSYVGDEAQS KRGILTLKYP IEHGIVTINWD DMEKIWHHTF YNELRVAPEE
101 HPVLLTEAPL NPKANREKMT QIMFETFNTP AMYVAIQAVL SLYASGRTTG
151 IVMDSGDGVT HTVPIYEGYA LPHAILRLDL AGRDLTDYLM KILTERGYSF
201 TTTAEREIVR DIKERLCYVA LDFEQEMATA ASSSSLEKSY ELPDGQVITI
251 GNERFRCPEA LFQPSFLGME SCGIHETTFN SIMKCDVDIR KOLYANTVLS
301 GGTMYPGIA DRMKEITAL APSTMKIKII APPERKYSVW IGGSILASLS
351 TFQMMWISKQ EYDESGPSIV HRKCF
```

(B)

 **MASCOT Search Results**

**Protein View: CAP1\_HUMAN**

Adenylyl cyclase-associated protein 1 OS=Homo sapiens OX=9606 GN=CAP1 PE=1 SV=5

Database: SwissProt  
Score: 145  
Expect: 6.4e-011  
Monoisotopic mass (M<sub>r</sub>): 51869  
Calculated pI: 8.24  
Taxonomy: [Homo sapiens](#)

Sequence similarity is available as [an NCBI BLAST search of CAP1\\_HUMAN against nr.](#)

**Search parameters**

Enzyme: Trypsin: cuts C-term side of KR unless next residue is P.  
Mass values searched: 97  
Mass values matched: 19

**Protein sequence coverage: 38%**

Matched peptides shown in **bold red**.

```
1 MADMQLVER LERAVGRLEA VSHTSDMRHG YADSPSKAGA APYVQAFDSL
51 LAGFVAEYLK ISKEIGGDVQ KHAEMVHTGL KLERALLVTA SQCQQPAENK
101 LSDLLAPISE QIKEVITFRE KNRGSKLFNH LSAVSESIQA LGWVAMAPKP
151 GPYVKEMNDA AMFYTNRVLK EYKDVKKHV DWVKAYLSIW TELQAYIKEF
201 HTTGLAWSKT GPVAKELSGL PSGFSAGSCP PPPPPCPPPP PVSTISCSYE
251 SASRSSLFAQ INQGESITHA LKHVSDDMKT HKNPALKAQ GPVRSQPKPF
301 SAPKQTSPTS PKRATKEPA VLELEGKKWR VENDENVSNL VIEDTELRQV
351 AYIYKCVNTT LQIKGKINSI TVDNCKKGLL VFDDVVGIVE IINSKDVKQV
401 VMGRVPTISI NKTDGCHAYL SKNSLDCEIV SAKSSSEMNVL IPTEGGDFNE
451 FPVPEQFKTL WNGQKLVITV TEIAG
```

**Figure 3.3.** MASCOT analysis of trypsin digested peptides obtained from the (A) 46 kDa and (B) 57 kDa protein.

### **3.3.2 CAP-1 expression and immunostaining on THP-1 DCs**

To verify the presence of CAP-1 on THP-1 DCs, different induction strategies were utilized on THP-1 monocyte. Anti-CAP-1 antibody was incubated with THP-1 cells after differentiation with 50 mM PMA for 2 days (PMA group). THP-1 cells treated with 50 mM PMA for 2 days, followed by 20 ng/mL IL-4 for 2 days (PMA + IL-4 group) were also incubated with anti-CAP-1 antibody. The cell surface CAP-1 on THP-1 cells was quantified by the method described in Materials and Methods. Non-treated monocyte THP-1 cells were set as the control group. The results showed that CAP-1 was highly induced in THP-1 DCs by combination with PMA and IL-4 compared to that with THP-1 cells by PMA (Figure 3.4). The results not only confirmed the existence of CAP-1 on the surface of THP-1 DCs but also revealed inductions of CAP-1 during the differentiation process.

After clarifying the expression of CAP-1 on THP-1 DCs, immunofluorescence staining for CAP-1 was performed. The observation showed CAP-1 is evenly distributed in the cells (Figure 3.5). This fluorescence staining image further determined the presence of the protein on THP-1 DCs.

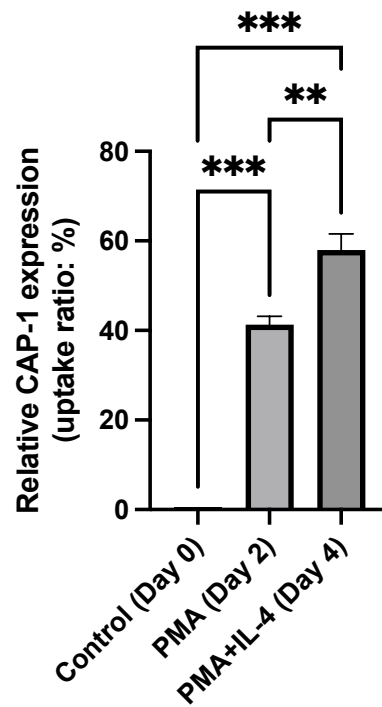


**Figure 3.4** CAP-1 expression in THP-1 DC differentiated with PMA, and PMA + IL-4. (Means  $\pm$  SD. \*\*  $p < 0.01$ , \*\*\*  $p < 0.001$ ).

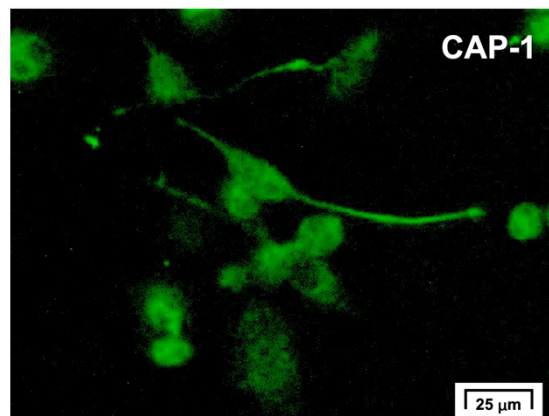


**Figure 3.5.** Immunostaining of CAP-1 on THP-1 DCs with anti-CAP-1 antibody and FITC-anti-IgG secondary antibody. The scale bars are 25  $\mu$ m.

### 3.3.3 Western Blotting Analysis for surface receptors

In the present study, we differentiated monocyte THP-1 cells into dendritic cells to understand the production of specific cytokines by various lactic acid bacteria. The high expression of DC-SIGN on THP-1 DCs has been determined in the previous experiment in our laboratory. Mincle is a type of C-type lectin induced on the surface of macrophages and is used as a pattern recognition receptor for various lactic acid bacteria [153]. To confirm the expressions of CAP-1, DC-SIGN, and Mincle, on the THP-1 DC, the western blotting analysis was performed with specific antibodies. The results showed that DC-SIGN appeared on the cell extract around 45 kDa (Figure 3.6 A), however, no signal for Mincle was observed in THP-1 DC (Figure 3.6 B).

The CAP-1 antibody reacted with a 57 kDa band corresponding to CAP-1 in gel extracted purified protein (Figure 3.6 D) and THP-1 cell extract (Figure 3.6 C). The results suggest a high affinity of anti-CAP-1 antibody to the cell, the continued experiments are required to confirm the function of Actin for SlpB binding. While CAP-1 is the main SlpB binding receptor on the cell surface has been more clearly demonstrated by WB results.



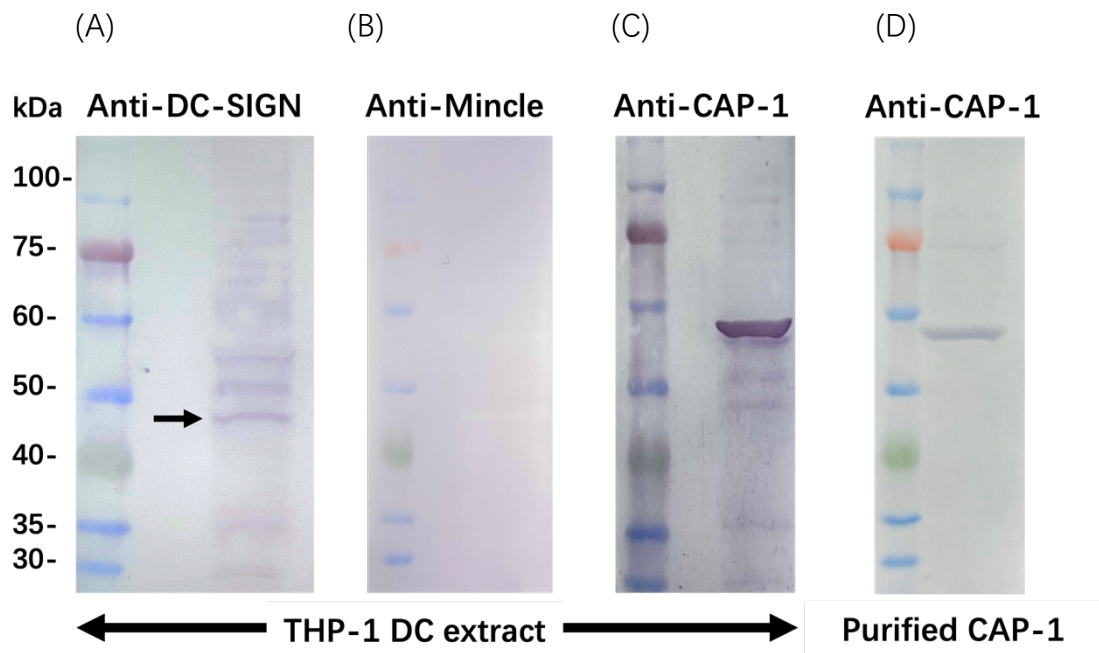


**Figure 3.6.** Western blotting analysis of (A) anti-DC-SIGN antibody (B) anti-macrophage-inducible C-type lectin (Mincle) antibody (C) anti-CAP-1 antibody with crude extract of THP-1 cells and (D) anti-CAP-1 antibody with affinity purified 57 kDa (CAP-1) protein.

### 3.3.4 SlpB Binding to THP-1 DCs by Antibodies

For further understanding of the role of various cell surface proteins on THP-1 DC in SlpB binding, each anti-Mincle antibody, anti-DC-SIGN antibody, anti-CAP-1 antibody, or anti-Actin antibody was added into THP-1 DCs before adding <sup>Cy3</sup>SlpB. Anti-CAP-1 antibody significantly inhibited the binding of <sup>Cy3</sup>SlpB to THP-1 cells compared to the control sample (-antibody), indicating the high binding ability of SlpB to CAP-1. It's worth noting that, the expression level of <sup>Cy3</sup>SlpB in the anti-DC-SIGN group was not highly reduced indicating <sup>Cy3</sup>SlpB can still bind to cells if anti-DC-SIGN was added. Anti-Mincle antibody did not inhibit the binding of <sup>Cy3</sup>SlpB (Figure 3.7.A), suggesting less expression of Mincle on THP-1 DCs. Considering with WB results, the inhibitory effect of anti-Actin antibody on SlpB binding may be due to the high binding between Actin antibody and CAP-1, research has been should the existing binding sequence area of CAP-1 to Actin [148], so the anti-Actin antibody suppression to SlpB may due to the occupying of anti-Actin to the original binding site between slpB and CAP-1, resulting in the suppression of <sup>Cy3</sup>SlpB expression in the results (Figure 3.7 B).

The results provide more evidence of the strong affinity that exists between CAP-1 and SlpB and further reveal the possibility of CAP-1 as a SlpB receptor on DCs.

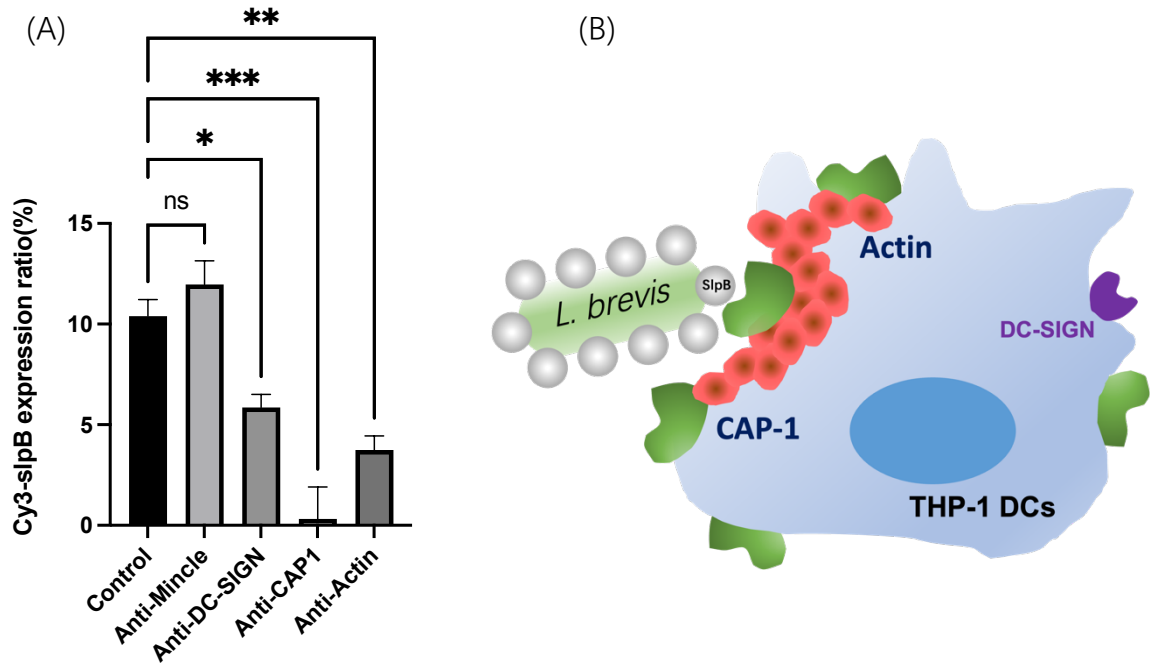


**Figure 3.7.** (A)  $^{Cy3}$ SlpB was incubated with THP-1 DCs with normal mouse serum (Control), anti-Mincle antibody, anti-DC-SIGN antibody, anti-CAP-1 antibody, and anti-Actin antibody for 1 h. (Means  $\pm$  SD. \*  $p < 0.05$ , \*\*  $p < 0.01$ , \*\*\*  $p < 0.001$ ). (B) Illustration for *L. brevis* JCM 1059 binding of SlpB with CAP-1 and Actin interaction.

### 3.3.5 Immunostaining of CAP-1 and Actin on THP-1 DCs

Due to CAP-1 and Actin antibodies are the same mouse homologs, they cannot be labeled with different fluorescent secondary antibodies. Therefore, the fluorescent dyes FITC and Cy3 are used to directly mark the anti-CAP-1 and anti-Actin antibodies. The presence and distribution of two proteins on the cell surface can be clearly observed in the micrographs. CAP-1 distributes broadly in the cells (Figure 3.8 A). And Actin is particularly congregated at the surface edge of congregate (Figure 3.8 B). The merged picture showed Actin and CAP-1 have an overlapped location area (Figure 3.8.C). This may also explain the WB results and the antibody competition results, the suppression expression of <sup>Cy3</sup>slpB by anti-Actin is not the binding affinity between SlpB and Actin but caused by the SlpB-CAP-1 binding region blocked by Actin-CAP-1 overlapped location.

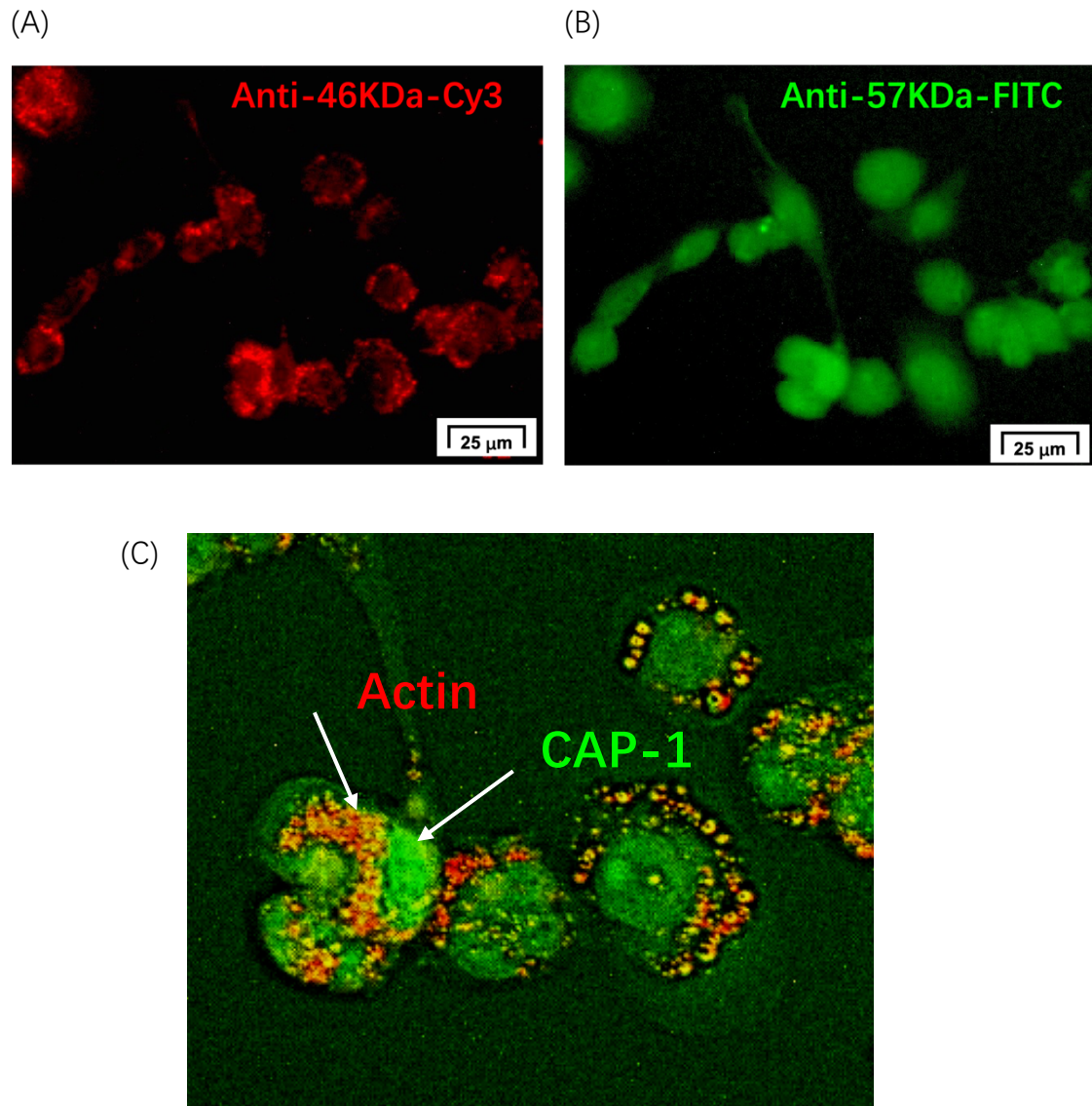


**Figure 3.8.** (A) Immunostaining of Actin on THP-1 DCs with Cy3-anti-Actin antibody and (B) CAP-1 with FITC-anti-CAP-1 antibody. (C) the merged immunostaining image of Actin (red) and CAP-1 (Green). The scale bars are 25 μm.

### 3.4 Summary

In this chapter, a 57 kDa protein purified from THP-1 DCs has been identified as adenylyl cyclase-associated protein 1 (CAP-1) and predicted as a novel receptor on THP-1 DCs for SlpB.

The potential SlpB binding proteins from THP-1 DCs extract were captured by SlpB-resin, and two major bands around 46 kDa and 57 kDa were detected in SDS-10%PAGE after 1M NaCl-PB elution (Figure 3.1). After protein isolation and purification from the gel, proteome analysis by TOF MS and sequence comparison on MASCOT Database were performed. Eventually, the 46 kDa protein was high matched with Actin and 57 kDa protein was high matched with CAP-1 (Figure 3.3).

To clearly the expression of the predicted proteins on cells, CAP-1 expression at various cell differentiation stages was measured through flow cytometry analysis. Immunofluorescence labeling CAP-1 by anti-CAP-1 against FITC-Anti-IgG secondary antibody. The results showed that CAP-1 was highly expressed in DC cells induced by complete PMA/IL-4 stimulation compared with PMA middle stimulation period and no stimulation monocyte THP-1 cells group (Figure 3.4). Meanwhile, through Western blotting experimental analysis further confirms the expression of each protein on the THP-1 DCs. The antibody to CAP-1 is highly reactive on both cell crude extracts and purified 57 kDa protein (Figure 3.6. C, B), fully validating the presence of CAP-1 on cells.

To further decide the binding affinity of each protein with SlpB, a cell competitive binding experiment was conducted with the protein antibodies and SlpB. Each antibody was added to the fully differentiated THP-1 cells culture

medium, followed by the addition of fluorescent Cy3 labeled SlpB. In the results, the antibody against CAP-1 showed significant inhibition of <sup>Cy3</sup>SlpB expression (Figure 3.7.A). Finally, it can be concluded that CAP-1, as a significantly expressed protein on DCs, has a high affinity to SlpB and considered is a major and novel receptor for slpB.

# Chapter 4 Prediction of major SlpB regions involved in bindings with bacteria and THP-1 DCs

## 4.1 Introduction

As a C-type lectin receptor, DC-SIGN and Mincle containing a Glu-Pro-Asn (EPN) carbohydrate-recognition domain can bind to glucose-, mannose- and N-acetylglucosamine-containing oligosaccharides [140, 141]. In the present study, although CAP-1 has no clear EPN sequence and has a low homology to DC-SIGN and Mincle, SlpB showed binding to CAP-1 and partly to DC-SIGN through the competition experiments with specific antibodies in Chapter 3. This result suggests the potential recognition of carbohydrates on SlpB by DC-SIGN. However, the interaction of CAP-1 with SlpB via the carbohydrate structure of SlpB remains unclear.

Therefore, in this chapter, the main object is to verify the functional SlpB peptides' response to bacterial and CAP-1 binding. In order to identify the specific binding peptide fragments, SlpB purified from *L. brevis* JCM 1059 was treated with chymotrypsin, and digested peptides were tested for the binding abilities of two different LAB strains *L. brevis* JCM 1059 and *L. plantarum* JCM 1149, and CAP-1 in THP-1 DCs. The peptides binding with CAP-1 were evaluated by comparative analysis of the disappeared peptide peak after the binding by reversed phase high performance liquid chromatography (RP-HPLC). Peptide fragments interacting with bacterial cell surface were also evaluated and identified by observation of disappeared peptides by HPLC after incubation with bacterial cells. Then, each



isolated peptide was labeled with fluorescent and tested the binding to CAP-1 and also the bacterial cell surface. Finally, important SlpB regions needed for bindings with *L. brevis* JCM 1059 and *L. plantarum* JCM 1149 and CAP-1 were predicted.

## 4.2 Materials and Methods

### 4.2.1 SlpB digestion and HPLC analysis

SlpB isolated from JCM 1059 as described in Chapter 2. SlpB was digested by  $\alpha$ -chymotrypsin, 50:1 (w/w) for 2 h partial digestion or 24h complete digestion at 37°C. Reversed-phase HPLC (RP-HPLC) analysis with 4.6 mm  $\times$  150 mm C18 column (XBridge BEH, Waters Company, Milford, MA, USA) was utilized to distinguish the digested SlpB fragments. The separation protocol was a 30 min performed 0% to 100% solvent B in solvent A linear gradient at a 1 mL/min flow rate. (Solvent A: 0.1% TFA in H<sub>2</sub>O; Solvent B: 0.1% TFA in acetonitrile). Trifluoroacetic acid (TFA), acetonitrile, and  $\alpha$ -chymotrypsin were purchased from Nacalai Tesque, Inc. (Kyoto, Japan).

### 4.2.2 Identification of bacteria binding fragments

2 h chymotrypsin partial digested SlpB (50  $\mu$ g) fragments (CT-2H-SlpB) were co-culture with 5M LiCl treated *L. brevis* JCM 1059 (*L. brevis*-Supernatant) and *L. plantarum* JCM 1149 (*L. plantarum*-Supernatant) ( $5 \times 10^8$ ) in 0.5 mL PBS at 30°C for 2 h. After incubation, the supernatant was collected by centrifugation (6000  $\times g$  for 10 min), then 1:1 (v/v) mixing with solvent A and applying the sample for HPLC analysis. Next, the chromatograms were compared between CT-2H-SlpB and supernatant groups under the same enzymatic hydrolysis conditions. The peaks that disappeared or decreased in the chromatogram of the supernatant group were predicted as possible bacteria binding peptides. Collect the target peptides, vacuum remove TFA from the peptide collection solution, and freeze-drying the sample to remove water from the sample. Cy3 fluorescence labeling of

the obtained peptide dry powder and re-binding with the strain was performed to compare the fluorescence expression of each Cy3 labeled fluorescent peptide on the strain, eventually determining the peptide fragment that is highly bound to the strain. Suspended the Cy3 labelled peptide contained bacteria into a microwell plate and Cy3 fluorescence was measured using a plate reader (Thermo Fisher Scientific, Varioskan LUX SkanIt Software 4.0). ZipTip with 0.6  $\mu$ L C<sub>18</sub> resin (Merck Millipore, Cork, Ireland) pipette tips were used to capture the peptides with Cy3 labelled and remove the un-labelled Cy3 dye following the manufacturer's protocol.

#### **4.2.3 Identification of CAP-1 binding fragments**

24 h chymotrypsin complete digested SlpB (10  $\mu$ g) fragments (CT-24H-SlpB) were co-cultured with CAP-1 captured microwell plate. To build the CAP-1-CT-24H-SlpB binding microplate, 1/1000 diluted Anti-CAP-1 antibody was coated on the microplate for 2 h at room temperature followed with 30 min 1% BSA-PBS block, then 1/500 diluted CAP-1 contained THP-1 DCs extract was added for 2 h at room temperature and continue with an overnight coating at 4°C. the next day, washed the plate with PBS twice to remove the uncaptured CAP-1 and added the CT-24H-SlpB for 2 h at room temperature. Then collect the supernatant (CAP-1-Supernatant) from the microplate and applied to the sample for HPLC analysis.

The same compression method described above was used for binding between CT-24H-SlpB and CAP-1. The collected target peptides were also fluorescent labeled by Cy3 and tested for binding to CAP-1 captured on a microwell plate. Finally, Cy3 fluorescence originating from the bound peptide was

measured by using the plate reader.

#### **4.2.4 Glycan competition test with SIpB on THP-1 DCs**

$5 \times 10^5$ /mL THP-1 DCs were differentiated as described in Chapter 2, harvested by cold PBS and were fixed in 1% PFA for 10 min at 4 °C. To evaluate the <sup>Cy3</sup>SIpB binding to THP-1 DCs, incubation at 37 °C for 1 h followed by the addition of <sup>Cy3</sup>SIpB with or without galactose (Sigma-Aldrich, St. Louis, MO, USA) or mannose (Nacalai Tesque Inc., Kyoto, Japan) (0.5 mg/mL), and THP-1 DCs were collected and processed via flow cytometry. Flow cytometric measurements were conducted at 550/570 nm.

#### **4.2.5 SIpB deglycosylation and THP-1 DCs binding test**

1/1000 diluted anti-CAP-1 antibody was applied to a microwell plate and incubated at 4 °C for 24 h before being incubated for 2 h at 25 °C to capture CAP-1 in THP-1 DC cell extract. The plates were then incubated with deglycosylated <sup>Cy3</sup>SIpB for 2 h at 25 °C. 20 g of <sup>Cy3</sup>SIpB were combined with 4 g of recombinant glycosidase (PNGase F PRIMETM, N-Zyme Scientifics, PA, USA) and incubated for 24 h at 37 °C to digest the polysaccharides from SIpB. A plate reader was used to quantify Cy3 fluorescence from <sup>Cy3</sup>SIpB.

#### **4.2.6 Peptide analysis and prediction**

The predicted peptides were collected from HPLC effluent, Solvent A contained TFA evaporated by vacuum chamber and freeze drying to completely remove the remaining water. Re-dissolving the peptide powder in PBS and finally

analyzed by mass spectrometry using an UltrafleXtreme TOF/TOF MS analyzer. SWISS-MODEL (<https://swissmodel.expasy.org/>) was utilized to search the SlpB template and the high score matched crystal structures were selected for 3D model building. The NetSurfP-2.0 server was applied to predict the 2D structure of SlpB with surface accessibility, secondary structure, disorder, and phi/psi dihedral angles of amino acids in the SlpB sequence (<https://services.healthtech.dtu.dk/service.php?NetSurfP-2.0>). The basic physical and chemical information including Isoelectric point and hydrophilicity was evaluated through the ProtParam tool (<https://web.expasy.org/protparam/>).

#### **4.2.7 Statistical Analysis**

Statistical significance was analysed using GraphPad Prism software version 9.1. Each data point represents the mean of triplicated test samples and SD. Statistically significant differences were set at  $p < 0.05$  by using one-way analysis of variance (ANOVA) followed by Duncan's test.

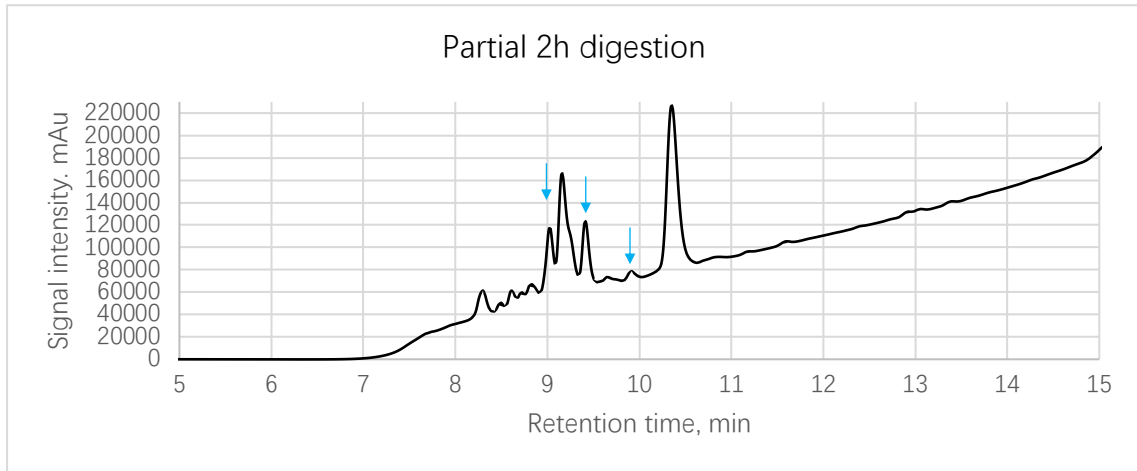
## 4.3 Results

### 4.3.1 Peptide fragments at different enzymatic hydrolysis times

Short SlpB peptide fragments were prepared to identify the polysaccharide-based binding to CAP-1, and longer peptide fragments were prepared for bacterial binding. Therefore, SlpB derived peptide fragments by chymotrypsin were prepared by different treatments. Peptide profiles for shorter time treatment (2 h, partial digestion) and longer time treatment (24 h, complete digestion) were compared by HPLC analysis. Most of the peaks in 2 h and 24 h hydrolysates showed similar elution profiles, but various peaks were specific to hydrolysates by 2 h or 24 h (Figure 4.1 A, B). Some peptides were detected at 9-10 min in 2 h hydrolysate (Figure 4.1 A, arrows), but specific peptides in 24 h hydrolysates were eluted earlier retention time at 8 min (Figure 4.1 B, arrows).

The results suggest that 24 h hydrolysate contains shorter peptides than 2 h hydrolysate. Therefore, 24 h of completely digested SlpB fragments were used for CAP-1 binding assay and 2h of partially digested SlpB fragments were used for bacteria binding.

(A)



(B)

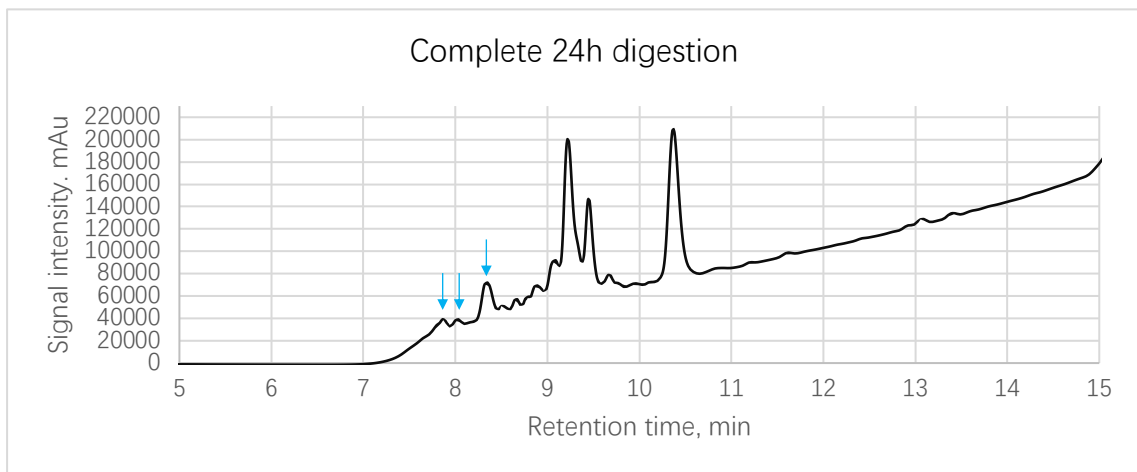


**Figure 4.1.** Chymotrypsin digested SIpB peptides enriched in different treatment times in HPLC analysis. Peptides were treated for 2h (A) and 24 h (B). Arrows indicate specific peptides in the fractions.

### 4.3.2 Identification of binding fragments to bacteria

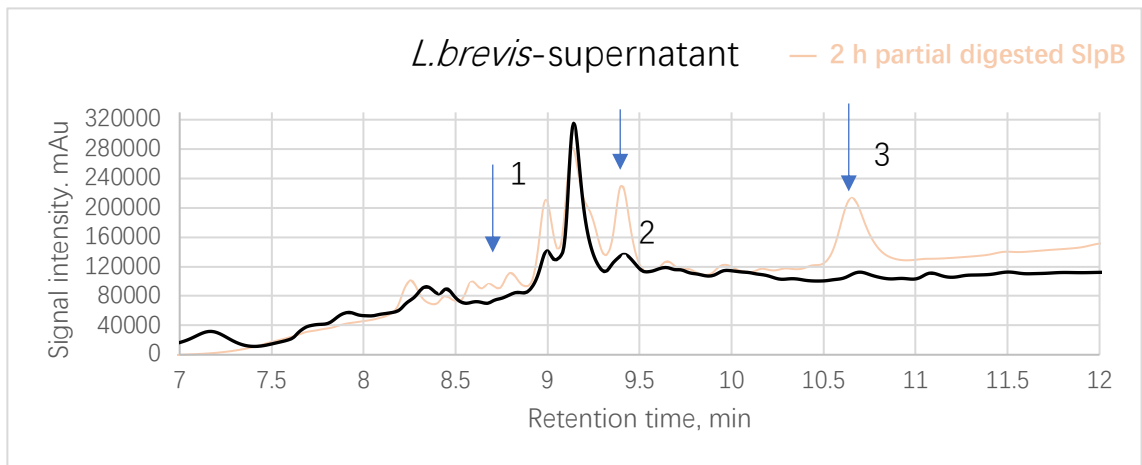
Partial digested SlpB fragments (2 h) were mixed with *L. brevis* JCM 1059 or *L. plantarum* JCM 1149, and both peak profiles between *L. brevis*-unbound peptides and *L. plantarum*-unbound peptides with 2h partial digested SlpB showed reductions of some major peptides (Peptide-1, -2 and -3). (Figure 4.2 A, B). Unbound Peptide-1, -2, and -3 from SlpB chymotrypsin hydrolysate were observed in the *L. brevis* and in the *L. plantarum*. Peptide-2 reduced the peak height in both bacteria groups, and another 2 peptides are different in the two bacteria groups.

Based on the results, the peptide fragments were carefully divided into 7 fragments (Figure 4.2 C), and fluorescently labeled the collected peptides to separately mix with *L. brevis* JCM 1059 or *L. plantarum* JCM 1149. The fluorescence intensity of the bacteria after mixing and washing treatment was measured to detect the binding ability of each peptide to the bacteria. The results showed a high binding ability of F1 to *L. plantarum* JCM 1149 compared with *L. brevis* JCM 1059, a higher binding ability of F6 and F7 to *L. brevis* JCM 1059 compared with *L. plantarum* JCM 1149 (Figure 4.3 A). And to compare the expression of 7 peptides within *L. brevis* JCM 1059 or *L. plantarum* JCM 1149, F6 showed the highest expression among all tested peptides binding with *L. brevis* JCM 1059 (Figure 4.3 B). F1 showed a significantly high expression on the binding with *L. plantarum* JCM 1149 to all other 6 peptides (Figure 4.3 C). The results basically matched with the HPLC prediction, F1 appears around 8 to 9 min as the main binding peptide for *L. plantarum* JCM 1149, and F6 and F7 appear around 9.5 to 11 min are showed higher binding expression for *L. brevis* JCM 1059.

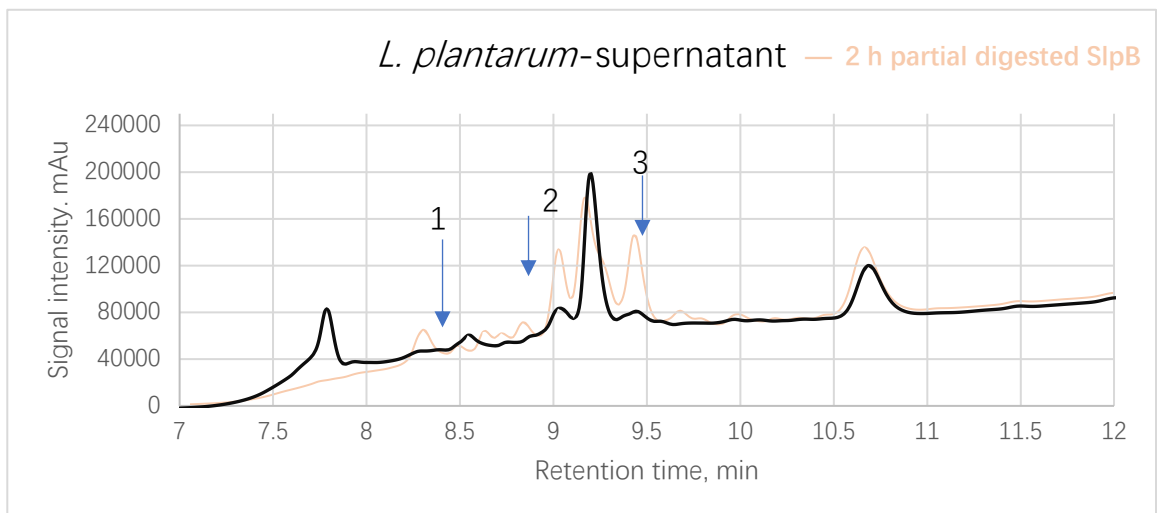


In summary, among the 7 collected peptides, F1 can highly bind to *L. plantarum* JCM 1149, while F6 and F7 showed high binding capacity to *L. brevis* JCM 1059. Considering these 3 peptides are the functional bacterial binding peptides of SlpB can be further determined through proteome sequence analysis to continue understanding the SlpB structure.

(A)



(B)



(C)

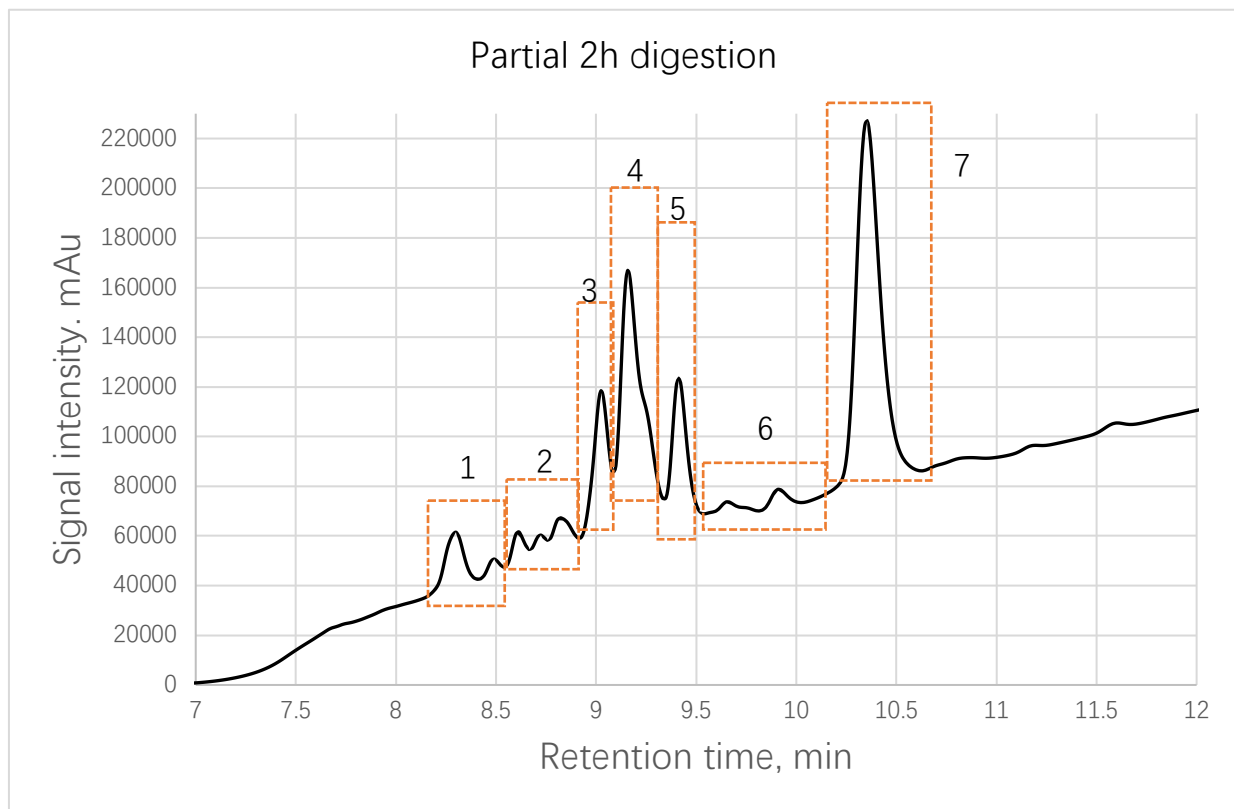


**Figure 4.2** (A) HPLC analysis of SlpB unbound peptides from *L. brevis* JCM 1059 and (B) *L. plantarum* JCM 1149 coinubation. SlpB was treated with chymotrypsin by a 2 h digestion. (C) Collected Fragment 1 to 7 from 2 h chymotrypsin treated SlpB. Arrows in (A) and (B) indicate specific unbound peptides.

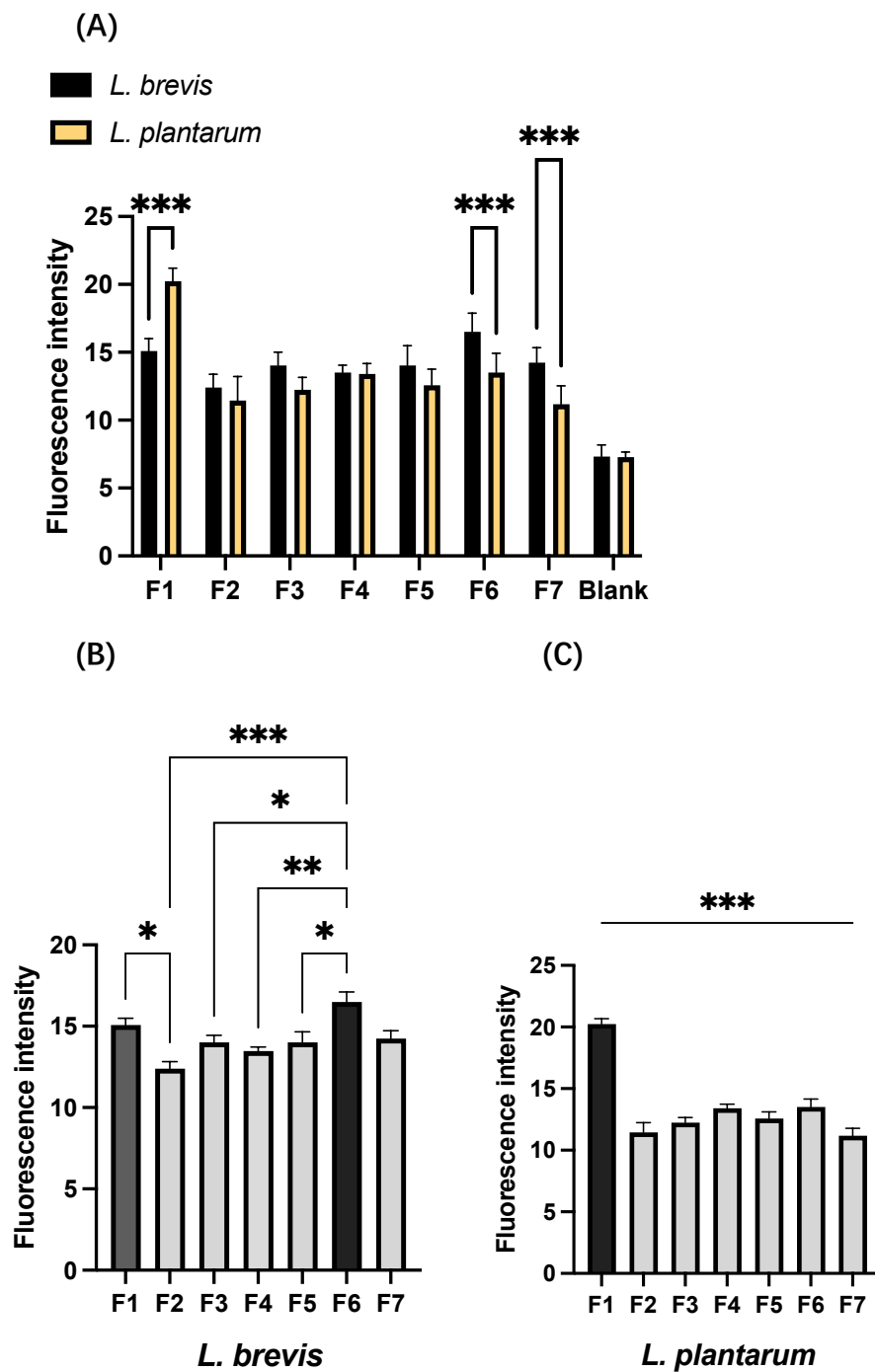


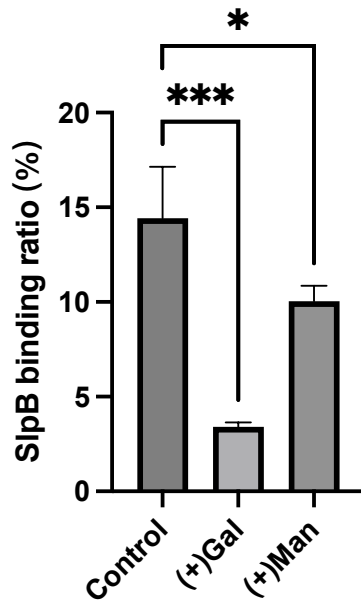
**Figure 4.3** (A) Fluorescence comparison between *L. brevis* JCM 1059 binding group and *L. plantarum* JCM 1149 binding group for 7 Cy3 labeled peptides. (B) 7 Cy3 labeled peptides binding expression on *L. brevis* JCM 1059 and (C) *L. plantarum* JCM 1149. (Means  $\pm$  SD. \*  $p < 0.05$ , \*\*  $p < 0.01$ , \*\*\*  $p < 0.001$ ).

### 4.3.3 Involvement of polysaccharide of SlpB for CAP-1 binding

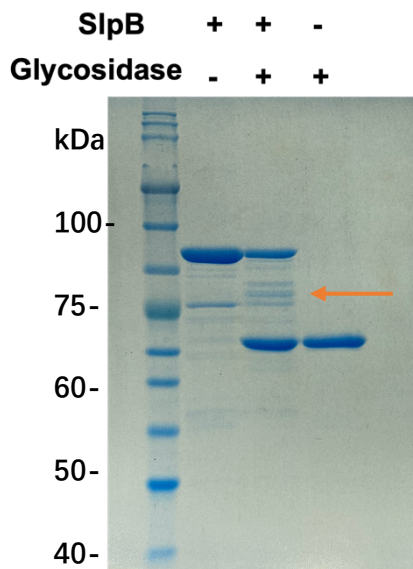
As discussed in the introduction, CAP-1 has been considered as a C-type lectin that may bind with the structure of the carbohydrate on protein, thus it is necessary to verify whether the glycan structure exists on SlpB and the involvement in SlpB-CAP-1 binding. Galactose (Gal) and mannose (Man) suppressed the interaction of SlpB to CAP-1 (Figure 4.4 A), indicating the ability of CAP-1 binding to glycan and its importance in the binding with SlpB. Further, with glycosidase treatment, several bands likely released from SlpB were observed from SDS-10% PAGE gel (Figure 4.4 B), illustrating that SlpB can be deglycosylated, thus suggesting SlpB is a glycoprotein.

According to these results, CAP-1 could identify carbohydrates on SlpB and perform the function of a C-type lectin-like protein. <sup>Cy3</sup>SlpB was detected on the CAP-1-coated microplate after CAP-1 was captured on the microplate using an anti-CAP-1 antibody to verify the presence of carbohydrates on SlpB. When <sup>Cy3</sup>SlpB was pre-treated with glycosidase, it was not able to be captured by CAP-1 (Figure 4.4 C). Demonstrates that CAP-1 has C-type lectin-like activity and interacts with carbohydrates on SlpB.

(A)



(B)



(C)

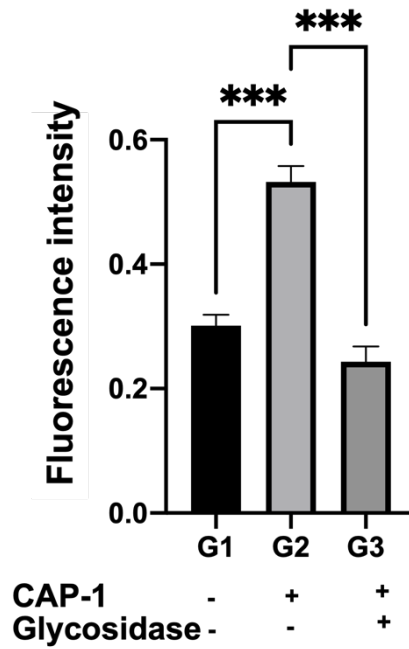


**Figure 4.4** (A)  $^{Cy3}$ SlpB and THP-1 DC binding with or without galactose (Gal) and mannose (Man). (B) SDS-10%PAGE analysis of SlpB and de-glycosylated SlpB. Arrows indicate the de-glycosylated SlpB. (C) Binding between CAP-1 and  $^{Cy3}$ SlpB or glycosidase treated  $^{Cy3}$ SlpB. (Means  $\pm$  SD. \*  $p < 0.05$ , \*\*\*  $p < 0.001$ ).

#### **4.3.4 Identification of binding fragments to CAP-1**

Complete digested SlpB fragments for 24 h were prepared by the same methods as used for 2 h hydrolysate. After digestion, the hydrolysate was incubated with CAP-1 coated on a microwell plate. The unbound peptides after incubation (CT-24h-SlpB-CAP-1) were compared by HPLC analysis. Several peaks were reduced in the CT-24h-SlpB-CAP-1 group (Figure 4.5, blue arrows). 6 fragments were collected from CT-24H-SlpB, including F0 that only appear under 24 h digestion, F1, F3, F4, F5, and F7 appear at the same retention time as 2h treatment. With the same fluorescent labelling, F0, F3, F4 and F5 showed a significant expression of CAP-1 binding compared with the control group (Figure 4.6). These fragments are different than bacteria binding fragments. Not only had the functional CAP-1 binding peptides in this experiment, but the different binding peptides also suggest a different function region for bacteria binding and cell binding of SlpB.

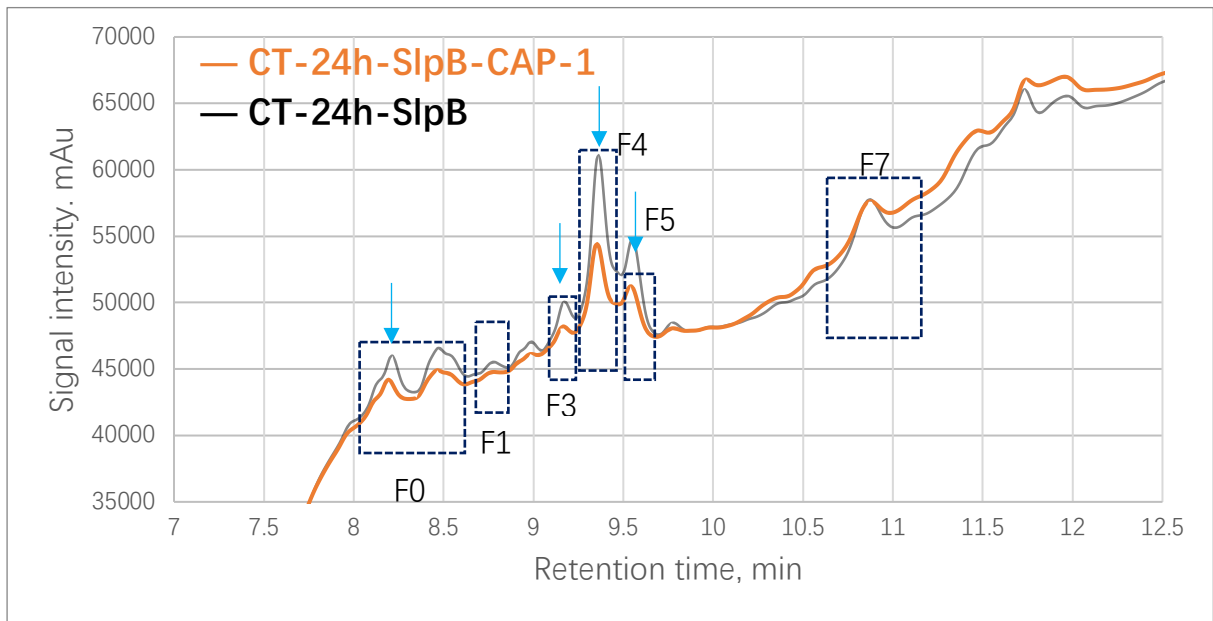


**Figure 4.5** HPLC analysis of SlpB peptides released from CAP-1 binding supernatant (orange) and 24h chymotrypsin digested SlpB (grey). Collected 6 Fragments from 24h chymotrypsin treated SlpB. F0 is a novel peptide from 24h chymotrypsin digested SlpB, F1, F3, F4, F5, and F7 appear at the same retention time as 2h treatment. Arrows (blue) indicate specific unbound peptides.

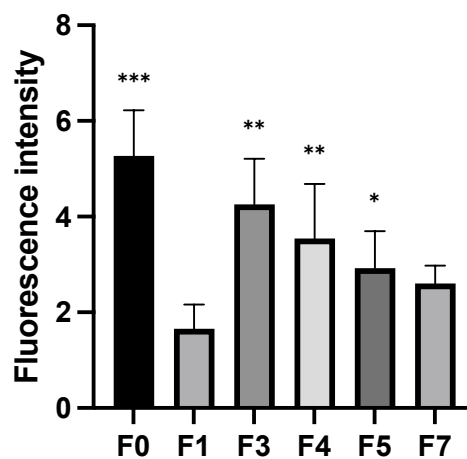


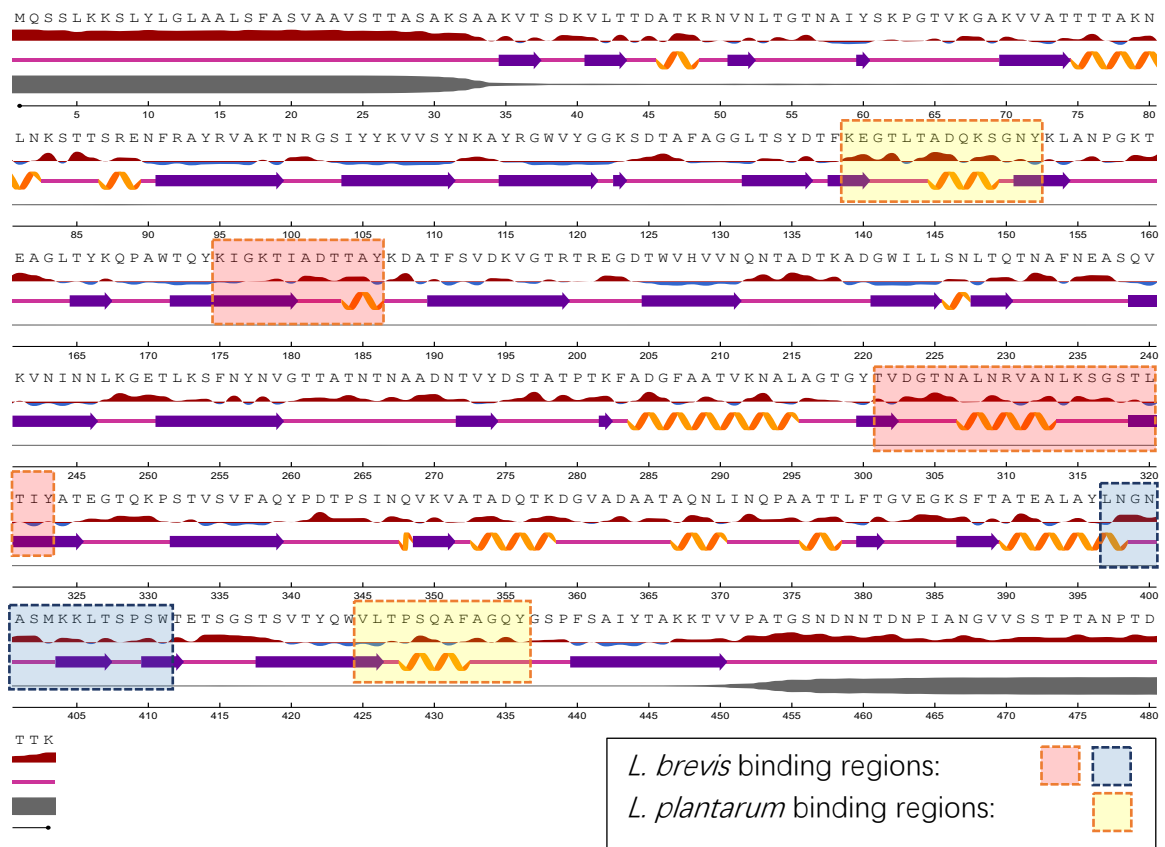
**Figure 4.6** Cy3 labeled 6 peptides binding expression with CAP-1 (Means  $\pm$  SD. \*  $p < 0.05$ , \*\*  $p < 0.01$ , \*\*\*  $p < 0.001$ ).



#### 4.3.5 Prediction of bacteria binding peptides

Based on the TOF MS analysis, several peptides sequence were predicted for bacteria binding. From F1, that showed high binding ability with *L. plantarum*, <sup>139</sup>KEGTLTADQK SGN<sup>152</sup> (pI=6.01) and <sup>425</sup>VLTPSQAFAG QY<sup>436</sup> (pI=5.49) were found. The calculation results of pI showed a positive charge of these 2 peptides binding with *L. plantarum*. From F6, <sup>175</sup>KIGKTIADTT AY<sup>186</sup> (pI=8.05) and <sup>301</sup>TVDGTNALNR VANLKSGSTL TIY<sup>324</sup> (pI=8.25) were predicted as the *L. brevis* high binding peptides. <sup>397</sup>LNGNASMKKL TSPSW<sup>411</sup> (pI=10.00) from F7 with *L. brevis* binding ability peptide also has been found and the peptides pI indicate a negative charge of these 3 *L. brevis* binding peptides. All peptide binding regions were located on a 2D SlpB structure (Figure 4.7). and showed no overlapping in the peptides that bind to the two strains. Based on the secondary structure, all peptides showed a helix structure. The grand average of hydropathicity (GRAVY) calculation showed all predicted peptides exhibited a hydrophobic characteristic.

The 3D structure model of SlpB revealed a clearer image of the peptides' location (Figure 4.8 A). The binding sites between SlpB and bacteria are in the center of the protein structure or around the C-terminus. The regions that combine with *L. brevis* are on the structure's outer side (Figure 4.8 B), whereas the regions that combine with *L. plantarum* are on the structure's inner side (Figure 4.8 C). It deserves to be noted that there are no strain-binding peptides at the N-terminus. And in this area, N-glycan binding amino acid Asn has been spotted (Figure 4.8 A), suggesting an expected corresponding CAP-1 binding region.



**Relative Surface Accessibility:** ▲ Red is exposed and blue is buried, thresholded at 25%.  
**Secondary Structure:** 🌀 Helix, ➡ Strand, — Coil.  
**Disorder:** ◆ Thickness of line equals probability of disordered residue.

**Figure 4.7** Homology model of SlpB predicted by the NetSurfP-2.0 server. *L. brevis* and *L. plantarum* high binding regions were added.

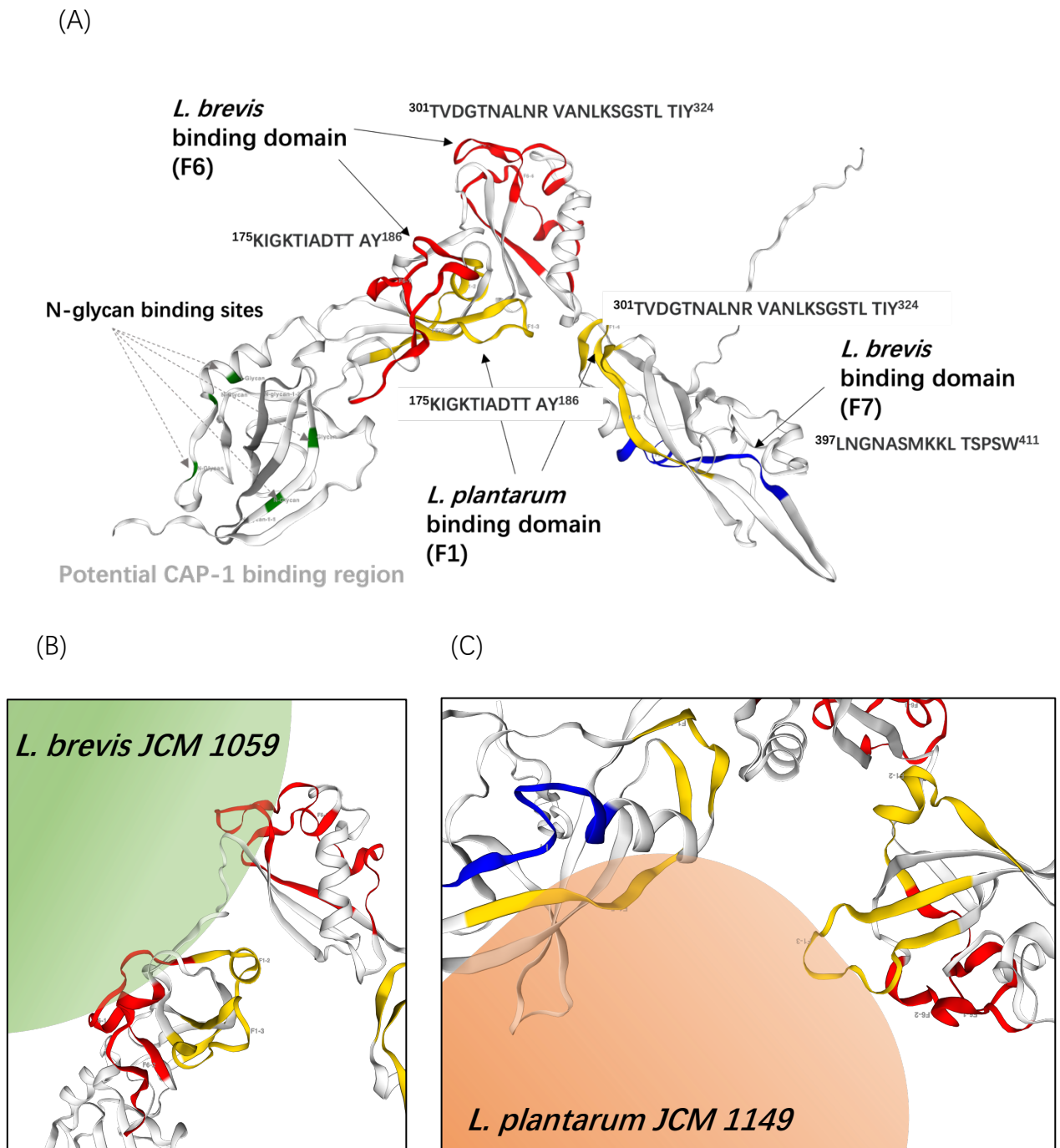


**Figure 4.8** (A) Prediction of peptides interactions with *L. brevis* JCM 1059 and *L. plantarum* JCM 1149 on SlpB 3D structure. The 3D structure of SlpB was constructed by using SWISS-MODEL. (B) the domain region of SlpB binding with *L. brevis* JCM 1059 and (C) *L. plantarum* JCM 1149.

## 4.4 Summary

In this chapter, the protein structure of SlpB is further disassembled and analyzed. Under different enzymatic hydrolysis methods, the binding peptides to bacteria and CAP-1 have been fully investigated with chymotrypsin hydrolysate.

In the selection of enzymatic hydrolysate, although trypsin is used in hydrolysis, the cleavage sites were limited in the C-terminal region [142], in order to obtain as small and many peptide fragments as possible for subsequent analysis, chymotrypsin was finally selected as a cutting enzyme to be able to cut the C-terminal side of tyrosine, phenylalanine, tryptophan, and leucine of SlpB [143]. And through experiments, peptide fragments with more subtle differences at different enzymatic hydrolysis times were further observed (Figure 4.1).

By using different digestion time collected slpB peptides, the functional binding peptides to bacteria and CAP-1 have been found. Totally 8 peptides from F0 to F7 have been collected, among these 8 peptides, F0 is CT-24H-SlpB produced peptide (Figure 4.5). F1 to F7 existed both in CT-2H-SlpB and CT-24H-SlpB. The binding results showed F1 is a major *L.plantarum* binding peptide (Figure 4.3 A, C), F6 and F7 have more strong binding ability to *L.brevis* (Figure 4.3 A, B). F0, F3, F4, F5 are the CAP-1 binding peptides (Figure 4.6). All the experiments not only selected functional peptides but results also showed that SlpB has different main functional binding domains in different strains and immune cells. With the determination and analysis of peptide fragment sequences, the structural description of SlpB will be further improved. With the TOF MS analysis, each bacteria binding peptide sequence has been predicted. *L.*

*plantarum* binding peptides are <sup>139</sup>KEGTLTADQK SGN<sup>152</sup> and <sup>425</sup>VLTPSQAFAG QY<sup>436</sup>. *L. brevis* major binding peptides are <sup>175</sup>KIGKTIADTT AY<sup>186</sup>, <sup>301</sup>TVDGTNALNR VANLKSGSTL TIY<sup>324</sup> and <sup>397</sup>LNGNASMKKL TSPSW<sup>411</sup>. With the 3D model, the location of these peptides on SlpB has been fully revealed (Figure 4.8 A).

Further studies of the receptor CAP-1 on THP-1DCs found that CAP-1, as a possible C-type lectin protein, has the possibility of binding to sugar structures. Therefore, it is necessary to further discuss the presence of sugar structure on SlpB and the effect on the binding effect during the binding process of SlpB-CAP-1. Through experimental design, it was confirmed that polysaccharides including galactose and mannose affect the binding expression of SlpB on CAP-1 (Figure 4.4 A). Further hydrolysis treatment changed the position of the SlpB band on the gel (Figure 4.4 B). Compare the binding expression on CAP-1 of deglycosylated SlpB and normal SlpB (Figure 4.4 C), it was finally determined that SlpB is a glycoprotein, and the existing polysaccharide structure affects the binding to CAP-1, which further verifies the possibility of CAP-1 as a C-type lectin receptor on THP-1 DCs.

# Chapter 5 Discussion and conclusion

## 5.1 Discussion

### 5.1.1 SlpB on *L. brevis* JCM 1059 plays important role for bacterial uptake by THP-1 DCs

In Chapter 2, Slps with the ability to interact with THP-1 DC cells were first screened. Among the 12 test strains isolated Slps coupled with microbeads, 5 strains include *L. helveticus* JCM 1120, *L. acidophilus* JCM 1132, *L. brevis* JCM 1059, *L. plantarum* JCM 1100, and *L. kefir* JCM 5818 showed high DC uptake of Slps-beads (Figure 2.3). The results of the determination of DC uptake and cytokine IL-12 production of 6 tested strains showed that *L. helveticus* JCM 1120, *L. acidophilus* JCM 1132, and *L. brevis* JCM 1059 not only have a high THP-1 DC uptake ratio, but also promote the secretion of IL-12 by cells. Compare the exist Slps of these strains, *L. helveticus* JCM 1120, *L. acidophilus* JCM 1132 has SlpA, one Slp that has been reported to have the binding ability to DC-SIGN receptors on DCs and thus triggers the immune regulation [144, 124]. And the Slps isolated from *L. brevis* JCM 1059 not only exhibited high immune regulation potential with high DC uptake and cytokine production as SlpA, but the strain also produced a single Ip around 50kDa clearly and obviously than other tested LAB (Figure 2.2).

To further confirm the Slps ability, choose *L. plantarum* JCM 1149 which didn't show a clear band on SDS-PAGE gel under 5M LiCl treatment, *L. acidophilus* JCM 1132 which produce SlpA and *L. brevis* JCM 1059 which produce a 50kDa Slp, compare the THP-1 DC uptake ratio again with same culture treatment condition, and the result showed JCM 1059 can significantly improve the uptake

ratio compared to both *L. acidophilus* JCM 1132 and *L. plantarum* JCM 1149 (Figure 2.4 A). Next to compare the absorption ability of *L. brevis* JCM 1059 with or without 5M LiCl treatment, to verify the impact of the presence of 50 kDa Slp on the bacteria-THP-1 DCs interaction. And the result revealed the uptake ratio of *L. brevis* JCM 1059 was significantly reduced in the Slp removed group (Figure 2.4 B), demonstrating the important role of this 50 kDa Slp in the absorption process of strain into DC cells.

Therefore, protein sequence analysis was performed on this Slp and identified as SlpB original source from *Lactobacillus brevis*. It belongs to the surface layer protein as SlpA, however, based on protein sequence comparison, it only has a 19.5% sequence overlap rate with SlpA indicating a different protein structure from SlpA (Figure 2.5 D). Also, in the previous experiment in our laboratory, competition experiments with SlpA also showed that SlpB has a different binding receptor on DC cells other than DC-SIGN, the SlpA binding receptor on DCs. There have been no reports on the receptors of SlpB on immune THP-1 DC cells and the immune regulatory mechanism of SlpB during bacteria and the immune cell recognition process. Thus, based on all required experimental results, after identifying SlpB on *L. brevis* JCM1059 as the major Slp, further research will be conducted on the immune function evaluation of SlpB.

### **5.1.2 SlpB can coat other LAB strains and enhance the bacterial immune ability**

The application of SlpB on other lactobacilli has also been examined in Chapter 2. As a surface layer protein, SlpB can be isolated from the surface of the original strain by disrupting hydrogen bonds through solvents such as LiCl [131].

At the same time, Slps also have the ability to self-assemble, which can quickly aggregate and re-cover on the cell surface through noncovalent interactions [46]. Therefore, SlpB can not only be isolated from *L. brevis* JCM 1059 but can also re-cover on other strain cell body surface theoretically. And our experiment successfully verified that SlpB has a very efficient encapsulation ability on the surface of other lactobacilli except for the original JCM 1059.

After fluorescent labelling of SlpB with Cy3 and *L. plantarum* JCM 1149 with FITC, through a fluorescence microscope observed a red fluorescent SlpB uniformly covered the *L. plantarum* JCM 1149 bacterial body (green) (Figure 2.6 A). And by mixing different concentrations of Cy3-SlpB with the same amount of *L. plantarum* JCM 1149 bacterial numbers, the fluorescence intensity of JCM 1149 was measured. The results showed that as the concentration of SlpB increased, the fluorescence intensity of JCM 1149 did not continue to increase, there was no significant increase after reaching a certain fluorescence intensity (Figure 2.6 B). The results demonstrated the single-layer coverage characteristics of SlpB, and it was calculated that 1 $\mu$ g slpB could cover  $1.13 \times 10^7$  *L. plantarum* JCM 1059, providing an accurate coating dosage for the subsequent combination experiments. On this basis, the coating ability of SlpB on other strains was further determined, using 6 strains of *Lactobacillus* strains, including JCM 1059 and JCM 1149, and the remaining four strains were *L. helveticus* JCM 1120, *L. acidophilus* JCM 1132, *L. lactis* IL1403 and *L. amylovorus* JCM 1126. These strains were previously treated with LiCl to remove their original Slps. And the results showed that all strains could be stably covered by SlpB (Figure 2.7), illustrating the self-assembly ability of SlpB and the possibility of its application to other strains.



Further determination of the immune performance of each strain coated by SlpB. Co-culture the SlpB coated strains with THP-1 DCs then measure the uptake ratio of DCs in each strain adding group. The results showed that for all four tested strains, *L. brevis* JCM 1059, *L. plantarum* JCM 1149, *L. amylovorus* JCM 1126 and *L. lactis* IL1403 significantly increased the uptake rate into DCs (Figure 2.8). Without removing the original Slps, in laboratory pre-experiments, *L. plantarum* JCM 1149, *L. amylovorus* JCM 1126 and *L. lactis* IL1403 all showed very low DC uptake performance. While, with the SlpB coating assistant, all 4 tested stains significantly increased the uptake ratio into THP-1 DCs, especially *L. plantarum* JCM 1149.

Continue to measure the cytokines secreted by DCs that regulate cell immunity in each strain group. IL-12, IL-10 and IL-6 have been detected in *L. brevis* JCM 1059 and *L. plantarum* JCM 1149 co-culture group, and the results showed the most obvious increased IL-12 production (Figure 2.9 A, Figure 2.10 A), not only significantly increased the IL-12 production but the production amount is high. Although IL-10 and IL-6 also showed increased potential, the secretion amount is limited. Considering that DCs secreted IL-12 can promote Th1 cell differentiation and proliferation. further, promote the secretion of IFN- $\gamma$  [145], and strengthen the host's ability to clear intracellular pathogens. Since IL-12 plays a very important role in regulating cellular immune response and can be highly stimulated by SlpB coated bacteria, the following experiments will continue to test IL-12 as the main measure of cytokine. The IL-12 production of other strain groups was measured, and the DC uptake ability also be compared among the four groups. The results showed that not only did all groups significantly increase

IL-12 secretion (Figure 2.12 A, B), but the increase also positively correlated with cell uptake ratio (Figure 2.12 C). Specifically, under the coating of SlpB, the adhesion of the strain on the DCs is first increased, allowing DC to recognize the strain and initiate the immune presentation process, promoting the secretion of IL-12 by DCs and further activating the immune system.

Based on *in vitro* tests, *in vivo* experiments were conducted to determine the activity of SlpB in the mouse intestine and its adhesion effect on intestinal immune lymphoid tissue, Peyer's patches. The (+) SlpB/ (-) SlpB <sup>Cy3</sup>*L. plantarum* JCM 1149 was gavaged into the mouse and the intestine containing the Peyer's patches tissue was collected. The frozen sections were utilized and then the section was observed under the microscope. Not only the SlpB coated <sup>Cy3</sup>*L. plantarum* JCM 1149 can obviously be observed on Peyer's patches tissue (Figure 2.14 B), but through the bacteria counting comparison, it is clearly demonstrated that SlpB can significantly improve the adhesion of *L. plantarum* JCM 1149 on mouse Peyer's patches (Figure 2.15 C). This indicates the stability of SlpB in mice and the possibility of its application in more *in vivo* experiments.

### **5.1.3 NF- $\kappa$ B involved in TLRs signal pathway triggered by SlpB in THP-1 DCs**

In order to explore the signaling pathway mechanism of THP-1 DCs from SlpB coated bacteria adsorption to cytokine IL-12 production more clearly, experiments were designed in Chapter 2 to co-culture *L. brevis* JCM 1059 and THP-1 DCs with or without SlpB coating, collect THP-1 Dc cells and extract the cell RNA, and perform sequencing analysis. After data calculation and database analysis comparison, in the SlpB (+) group, 697 genes including immune response,

cytokine and chemokine production, transcriptional regulation, and adhesion were upregulated in DC cells. High expression of genes centered around TRAF1, NF- $\kappa$ B, ICAM1 (Figure 2.13). In the signaling pathways involved in intestinal immune regulation, NF- $\kappa$ B and TLRs signaling pathways can interact with each other. TLRs identify the PAMPs and DAMPs of pathogens such as bacteria, viruses, or fungi to activate the downstream signaling pathways. Activating cytoplasmic proteins such as IRAK, TRAF6, or TAK1, ultimately leads to the degradation of I $\kappa$ B and activates NF- $\kappa$ B [72, 73]. And the involved coding genes have been upregulated by SlpB coating *L. brevis* JCM 1059 group (Table 2.2). The activated NF- $\kappa$ B enters the nucleus and binds to specific NF- $\kappa$ B binding sites on the DNA sequence, regulating the transcription and expression of multiple NF- $\kappa$ B dependent genes [72]. For example, IL-1, IL-6, TNF- $\alpha$  Inflammatory mediator genes can be expressed through NF- $\kappa$ B activation, apoptosis related Bcl-xL, cIAP and other apoptosis regulator genes can be activated by NF- $\kappa$ B, while genes related to intestinal immunity such as ICAM1, VCAM1, E-selectin, and MHC-II antigen presenting molecules can also be activated and expressed through NF- $\kappa$ B [146, 147]. Although more specific gene expression experiments are needed to clear the signal pathway, through this experiment, it can be basically determined that all relevant genes are involved. This indicates that the process of DC adsorption and recognition of SlpB (+) *L. brevis* JCM 1059, initiated a signaling pathway with NF- $\kappa$ B as the core and TLRs actively participated in. This further explains the immune regulation active under the interaction of lactobacilli and DCs.

Above all, the essential key factor to activate this signaling pathway is SlpB. Without the involvement of SlpB, the strain couldn't successfully adhere to the

surface of THP-1 DCs and be further recognized, and the continued immune presentation will not occur. Demonstrate the importance of SlpB in immune regulation.

#### **5.1.4 CAP-1 as a novel receptor for SlpB on THP-1 DCs**

In Chapter 3, the SlpB binding receptor has been fully revealed. Since the important immune regulatory role of SlpB has been identified, and THP-1 DC initiates the immune regulatory pathway by recognizing SlpB, it is necessary to clarify the recognition receptors of SlpB on THP-1 DCs. As mentioned above, it has been verified in our laboratory experiments that DC-SIGN is not the only receptor for SlpB, so there must be a novel unidentified receptor for SlpB on DCs.

Therefore, the experiment was designed to obtain possible SlpB binding proteins from the surface of THP-1 DCs first. The cultured THP-1 DCs were lysed by 1% Triton-PBS to acquire cell surface proteins and mixed with SlpB-resin. During the mixing process, potential protein receptors that can bind to SlpB will remain in the resin and can be recovered through NaCl elution. Proteins that eluted under high concentrations of NaCl exhibit high affinity with SlpB.

According to the SDS-PAGE result, two protein bands on 46kDa and 57kDa were still clearly present by 1M NaCl eluent (Figure 3.1). Cut and recover the proteins on these two protein bands then identify the protein sequence. Finally, through database comparison, peptide from the 46 kDa protein was matched as Actin (Figure 3.2 A), and the 57kDa protein was matched as CAP-1 (Figure 3.2 B), indicating a high possibility of these two proteins being Actin and CAP-1. Especially CAP-1 has been clarified and expressed on DCs and has immune

regulatory functions in current research [139]. To confirm the presence of these two proteins on our laboratory cultured THP-1 DCs, fluorescent staining was used to label the Anti-CAP-1 antibody against the protein. After mixed cultivation with DCs, not only fluorescence was displayed but showed CAP-1 was evenly covered on the cell surface (Figure 3.5).

Meanwhile, CAP-1 expression was measured in different THP-1 DC stimulation periods. CAP-1 protein antibodies were added to the cell culture medium on day 0 of undifferentiated THp-1 cells, day 2 of PMA stimulation, and day 5 of complete differentiation after the addition of IL-4. The fluorescence intensity of the cells was measured by flow cytometry. The results showed that CAP-1 could not be expressed on the surface of undifferentiated THP-1 monocytes on day 0. While in the middle stage of differentiation by PMA, CAP-1 has gradually begun to be expressed. Ultimately, significantly expressed on the surface of complete differentiated DC cells compared to the day 2 stimulation group (Figure 3.4). The results confirmed the presence and high expression of CAP-1 on the surface of our laboratory induced THP-1 DCs.

Western blotting was also performed to determine the presence of each protein, considering that the THP-1 cells can be differentiated into dendritic cells or macrophage cells, the specific antigens of the two cells were used to determine the cell type. And according to the WB results, it can observe that the DC-SIGN antibody exhibits a clear band at 45kDa after reacting with THP-1 DCs extract (Figure 3.6 A), while the antibody against Mincle showed no band (Figure 3.6 B) after the reaction. indicating that the cells induced in our laboratory are indeed dendritic cells with high expression of DC-SIGN. Continuing the WB experiment,

the antibody against CAP-1 showed strong binding specificity, with a very clear band at the 57kDa position and also a clear band on the purified CAP-1 protein (Figure 3.6 C, D). The results fully confirmed the presence of CAP-1 on the surface of DC cells induced by our laboratory. However, another candidate SlpB binding protein receptor Actin showed high affinity to CAP-1. Although the original Actin 46kDa band could also be observed, a stronger and clearer band was also observed at the 57kDa, CAP-1 protein band position. The results indicate a high affinity between Actin and CAP-1. To explain this result, the protein sequence of CAP-1 was analyzed. Existing studies have shown a bind region in the CAP-1 sequence that can bind to Actin [148], which explains the WB results of Actin. And Actin as a highly conserved protein, is widely present in various types of cells. For DC, Actin interacts with other proteins to form a cellular skeleton network, enabling cells to quickly change the form and promote the extension and contraction of cell membranes, playing a more important role in the formation and maintenance of cellular morphological protrusions [149, 150]. Although it is a very important protein present in DCs, the objective of this experiment is to find a special protein receptor in DCs that can recognize SlpB. Therefore, compared to Actin, CAP-1 has been considered the binding receptor to SlpB.

The antibody competition experiments also confirmed this hypothesis. Because each protein receptor has a higher priority in binding to its respective antibody, the binding domain of the receptor that can bind to SlpB will be occupied by its antibody, thus inhibiting the binding of SlpB on the cell surface. add Cy3-SlpB to the experimental group with antibody and the decrease in cell fluorescence intensity indicate the SlpB binding suppression. The experimental

results showed that the expression of SlpB in the Anti-CAP-1 adding group was almost completely inhibited (Figure 3.7 A), indicating that the antibody to CAP-1 and SlpB had the same binding protein and binding domain. The results confirmed that CAP-1 was a new highly binding receptor protein of SlpB on DCs. In the experiment, the Actin group also showed inhibition of SlpB expression (Figure 3.7 A). Considering the binding of Actin and CAP-1 may occupy the binding position of SlpB on CAP-1, thus partially suppressing the expression of slpB (Figure 3.7 B). Combining the binding domain of CAP-1 with Actin and the results of WB, this explanation is acceptable. And the fluorescence labeling of the two protein receptors can also illustrate this result. On the same THP-1 DC, antibody fluorescence staining of Actin and CAP-1 respectively shows that although actin occupies the edge position of the cell (Figure 3.8 A, B), CAP-1 and actin overlap at the cell morphological protrusions (Figure 3.8 C). If these positions are preferentially occupied by the Actin antibody, SlpB cannot bind to CAP-1 in the overlapping region, which leads to the restriction of SlpB fluorescent expression in THP-1 DCs.

In summary, through the experiments in Chapter 3, the entire process from collecting DC cell surface proteins, isolating, and identifying SlpB binding candidate proteins, and ultimately screening a novel receptor protein with high binding affinity to SlpB on the surface of THP-1 DCs was completed. CAP-1 has been identified as the important receptor for SlpB, further explaining the mechanism of immune activity under the involvement of SlpB.

### 5.1.5 The exploration of SlpB functional binding peptides

Finally, the structure of SlpB has been investigated in Chapter 4. As a macromolecular protein, SlpB must have the N-terminus responsible for the beginning of the amino acid sequence and the C-terminus responsible for the carboxylic acid sequence [151]. The N-terminus and C-terminus play different roles in the structure of the Slps in lactobacilli, and their binding targets are also different. For example, the C-terminal typically contains a hydrophobic tail structure containing a free carboxyl group (-COOH). This structure enables Slps to interact with other surface components, promoting the re-aggregation and forming a stable surface protein structure again [152]. Therefore, in the exploration of SlpB structure, it is necessary to understand the region of SlpB protein responsible for binding to other lactobacilli and to CAP-1, the DC surface receptor. So, in the experiment, slpB was digested into small peptides, functionally evaluate, and obtain the peptides with bacteria or DCs binding ability.

Throughout the entire experimental process, it is first necessary to cut the protein as small as possible. Therefore, although trypsin was used for enzymatic hydrolysis of SlpB in the experiment of protein sequence analysis, in this experiment, chymotrypsin that has more cutting sites to slpB was selected. And compare the effect of digestion time on the cleavage of peptide fragments. The peptide profiles were preliminarily compared by using HPLC. The peak for the peptide fragment was determined between 7-12 min (Figure 4.1 A). After carefully comparing the peaks within the retention time, it was found the producing peak have differences between the 2 h and 24 h treatment methods. Under 24 h hydrolysis, two peptide fragments appear and do not exist under 2 h partial



digestion (Figure 4.1 B, C). Therefore, the larger peptide fragment under 2h partial digest was used for binding comparison with the LAB strains, while the peptide fragment of 24 h complete hydrolysis was used for binding comparison with CAP-1.

In the bacterial binding experiments, the SlpB peptides with 2h hydrolysis was mixed and compared with *L. brevis* JCM 1059 and *L. plantarum* JCM 1149, the supernatant after mixing was recovered and performed using HPLC. If there are peptides highly bound to the strain, the peak expression in the supernatant will be disappeared or reduced. It was found that there were peptides from the supernatant that reduced the same peak in both strains, as well as peptides that decreased only in the supernatant of one strain alone. After dividing each peptide peak into 7 fragments (Figure 4.2 C), F3 and F5 were decreased in both strain groups and F7 was only significantly reduced in the *L. brevis* JCM 1059 supernatant (Figure 4.2 A, B). some peptide peaks could not be compared through HPLC; Therefore, these 7 peptide fragments were directly collected. After fluorescence labeling of the recovered peptides, they were then combined with two strains to compare the fluorescence expression intensity of each fragment on the strains. Although the fluorescence intensity of each peptide fragment was significantly enhanced compared to the blank, in the comparison between groups, only the F1 peptide was highly expressed on *L. plantarum* JCM 1149 compared to the other six fragments (Figure 4.3 C). When comparing the F1 fluorescence intensity between *L. plantarum* JCM 1149 and *L. brevis* JCM 1059, the F1 fluorescence intensity on *L. plantarum* JCM 1149 was also significantly higher than that of *L. brevis* JCM 1059 (Figure 4.3 A). This indicates that the F1 peptide is a

highly bound peptide fragment to *L. plantarum* JCM 1149. F6 and F7, on the other hand, showed high expression on *L. brevis* JCM 1059, especially F6, which showed the most significantly higher expression (Figure 4.3 A, B).

Before conducting experiments on the binding of peptide fragments to CAP-1, the first thing to solve is the impact of the sugar structure on the binding of CAP-1 on SlpB. In the protein structure analysis of CAP-1, it is a similar EPN carbohydrate recognition domain of DC-SIGN, which has the possibility of binding to glycan on glycoproteins [140]. In the competitive binding experiments involving glucose and mannose, it was confirmed that both sugars can inhibit the binding of SlpB on DCs (Figure 4.4 A). Although most surface proteins of LAB do not possess a sugar structure, the glycosylation structure of Slps in *Lactobacillus brevis* has been reported [56]. The treatment of SlpB with glycosidases also confirmed that the protein structure of SlpB would change under the glycosidase treatment (Figure 4.4 B). And further experiments showed that slpB isolated from *L. brevis* JCM 1059 not only is a glycoprotein but also proved that the destruction of this glycosylated structure would directly affect the binding of SlpB to CAP-1 (Figure 4.4 C).

In the continued peptides binding experiment, four peptide fragments with significantly reduced peak heights were compared by mixing and recovering the peptide fragments on a CAP-1 covered microwell plate (Figure 4.5 A). In further fluorescence peptide binding experiments, the same 6 fragments F1-F5, F7 as 2 h digested peptides, and a peptide fragment F0 that only appeared after 24 h of enzymatic hydrolysis were used for binding to CAP-1 (Figure 4.5 B). The results were basically consistent with the results by HPLC analysis, F0, F3, F4 and F5 were

peptide fragments that could highly bind to CAP-1 (Figure 4.6). By comparing the bacteria binding HPLC results, it is clear to find that there are no overlap fragments between the peptide that bind to strains and those that highly bind to CAP-1. The results indicate that there are different binding areas to strains and CAP-1 on SlpB.

Based on this result, peptide fragments have been further collected for proteome sequence analysis. Eventually, obtained peptides with special binding functions predicted the locations on the 3D structure of SlpB (Figure 4.8). the 3D structure revealed the different binding regions for bacteria binding and predicted a potential CAP-1 interaction area with carbohydrate binding ability.

## 5.2 Conclusion

All in all, during my doctoral studies, the surface layer protein isolated from *L. brevis* JCM 1059 was identified as SlpB. This SlpB is crucial for bacteria binding to THP-1 DCs and subsequently producing pro-inflammatory IL-12. SlpB can not only stably coated on the surface of different lactobacilli, improve the immune THP-1 DCs uptake ratio of tested lactobacilli, and enhance the secretion of IL-12, but also allow the coated lactobacilli *L. plantarum* JCM 1149 stable survival in mice's intestine. The experiment continued to use the prepared SlpB coated affinity resin to purify the SlpB binding receptor on THP-1 DCs, and ultimately identified a new SlpB receptor CAP-1, which plays a crucial role in the immunomodulatory effect of *L. brevis* JCM 1059 on THP-1 DCs. In the analysis of the structure of SlpB, it was further found that CAP-1 is a C-type like lectin, and its binding with SlpB is due to interaction with the glycosylation structure of SlpB. By enzymatic cleavage of slpB, it is more clearly understood that there are different peptide fragments of SlpB that separately bind to strains and CAP-1. TOF-MS analyses of the purified peptides revealed the binding of <sup>139</sup>KEGTLTADQK SGNY<sup>152</sup> and <sup>425</sup>VLTPSQAFAG QY<sup>436</sup> with *L. plantarum* JCM 1149 and <sup>175</sup>KIGKTIADTT AY<sup>186</sup>, <sup>301</sup>TVDGTNALNR VANLKSGSTL TIY<sup>324</sup> and <sup>397</sup>LNGNASMKKL TSPSW<sup>411</sup> with *L. brevis* JCM 1059. Further developing the sequence of these peptide fragments improved our understanding of the structure of SlpB and deepen our understanding of the important mechanism of lactobacilli in initiating immune regulation through immune recognition between SlpB and receptor CAP-1 on THP-1 DCs

## Reference

- [1] Mokoena MP, Omatola CA, Olaniran AO. Applications of Lactic Acid Bacteria and Their Bacteriocins against Food Spoilage Microorganisms and Foodborne Pathogens. *Molecules*. 2021 Nov 22;26(22):7055.
- [2] Hemarajata P, Versalovic J. Effects of probiotics on gut microbiota: mechanisms of intestinal immunomodulation and neuromodulation. *Therap Adv Gastroenterol*. 2013 Jan;6(1):39-51.
- [3] Gebrayel, P., Nicco, C., Al Khodor, S. et al. Microbiota medicine: towards clinical revolution. *J Transl Med* 20, 111 (2022).
- [4] Anjana, Tiwari SK. Bacteriocin-Producing Probiotic Lactic Acid Bacteria in Controlling Dysbiosis of the Gut Microbiota. *Front Cell Infect Microbiol*. 2022 May 16; 12:851140.
- [5] Shi C, Maktabdar M. Lactic Acid Bacteria as Biopreservation Against Spoilage Molds in Dairy Products - A Review. *Front Microbiol*. 2022 Jan 26; 12:819684.
- [6] Zheng, D., Liwinski, T. & Elinav, E. Interaction between microbiota and immunity in health and disease. *Cell Res* 30, 492–506 (2020).
- [7] Ménard S, Candalh C, Bambou JC, et al. Lactic acid bacteria secrete metabolites retaining anti-inflammatory properties after intestinal transport. *Gut*. 2004 Jun;53(6):821-8.
- [8] Park HJ, Lee SW, Hong S. Regulation of Allergic Immune Responses by Microbial Metabolites. *Immune Netw*. 2018 Feb 26;18(1): e15.
- [9] De Vries, M.C., Vaughan, et al. (2006) *Lactobacillus plantarum*—Survival,

Functional and Potential Probiotic Properties in the Human Intestinal Tract. International Dairy Journal, 16, 1018-1028.

[10] Hur, H.J., Lee, et al. (2010) Production of Nitric Oxide, Tumor Necrosis Factor- $\alpha$  and Interleukin-6 by RAW264.7 Macrophage Cells Treated with lactic acid bacteria Isolated from Kimchi. Biofactors, 21, 123-125.

[11] Pelicano E, Souza PD, Souza HD, et al. Effect of different probiotics on broiler carcass and meat quality[J]. Revista Brasileira de Ciência Avícola, 2003, 5(3): 207-214

[12] Famularo G, De Simone C, Pandey V, et al. Probiotic lactobacilli: an innovative tool to correct the malabsorption syndrome of vegetarians? Med Hypotheses. 2005;65(6):1132-1135.

[13] Yano JM, Yu K, Donaldson GP, et al. Indigenous bacteria from the gut microbiota regulate host serotonin biosynthesis [published correction appears in Cell. 2015 Sep 24; 163:258]. Cell. 2015;161(2):264-276.

[14] Gershon MD, Tack J. The serotonin signaling system: from basic understanding to drug development for functional GI disorders. Gastroenterology. 2007;132(1):397-414.

[15] Siezen RJ, van Hylckama Vlieg JE. Genomic diversity and versatility of *Lactobacillus plantarum*, a natural metabolic engineer. Microb Cell Fact. 2011;10 Suppl 1(Suppl 1): S3.

[16] Madani G, Mirlohi M, Yahay M, et al. How much in vitro cholesterol reducing activity of lactobacilli predicts their in vivo cholesterol function? Int J Prev Med. 2013 Apr;4(4):404-13.

- [17] Yamasaki M, Minesaki M, Iwakiri A, et al. *Lactobacillus plantarum* 06CC2 reduces hepatic cholesterol levels and modulates bile acid deconjugation in Balb/c mice fed a high-cholesterol diet. *Food Sci Nutr*. 2020 Oct 26;8(11):6164-6173.
- [18] Ren J, Sun K, Wu Z, et al. All 4 bile salt hydrolase proteins are responsible for the hydrolysis activity in *Lactobacillus plantarum* ST-III. *J Food Sci*. 2011;76(9):M622-M628.
- [19] Belkaid Y, Hand TW. Role of the microbiota in immunity and inflammation. *Cell*. 2014 Mar 27;157(1):121-41.
- [20] Liboni KC, Li N, Scumpia PO, et al. Glutamine modulates LPS-induced IL-8 production through I $\kappa$ B/NF- $\kappa$ B in human fetal and adult intestinal epithelium. *J Nutr*. 2005;135(2):245-251.
- [21] Arrieta MC, Bistritz L, Meddings JB. Alterations in intestinal permeability. *Gut*. 2006 Oct;55(10):1512-20.
- [22] Barrett KE. New ways of thinking about (and teaching about) intestinal epithelial function. *Adv Physiol Educ*. 2008;32(1):25-34.
- [23] Amabebe E, Anumba DOC. The Vaginal Microenvironment: The Physiologic Role of Lactobacilli. *Front Med (Lausanne)*. 2018 Jun 13; 5:181.
- [24] Mattar AF, Teitelbaum DH, Drongowski RA, et al. Probiotics up-regulate MUC-2 mucin gene expression in a Caco-2 cell-culture model. *Pediatr Surg Int*. 2002;18(7):586-590.
- [25] Mazziotta C, Tognon M, Martini F, et al. Probiotics Mechanism of Action on Immune Cells and Beneficial Effects on Human Health. *Cells*. 2023 Jan 2;12(1):184.

- [26] Mei L, Chen Y, Wang J, et al. *Lactobacillus fermentum* Stimulates Intestinal Secretion of Immunoglobulin A in an Individual-Specific Manner. *Foods*. 2022 Apr 25;11(9):1229.
- [27] Ding YH, Qian LY, Pang J, et al. The regulation of immune cells by Lactobacilli: a potential therapeutic target for anti-atherosclerosis therapy. *Oncotarget*. 2017 Jun 2;8(35):59915-59928.
- [28] Alain L. Servin, Antagonistic activities of lactobacilli and bifidobacteria against microbial pathogens, *FEMS Microbiology Reviews*, Volume 28, Issue 4, October 2004, Pages 405–440
- [29] Gieryńska M, Szulc-Dąbrowska L, Struzik J, et al. Integrity of the Intestinal Barrier: The Involvement of Epithelial Cells and Microbiota-A Mutual Relationship. *Animals (Basel)*. 2022 Jan 8;12(2):145.
- [30] Kong S, Zhang YH, Zhang W. Regulation of Intestinal Epithelial Cells Properties and Functions by Amino Acids. *Biomed Res Int*. 2018 May 9; 2018:2819154.
- [31] Vancamelbeke M, Vermeire S. The intestinal barrier: a fundamental role in health and disease. *Expert Rev Gastroenterol Hepatol*. 2017 Sep;11(9):821-834.
- [32] Yuan Q, Peng N, Xiao F, et al. New insights into the function of Interleukin-25 in disease pathogenesis. *Biomark Res* 11, 36 (2023).
- [33] Wu RQ, Zhang DF, Tu E, et al. The mucosal immune system in the oral cavity—an orchestra of T cell diversity. *Int J Oral Sci* 6, 125–132 (2014).
- [34] Taylor A, Verhagen J, Blaser K, et al. Mechanisms of immune suppression by interleukin-10 and transforming growth factor-beta: the role of T regulatory cells.



Immunology. 2006 Apr;117(4):433-42.

[35] Lebeer S, Vanderleyden J, De Keersmaecker SC. Genes and molecules of lactobacilli supporting probiotic action. *Microbiol Mol Biol Rev.* 2008 Dec;72(4):728-64, Table of Contents.

[36] Delcour J, T Ferain, M Deghorain, et al. 1999. The biosynthesis and functionality of the cell-wall of lactic acid bacteria. *Antonie van Leeuwenhoek* 76:159-184.

[37] Avall-Jaaskelainen S, and A Palva. 2005. *Lactobacillus* surface layers and their applications. *FEMS Microbiol. Rev.* 29:511-529.

[38] Zhao T, Wang H, Liu Z, et al. Recent Perspective of *Lactobacillus* in Reducing Oxidative Stress to Prevent Disease. *Antioxidants (Basel).* 2023 Mar 21;12(3):769.

[39] Kong Y, Olejar K J, On S L W, et al. The Potential of *Lactobacillus spp.* for Modulating Oxidative Stress in the Gastrointestinal Tract. *Antioxidants.* 2020; 9:610.

[40] Wang C, Sun J, Lassabliere B, et al. (2019). Potential of lactic acid bacteria to modulate coffee volatiles and effect of glucose supplementation: fermentation of green coffee beans and impact of coffee roasting. *J. Sci. Food Agr.* 99 409–420.

[41] Du Y, Li H, Shao J, et al. Adhesion and Colonization of the Probiotic *Lactobacillus plantarum* HC-2 in the Intestine of *Litopenaeus Vannamei* Are Associated With Bacterial Surface Proteins. *Front Microbiol.* 2022 Apr 13; 13:878874.

[42] Chauvière G, Coconnier MH, Kernéis S, et al. Adhesion of human *Lactobacillus acidophilus* strain LB to human enterocyte-like Caco-2 cells. *J Gen Microbiol.*

1992;138 Pt 8:1689-1696.

[43] Greene JD, Klaenhammer TR. Factors involved in adherence of lactobacilli to human Caco-2 cells. *Appl Environ Microbiol.* 1994;60(12):4487-4494.

[44] Schneitz C, Nuotio L, Lounatma K. Adhesion of *Lactobacillus acidophilus* to avian intestinal epithelial cells mediated by the crystalline bacterial cell surface layer (S-layer). *J Appl Bacteriol.* 1993;74(3):290-294.

[45] Kos B, Susković J, Vuković S, et al. Adhesion and aggregation ability of probiotic strain *Lactobacillus acidophilus* M92. *J Appl Microbiol.* 2003;94(6):981-987.

[46] Hynönen U, Palva A. *Lactobacillus* surface layer proteins: Structure, function and applications. *Appl. Microbiol. Biotechnol.* 2013, 97, 5225–5243.

[47] Carasi P, Trejo FM, Pérez PF, et al. (2011) Surface proteins from *Lactobacillus kefir* antagonize in vitro cytotoxic effect of *Clostridium difficile* toxins. *Anaerobe* 18:135–142

[48] Ravi J, Fioravanti A. S-layers: The Proteinaceous Multifunctional Armors of Gram-Positive Pathogens. *Front Microbiol.* 2021 Apr 6; 12:663468.

[49] Rodrigues-Oliveira T, Belmok A, Vasconcellos D, et al. Archaeal S-Layers: overview and current state of the art. *Front. Microbiol.* 8: 2597. doi:10.3389/fmicb.2017.02597

[50] Banerji O, Lanzoni-Mangutchi P, Vaz F, et al. (2021). Structure and assembly of the S-layer determine virulence in *C. difficile*. *Res. Sq.*10.21203/rs.3.rs-79088/v1

[51] Avall-Jääskeläinen S, Palva A. *Lactobacillus* surface layers and their

applications. FEMS Microbiol Rev. 2005;29(3):511-529.

[52] Gatti M, Rossetti L, Fornasari ME, et al. Heterogeneity of putative surface layer proteins in *Lactobacillus helveticus*. Appl Environ Microbiol. 2005 Nov; 71(11): 7582-8.

[53] Navarre WW, Schneewind O. Surface proteins of gram-positive bacteria and mechanisms of their targeting to the cell wall envelope. Microbiol Mol Biol Rev. 1999;63(1):174-229.

[54] Sára M, Sleytr UB. S-Layer proteins. J Bacteriol. 2000; 182 (4): 859-868.

[55] Schäffer C, Messner P. Glycobiology of surface layer proteins. Biochimie. 2001;83(7):591-599.

[56] Kuniyoshi Masuda, Tomio Kawata. Distribution and chemical characterization of regular arrays in the cell walls of strains of the genus *Lactobacillus*, FEMS Microbiology Letters, Volume 20, Issue 2, October 1983, Pages 145–150

[57] Toca-Herrera JL, Krastev R, Bosio V, et al. Recrystallization of bacterial S-layers on flat polyelectrolyte surfaces and hollow polyelectrolyte capsules. Small. 2005;1(3):339-348.

[58] Baumeister W, Wildhaber I, Phipps BM. Principles of organization in eubacterial and archaebacterial surface proteins. Can J Microbiol. 1989;35(1):215-227.

[59] Sleytr UB, Schuster B, Egelseer EM, Pum D. S-layers: principles and applications. FEMS Microbiol Rev. 2014;38(5):823-864.

[60] Goh YJ, Azcárate-Peril MA, O' Flaherty S, et al. Development and application of a upp-based counterselective gene replacement system for the study of the S-

layer protein SlpX of *Lactobacillus acidophilus* NCFM. Appl Environ Microbiol. 2009 May;75(10):3093-105.

[61] Johnson B, Selle K, O'Flaherty S, Goh YJ, et al. 2013. Identification of extracellular surface-layer associated proteins in *Lactobacillus acidophilus* NCFM. Microbiology 159: 2269–2282.

[62] Kajikawa A, Zhang L, LaVoy A, et al. Mucosal Immunogenicity of Genetically Modified *Lactobacillus acidophilus* Expressing an HIV-1 Epitope within the Surface Layer Protein. PLoS One. 2015 Oct 28;10(10): e0141713.

[63] Johnson BR, Hymes J, Sanozky-Dawes R, et al. Conserved S-Layer-Associated Proteins Revealed by Exoproteomic Survey of S-Layer-Forming Lactobacilli. Appl Environ Microbiol. 2015 Oct 16; 82 (1): 134-45.

[64] Duan T, Du Y, Xing C, et al. Toll-Like Receptor Signaling and Its Role in Cell-Mediated Immunity. Front Immunol. 2022 Mar 3; 13:812774.

[65] Fore F, Indriputri C, Mamutse J, et al. TLR10 and Its Unique Anti-Inflammatory Properties and Potential Use as a Target in Therapeutics. Immune Netw (2020) 20(3): e21–1.

[66] Kawai T, Akira S. The Role of Pattern-Recognition Receptors in Innate Immunity: Update on Toll-Like Receptors. Nat Immunol (2010) 11(5):373–84.

[67] McClure R, Massari P. TLR-Dependent Human Mucosal Epithelial Cell Responses to Microbial Pathogens. Front Immunol (2014) 5:386.

[68] Lin SC, Lo YC, Wu H. Helical Assembly in the MyD88-IRAK4-IRAK2 Complex in TLR/IL-1R Signalling. Nature (2010) 465(7300):885–U2.

[69] Li SY, Strelow A, Fontana EJ, et al. IRAK-4: A Novel Member of the IRAK Family

With the Properties of an IRAK-Kinase. Proc Natl Acad Sci USA (2002) 99(8):5567–72.

[70] Kollwe C, Mackensen AC, Neumann D, et al. Sequential Autophosphorylation Steps in the Interleukin-1 Receptor-Associated Kinase-1 Regulate its Availability as an Adapter in Interleukin-1 Signaling. J Biol Chem (2004) 279(7):5227–36.

[71] Xie P. TRAF molecules in cell signaling and in human diseases. J Mol Signal. 2013 Jun 13;8(1):7.

[72] Liu T, Zhang L, Joo D, et al. NF- $\kappa$ B signaling in inflammation. Sig Transduct Target Ther 2, 17023 (2017).

[73] Kawai T, Akira S. Signaling to NF-kappaB by Toll-like receptors. Trends Mol Med 2007; 13: 460–469.

[74] Yang K, Puel A, Zhang S, et al. Human TLR-7-, -8-, and -9-mediated induction of IFN-alpha/beta and -lambda is IRAK-4 dependent and redundant for protective immunity to viruses. Immunity. 2005 Nov;23(5):465-78.

[75] Paradowska-Gorycka A, Wajda A, Stypinska B, et al. Variety of endosomal TLRs and Interferons (IFN- $\alpha$ , IFN- $\beta$ , IFN- $\gamma$ ) expression profiles in patients with SLE, SSc and MCTD. Clin Exp Immunol. 2021 Apr;204(1):49-63.

[76] Lu P, Sodhi CP, Hackam DJ. Toll-like receptor regulation of intestinal development and inflammation in the pathogenesis of necrotizing enterocolitis. Pathophysiology. 2014 Feb;21(1):81-93.

[77] Villena J, Kitazawa H. Modulation of Intestinal TLR4-Inflammatory Signaling Pathways by Probiotic Microorganisms: Lessons Learned from *Lactobacillus*

*jensenii* TL2937. Front Immunol. 2014 Jan 14; 4:512.

[78] Thepmalee C, Panya A, Junking M, et al. Inhibition of IL-10 and TGF- $\beta$  receptors on dendritic cells enhances activation of effector T-cells to kill cholangiocarcinoma cells. Hum Vaccin Immunother. 2018 Jun 3;14(6):1423-1431.

[79] Kramann N, Menken L, Hayardeny L, et al. Laquinimod prevents cuprizone-induced demyelination independent of Toll-like receptor signaling. Neurol Neuroimmunol Neuroinflamm. 2016;3(3): e233. Published 2016 May 17.

[80] Yu H, Lin L, Zhang Z, et al. Targeting NF- $\kappa$ B pathway for the therapy of diseases: mechanism and clinical study. Sig Transduct Target Ther 5, 209 (2020).

[81] Ghosh, S. & Hayden, M. S. New regulators of NF- $\kappa$ B in inflammation. Nat. Rev. Immunol. 8, 837–848 (2008).

[82] Sun, S. C. Controlling the fate of NIK: a central stage in noncanonical NF- $\kappa$ B signaling. Sci. Signal 3, pe18 (2010).

[83] Sullivan C.B., Porter R.M., Evans C.H., et al. TNF $\alpha$  and IL-1 $\beta$  influence the differentiation and migration of murine MSCs independently of the NF- $\kappa$ B pathway. Stem Cell Res Ther 5, 104 (2014).

[84] Zhang A, Wang Y, Ye Z, et al. Mechanism of TNF- $\alpha$ -induced migration and hepatocyte growth factor production in human mesenchymal stem cells. J Cell Biochem. 2010, 111: 469-475.

[85] Manna SK, Ramesh GT. Interleukin-8 induces nuclear transcription factor- $\kappa$ B through a TRAF6-dependent pathway. J Biol Chem. 2005;280(8):7010-7021.

[86] Haselager M, Thijssen R, West C, et al. Regulation of Bcl-XL by non-canonical

NF- $\kappa$ B in the context of CD40-induced drug resistance in CLL. *Cell Death Differ* 28, 1658–1668 (2021).

[87] Zhang L, Dittmer MR, Blackwell K, et al. TRAIL activates JNK and NF- $\kappa$ B through RIP1-dependent and -independent pathways. *Cell Signal*. 2015 Feb;27(2):306-14.

[88] Micheau O, Lens S, Gaide O, et al. NF-kappaB signals induce the expression of c-FLIP. *Mol Cell Biol*. 2001 Aug;21(16):5299-305.

[89] Attaf M, Legut M, Cole DK, et al. The T cell antigen receptor: the Swiss army knife of the immune system. *Clin Exp Immunol*. 2015 Jul;181(1):1-18.

[90] Tang C, Chen S, Qian H, et al. Interleukin-23: as a drug target for autoimmune inflammatory diseases. *Immunology*. 2012 Feb;135(2):112-24.

[91] Iwakura Y, Ishigame H. The IL-23/IL-17 axis in inflammation. *J Clin Invest*. 2006 May;116(5):1218-22.

[92] Riera Romo M. Cell death as part of innate immunity: Cause or consequence? *Immunology*. 2021 Aug;163(4):399-415.

[93] Taverniti V, Stuknyte M, Minuzzo M, et al. S-layer protein mediates the stimulatory effect of *Lactobacillus helveticus* MIMLh5 on innate immunity. *Appl Environ Microbiol*. 2013 Feb;79(4):1221-31.

[94] Klotz C, Barrangou R. Engineering Components of the *Lactobacillus* S-Layer for Biotherapeutic Applications. *Front Microbiol*. 2018 Oct 2; 9:2264.

[95] Jung C, Hugot JP, Barreau F. Peyer's Patches: The Immune Sensors of the Intestine. *Int J Inflam*. 2010 Sep 19; 2010:823710.

[96] Ramanan D, Cadwell K. Intrinsic Defense Mechanisms of the Intestinal

Epithelium. *Cell Host Microbe*. 2016 Apr 13;19(4):434-41.

[97] Kiyono H, Fukuyama S. NALT-versus Peyer's patch-mediated mucosal immunity. *Nat Rev Immunol*. 2004 Sep;4(9):699-710.

[98] Laidlaw B, Craft J, Kaech S. The multifaceted role of CD4<sup>+</sup>T cells in CD8<sup>+</sup>T cell memory. *Nat Rev Immunol* 16, 102–111 (2016).

[99] O'Sullivan, D. et al. Memory CD8<sup>+</sup> T cells use cell-intrinsic lipolysis to support the metabolic programming necessary for development. *Immunity* 41, 75–88 (2014).

[100] Hoffman W, Lakkis FG, Chalasani G. B Cells, Antibodies, and More. *Clin J Am Soc Nephrol*. 2016 Jan 7;11(1):137-54.

[101] Mörbe UM, Jørgensen PB, Fenton TM, et al. Human gut-associated lymphoid tissues (GALT); diversity, structure, and function. *Mucosal Immunol*. 2021;14(4):793-802.

[102] Lauriano E.R., Alesci A., Aragona M., et al. Immunohistochemistry of the Gut-Associated Lymphoid Tissue (GALT) in African Bonytongue (*Heterotis niloticus*, Cuvier 1829). *Int. J. Mol. Sci*. 2023, 24, 2316.

[103] Parra D, Korytář T, Takizawa F, et al. B cells and their role in the teleost gut. *Dev. Comp. Immunol*. 2016, 64, 150–166.

[104] Moradkhani A., Abdi R., Abadi M.S.-A., et al. Quantification and description of gut-associated lymphoid tissue in, shabbout, *Arabibarbus grypus* (actinopterygii: Cypriniformes: Cyprinidae), in warm and cold season. *Acta Ichthyol. Et Piscat*. 2020, 50, 423–432.

[105] Senda T, Dogra P, Granot T, et al. Microanatomical dissection of human



intestinal T-cell immunity reveals site-specific changes in gut-associated lymphoid tissues over life. *Mucosal Immunol.* 2019 Mar;12(2):378-389.

[106] Cerutti A, Cols M, Gentile M, et al. Regulation of mucosal IgA responses: lessons from primary immunodeficiencies. *Ann N Y Acad Sci.* 2011 Nov;1238(1):132-44.

[107] Zeuthen LH, Fink LN, Frokiaer H. Epithelial cells prime the immune response to an array of gut-derived commensals towards a tolerogenic phenotype through distinct actions of thymic stromal lymphopoietin and transforming growth factor-beta. *Immunology.* 2008 Feb;123(2):197-208.

[108] Harrison OJ, Powrie FM. Regulatory T cells and immune tolerance in the intestine. *Cold Spring Harb Perspect Biol.* 2013 Jul 1;5(7): a018341.

[109] Liu K. Dendritic Cells. *Encyclopedia of Cell Biology.* 2016:741-9.

[110] Chaplin DD. Overview of the immune response. *J Allergy Clin Immunol.* 2010 Feb;125(2 Suppl 2): S3-23.

[111] Mann ER, Li X. Intestinal antigen-presenting cells in mucosal immune homeostasis: crosstalk between dendritic cells, macrophages and B-cells. *World J Gastroenterol.* 2014 Aug 7;20(29):9653-64.

[112] Grainger JR, Askenase MH, Guimont-Desrochers F, et al. Contextual functions of antigen-presenting cells in the gastrointestinal tract. *Immunol Rev.* 2014 May;259(1):75-87.

[113] Adiko AC, Babdor J, Gutiérrez-Martínez E, et al. Intracellular Transport Routes for MHC I and Their Relevance for Antigen Cross-Presentation. *Front Immunol.* 2015; 6:335.

- [114] Eisenbarth SC. Dendritic cell subsets in T cell programming: location dictates function. *Nat Rev Immunol*. 2019 Feb;19(2):89-103.
- [115] Stagg AJ, Hart AL, Knight SC, et al. The dendritic cell: its role in intestinal inflammation and relationship with gut bacteria. *Gut*. 2003 Oct;52(10):1522-9.
- [116] Wykes M, MacPherson G. Dendritic cell-B-cell interaction: dendritic cells provide B cells with CD40-independent proliferation signals and CD40-dependent survival signals. *Immunology*. 2000 May;100(1):1-3.
- [117] MacLennan I, Vinuesa C. Dendritic cells, BAFF, and APRIL: innate players in adaptive antibody responses. *Immunity*. 2002;17(3):235-238.
- [118] Cyster JG, Allen CDC. B Cell Responses: Cell Interaction Dynamics and Decisions. *Cell*. 2019 Apr 18;177(3):524-540.
- [119] Buck BL, Altermann E, Svingerud T, et al. Functional analysis of putative adhesion factors in *Lactobacillus acidophilus* NCFM. *Appl Environ Microbiol*. 2005; 71(12): 8344–8351.
- [120] Hymes JP, Johnson BR, Barrangou R, et al. Functional analysis of an S-layer-associated Fibronectin-binding protein in *Lactobacillus acidophilus* NCFM. *Appl Environ Microbiol*. 2016;82(9):2676–2685.
- [121] Call EK, Goh YJ, Selle K, et al. Sortase-deficient lactobacilli: effect on immunomodulation and gut retention. *Microbiology*. 2015;161(Pt 2):311–321.
- [122] O'Flaherty SJ, Klaenhammer TR. Functional and phenotypic characterization of a protein from *Lactobacillus acidophilus* involved in cell morphology, stress tolerance and adherence to intestinal cells. *Microbiology*. 2010;156(Pt 11):3360–3367.

- [123] Lightfoot YL, Selle K, Yang T, et al. SIGNR3-dependent immune regulation by *Lactobacillus acidophilus* surface layer protein A in colitis. *EMBO J*. 2015;34(7):881-895.
- [124] Wakai T, Kano C, Karsens H, et al. Functional role of surface layer proteins of *Lactobacillus acidophilus* L-92 in stress tolerance and binding to host cell proteins. *Biosci Microbiota Food Health*. 2021;40(1):33-42.
- [125] Ramirez-Sánchez DA, Navarro-Lleó N, Bäuerl C, et al. Factors Affecting Spontaneous Endocytosis and Survival of Probiotic Lactobacilli in Human Intestinal Epithelial Cells. *Microorganisms*. 2022 May 31;10(6):1142.
- [126] Schär-Zammaretti P, Ubbink J. The cell wall of lactic acid bacteria: surface constituents and macromolecular conformations. *Biophys J*. 2003 Dec;85(6):4076-92.
- [127] Muscariello L, De Siena B, Marasco R. *Lactobacillus* Cell Surface Proteins Involved in Interaction with Mucus and Extracellular Matrix Components. *Curr Microbiol*. 2020 Dec;77(12):3831-3841.
- [128] Masuda K, Kawata T. Ultrastructure and partial characterization of a regular array in the cell wall of *Lactobacillus brevis*. *Microbiol Immunol*. 1979;23(10):941-953.
- [129] BAUMEISTER W, WILDHABER I, PHIPPS B M. Principles of organization in eubacterial and archaebacterial surface proteins[J]. *Can J Microbiol*, 1989, 35(1): 215-227.
- [130] Masuda K, Kawata T. Reassembly of the regularly arranged subunits in the cell wall of *Lactobacillus brevis* and their reattachment to cell walls. *Microbiol*

Immunol. 1980;24(4):299-308.

[131] Garrote GL, Delfederico L, Bibiloni R, et al. Lactobacilli isolated from kefir grains: evidence of the presence of S-layer proteins. *J Dairy Res.* 2004;71(2):222-230.

[132] Zarif JC, Hernandez JR, Verdone JE, et al. A phased strategy to differentiate human CD14+ monocytes into classically and alternatively activated macrophages and dendritic cells. *Biotechniques.* 2016;61(1):33-41.

[133] Deng Y, Govers C, Ter Beest E, et al. A THP-1 Cell Line-Based Exploration of Immune Responses Toward Heat-Treated BLG. *Front Nutr.* 2021; 7:612397.

[134] Gulubova MV, Ananiev JR, Vlaykova TI, et al. Role of dendritic cells in progression and clinical outcome of colon cancer. *Int J Colorectal Dis.* 2012;27(2):159-169.

[135] Andermann TM, Rezvani A, Bhatt AS. Microbiota manipulation with prebiotics and probiotics in patients undergoing stem cell transplantation[J]. *Curr Hematol Malig Rep*, 2016, 11(1):19- 28.

[136] Oh S.H., Kim S.H., Jeon J.H., et al. Cytoplasmic expression of a model antigen with M Cell-Targeting moiety in lactic acid bacteria and implication of the mechanism as a mucosal vaccine via oral route. *Vaccine* 2021, 39, 4072–4081

[137] Shono Y, Docampo MD, Peled JU, et al. Intestinal microbiota-related effects on graft-versus-host disease[J] *Int J Hematol.* 2015;101(5):428–437.

[138] Dominguez R, Holmes KC. Actin structure and function. *Annu Rev Biophys.* 2011; 40:169-86.

[139] Lee S, Lee HC, Kwon YW, et al. Adenylyl cyclase-associated protein 1 is a

receptor for human resistin and mediates inflammatory actions of human monocytes. *Cell Metab.* 2014 Mar 4;19(3):484-97.

[140] Hatakeyama T, Kamiya T, Kusunoki M, et al. Galactose recognition by a tetrameric C-type lectin, CEL-IV, containing the EPN carbohydrate recognition motif. *J. Biol. Chem.* 2011, 286, 10305–10315.

[141] Lee R.T., Hsu T-L, Ku S, et al. Survey of immune-related, mannose/fucose-binding C-type lectin receptors reveal widely divergent sugar-binding specificities. *Glycobiology* 2011, 21, 512–520.

[142] Olsen JV, Ong SE, Mann M. Trypsin cleaves exclusively C-terminal to arginine and lysine residues. *Mol Cell Proteomics.* 2004;3(6):608-614.

[143] Blow D M. The Structure of Chymotrypsin. In: Paul D B, editor. *The Enzymes*. Vol. 3. Academic Press; 1971. pp. 185–212.

[144]: Konstantinov SR, Smidt H, de Vos WM, et al. S layer protein A of *Lactobacillus acidophilus* NCFM regulates immature dendritic cell and T cell functions. *Proc Natl Acad Sci U S A.* 2008;105(49):19474-19479.

[145] Kriegel MA, Tretter T, Blank N, et al. Interleukin-4 supports interleukin-12-induced proliferation and interferon-gamma secretion in human activated lymphoblasts and T helper type 1 cells. *Immunology.* 2006 Sep;119(1):43-53.

[146] Zhang T, Ma C, Zhang Z, et al. NF- $\kappa$ B signaling in inflammation and cancer. *MedComm (2020).* 2021 Dec 16;2(4):618-653.

[147] Baška P, Norbury LJ. The Role of Nuclear Factor Kappa B (NF- $\kappa$ B) in the Immune Response against Parasites. *Pathogens.* 2022 Mar 2;11(3):310.

[148] Ksiazek D, Brandstetter H, Israel L, et al. Structure of the N-terminal domain

of the adenylyl cyclase-associated protein (CAP) from *Dictyostelium discoideum*. *Structure*. 2003;11(9):1171-1178.

[149] Leithner A, Altenburger LM, Hauschild R, et al. Dendritic cell actin dynamics control contact duration and priming efficiency at the immunological synapse. *J Cell Biol*. 2021 Apr 5;220(4): e202006081.

[150] Rodríguez-Fernández JL, Criado-García O. The Actin Cytoskeleton at the Immunological Synapse of Dendritic Cells. *Front Cell Dev Biol*. 2021; 9:679500.

[151] Sharma S, Schiller MR. The carboxy-terminus, a key regulator of protein function. *Crit Rev Biochem Mol Biol*. 2019 Apr;54(2):85-102.

[152] Avall-Jääskeläinen S, Hynönen U, Ilk N, et al. Identification and characterization of domains responsible for self-assembly and cell wall binding of the surface layer protein of *Lactobacillus brevis* ATCC 8287. *BMC Microbiol*. 2008; 8:165.

[153] Tanaka M, Saka-Tanaka M, Ochi K, et al. C-type lectin Mincle mediates cell death-triggered inflammation in acute kidney injury. *J Exp Med*. 2020 Nov 2;217(11): e20192230.

## Acknowledgement

As my doctoral thesis is nearing completion, I would like to express my sincere gratitude to all those who have provided assistance and support to me in completing this thesis.

Firstly, I would like to express my hearty appreciation to my supervisor. Prof. Yamamoto. not only provided me with valuable guidance and advice throughout the entire research process, but also patiently answered various questions I asked. His teachings have benefited me a lot. In the process of writing papers, I not only improved my academic ability, but also developed the habit of diligence, preciseness, and critical thinking.

Secondly, I would like to express my gratitude to all the Lab members, to Miyanaga-sensei for his support, to Ari-san for her assistance in the preliminary experiment, and to Lyu-san and Haku-san for selflessly sharing their experiences and insights. your support has played an important role in completing my paper.

In addition, I also want to thank my family and friends for their unconditional support and encouragement when I was writing my paper. your understanding and support have enabled me to overcome difficulties and focus on finishing this paper.

Finally, I would like to thank the university for providing a good learning environment and excellent educational resources. It is here that I have the chance to conduct research and receive comprehensive learning and practical opportunities.

Thank you again to everyone who has helped me. Without your support and assistance, I would not be able to successfully complete this thesis. I hope my study can be useful in related fields and provide some fresh ideas and motivation for both scholarly and practical applications.

Thank you all!